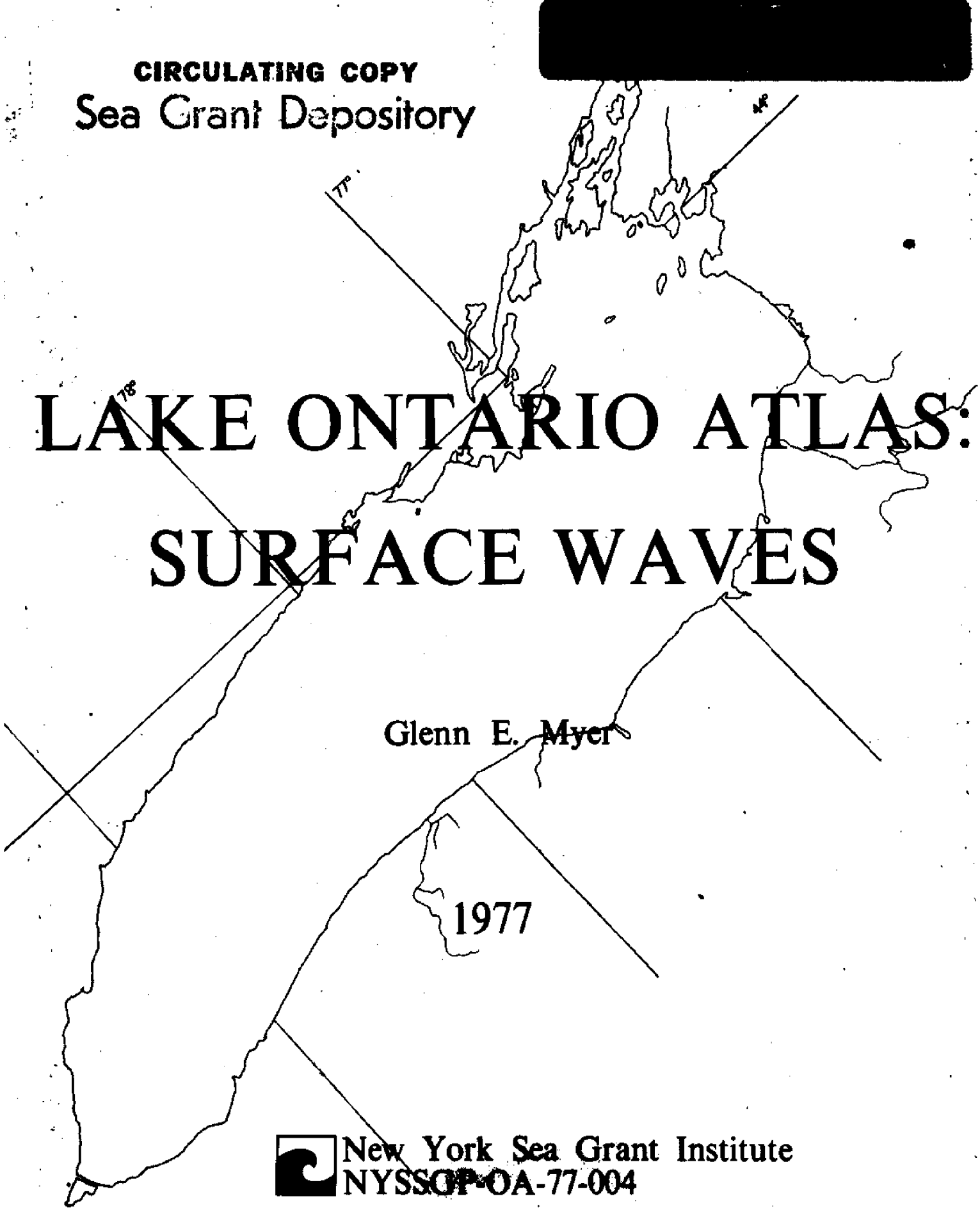

LAKE ONTARIO ATLAS: SURFACE WAVES

Glenn E. Myer

1977

New York Sea Grant Institute
NYSSGP-OA-77-004

THE LAKE ONTARIO ATLAS consolidates much of the available data on Lake Ontario into a series of monographs intended to be useful to industry and government. The eight monographs use graphics to aid interpretation of large amounts of data and to present information in summary form. The final product, a meld of the monographs, will be a nontechnical, graphic atlas for Lake Ontario.

LAKE ONTARIO ATLAS MONOGRAPHS

I	Biology	Donald C. McNaught, SUNY Albany
II	Chemistry	Eric R. Allen, SUNY Albany
III	Climatology	Cedric A. Grainger, SUC Oswego, and Bruce H. Bailey, SUNY Albany
IV	Currents	Jon T. Scott, SUNY Albany
V	Internal Waves	Dennis Landsberg, SUNY Albany
VI	Lake Temperatures	Eugene Chermack, SUC Oswego
VII	Land Use	Michael Dobson and Floyd Henderson, SUNY Albany
VIII	Surface Waves	Glenn E. Myer, SUC Plattsburgh

EDITORIAL STAFF

Editor	Ronald Stewart, Atmospheric Sciences Research Center, SUNY Albany
Reviewers	Kurt Anderson, New York State Power Pool Richard T. Nelson, Consultant Bernard Lettau, National Science Foundation Dennis Landsberg, SUNY Albany
Cartography	Michael Dobson, SUNY Albany
Production	Frances Richardson, New York Sea Grant Institute

ABSTRACT

THE SURFACE WAVES MONOGRAPH provides an analysis of gravity waves, seiche, wind tides, and long-term variations in lake level. A computerized analysis details the dynamics of each effect. Specific storm effects are analyzed and an example of hindcasting of wind velocity v. wave height is explained. This monograph will be useful for limnology, land use planning, shore erosion analysis, and coastal management.

Published by NEW YORK SEA GRANT INSTITUTE
State University of New York
99 Washington Avenue
Albany, NY 12246
$1.50
Printed in USA

LAKE ONTARIO ATLAS: Surface Waves

Glenn E. Myer

State University College at Plattsburgh

New York State Sea Grant Institute
State University of New York
99 Washington Avenue
Albany, New York 12246

1976

TABLE OF CONTENTS

Lake Ontario Surface Waves:
Temporal and Spatial Water Level Changes in Lake Ontario

Introduction

The Lake Ontario basin is a lowland bounded on the north by an escarpment of the Canadian Shield, on the east by the Adirondack Mountains, on the south by the Appalachian Plateau and on the west by the Niagara Escarpment. The watershed of the lake drains an area of approximately 75,600 Km^2 (27,200 mi^2) into the smallest of the five Great Lakes. The surface of the lake has an area of about 19,000 Km^2 (7,000 mi^2) and is located 75 m (245 ft) higher than the place at Father Point, Quebec where the St. Lawrence River makes its transition into the Gulf of St. Lawrence. Records of water levels through 1974 indicate that the average lake surface elevation has varied from 73.64 m to 75.66 m (241.45 ft to 248.06 ft), (St. Lawrence-Eastern Ontario Commission, 1975). Locally, the variations in water level have been greater than this. Some of the changes in water level have been aperiodic, others have followed a long period, and many were somewhat periodic but with short periods. This monograph has been written as a summary of much of what is now known about these locally observed time dependent water level variations in Lake Ontario.

For purposes of convenience the components of time dependent water level changes will be subdivided as much as possible based on the time scale of any periodicities which have been observed. This type of classification has been in general use and is treated in some detail by Bajorunas (1960), Kinsman (1965), and Liu (1972), the author will therefore only define the terms used in this monograph and give a general outline of the system of classification. It is recognized that the physical cause of the variation is probably more meaningful than the period. When similar periods may be caused by several physical phenomena this will be noted.

The long-term variations of lake level may be either periodic or aperiodic, generally showing components of both. These can be assumed to be a volumetric change and the lake level is usually assumed to be level, yielding the same time dependent variations of surface level at any location on the lake. The major factors causing this component of total water level change are precipitation, evaporation, runoff, and in some cases man-made and geological changes.

On Lake Ontario there exists an astronomical tide demonstrating both lunar and solar components. These are caused by the gravitational attraction of the moon and sun acting upon the water mass of the lake. The mean range of this tide is less on Lake Ontario than on the other four Great Lakes, having a total displacement of less than two centimeters (0.8 inch), (Graham, 1860; Harris, 1907; Dohler, 1964). Although these are interesting from an academic viewpoint, they may have limited importance compared with the more pronounced fluctuations of the lake surface in response to meteorological factors.

Probably wind tides and surges are responsible for some of the most dramatic changes of water level on Lake Ontario. Although both are generally regarded as forced lake-level oscillations that result from wind and are considered synonymous by some, they will be differentiated in this work following the criteria offered by Bajorunas (1960). Wind tides always have a single wave with length double that of the fetch in the wind direction. They build up slowly taking hours to reach equilibrium and may result from the wind only. Surges generally have shorter wavelengths and need only a few minutes to build up. They are forced by an atmospheric pressure gradient combined with strong winds. Energy is transferred if the atmospheric disturbance and gravity waves move at nearly equal speeds.

A wind tide will persist as long as the wind stress is sufficient to maintain the gradient of water height. The amount of the resulting rise in water level is known as a wind set-up. As the wind stress decreases, the stable surface of the wind tide cannot be sustained. The result is free oscillations of the lake surface with periods determined by the depth of the lake, the geometry of the lake, and the mode of the standing wave. These free oscillations which continue after the external forces that caused the initial set-up have ceased to act are termed seiches. On Lake Ontario these oscillations have periods ranging from about five hours to only a few minutes. There may also be some longer periods which represent rotational modes of free oscillation of the lake (Rao and Schwab, 1974).

At periods from about thirty seconds to five minutes there are waves often classified as infragravity waves. These include swell and surf beats. The swell is the result of the degeneration of the shorter period wind generated gravity waves as they travel from the generating area to a relatively calm region. Swells have longer periods and are more regular in shape than the wind generated waves from which they were formed. Liu (1972) indicates that swells rarely occur in the Great Lakes as the generating area usually covers the whole lake. The surf beats and other types of infragravity waves which were recognized from shallow water oceanic studies over thirty years ago have not been satisfactorily explained according to Munk (1962).

Wind generated waves in which the principal force involved in restoring the surface to an undeformed plane is gravity are often referred to as gravity waves. In general these have periods less than thirty seconds but greater than one second. They are characterized by a form which gives the lake surface the appearance of a series of intricate irregular moving ridges and hollows that gradually grow and shrink with time. Kinsman (1965) indicates that, at least for oceanic conditions, the general band of frequencies ascribed to wind generated gravity waves contains more wave energy than any other comparable band of frequencies of oscillation of the water surface.

The surface motions with the shortest periods are capillary waves or ripples. These are mainly controlled by the surface tension of the water. The ripples have very short wavelengths and appear as fine corrugations on the slope of longer waves. According to Liu (1972) these waves with periods less than one second play a less significant role in lake surface motion compared with other processes.

Figure 1 diagrammatically shows this classification of surface oscillations by periods. The graph shows a typical distribution of wave energy per unit frequency versus frequency.

The relative importance of the different types of surface disturbances and water level changes may be debated, depending on what process one is studying. The overall importance of the total effect of all these temporal changes in water height is apparent however. From the point of view of a researcher attempting to understand the residual complexities of circulation in Lake Ontario, it is recognized that these may only be rendered understandable in many cases after the regular motions such as seiches are first segregated. From a more applied perspective, there are at least three practical interests in these surface motions: navigation, shore protection, and electric power development. A knowledge of surface wave characteristics is essential in establishing design criteria for lake vessels, offshore structures and harbor breakwaters. Wave action, coupled with the longer term water level changes, is the primary agent responsible for shore erosion and deposition of material in navigation channels. The development of wave climate charts are demanded by the need for safe and economical navigation routes for vessels. The safe operation in harbors is greatly effected by long period surface changes, seiches, wind tides, and surges. Water supply and power storage capacity in possible hydro-electric development also has a prerequisite of knowledge of the temporal and spatial variations in the level of the water surface.

In this monograph the author has attempted to bring together in one source much of the information currently known about the temporal and spatial water level changes in Lake Ontario. In most cases only a summary of what appears to be the most generally informative and useful data is given. The reader is urged to check the references given for more detailed information. Some additional information regarding some of the more mathematically oriented methods used by some of the more recent studies is given in the appendicies.

During the past few years much has been learned about Lake Ontario, including much information from the International Field Year of the Great Lakes (IFYGL) program. Unfortunately, at the time of this writing much of this is either in the form of unpublished manuscripts or in some cases the data are still being analyzed. It has been possible to include some of this presently unpublished material through the kindness of several of the investigators who had been involved in the IFYGL program. This material has been referenced accordingly. The author has also included some analysis of IFYGL and other water level data which was done specifically for this monograph and is therefore unreferenced.

Long Term Variations in Lake Level

The water level records indicate that the entire surface of Lake Ontario is seldom, if ever, completely at rest. From the beginning to the end of any period, such as a month, there may be an appreciable change in the average level of the whole surface of the lake. This change corresponds to a change in the volume of the water in the lake during the time interval. This can be seen at several time scales. Figures 2 and 3 contain graphs of hourly water level versus time for three different stations on Lake Ontario recorded during one month. The first half of the month is represented in Figure 2 and the second half in Figure 3. Although differences between the curves caused by shorter period phenomena are apparent, the overall change in water level during the month due to a volumetric change is apparent in all stations. On a longer time scale a fairly regular increase and decrease in overall lake level can be observed on the graph in Figure 4 which shows the mean monthly water levels of Lake Ontario during a three year period. Longer term changes can be observed in Figure 5 where the mean annual water level at Oswego, N.Y. is graphed for the period from the 1860's through the present. It is apparent that, although all of these changes in level are of a volumetric nature and are therefore classified as long term variations, the changes seen in terms of these different time scales are of different origin.

The largest time scales include changes which are probably aperiodic. To accurately assess these long term changes an accurate water level record for a long period of time is required. Reliable United States records of water levels of all the Great Lakes date from about 1860. The Lake Survey Center, National Oceanographic and Atmospheric Administration maintains fifty permanent water level gauges on the Great Lakes and along their outflow rivers. Prior to 1970 these were maintained by the U.S. Corps of Engineers District Lake Survey. Canadian agencies, principally the Marine Sciences Directorate, Department of Environment, maintain thirty-three water level gauges on the Great Lakes system.

Unfortunately on Lake Ontario, as on many other lakes, the record kept at many of the stations are not continuous throughout the period of years of recorded data. Frequently there are periods when data for one or more of the stations are unavoidably absent. The method of recording the water level also has changed over the period of years, ranging from simple staff gauges to modern digital automatic recording stations. Although the change of the method of recording or the exact site of a gauge is not detrimental to the evaluation of data over periods of several years, they may inadvertently induce anomalies in records which might be used to detect changes in lake level over a period of a century or more. The effect of a new gauge site or the reestablishment of a gauge after a period of inactivity often results in a systematic error due to the gauge itself being set at a slightly different level. Fortunately, if several gauges have overlapping undisturbed periods of recording, these systematic errors can generally be detected and evaluated. A sample of this type of error is shown graphically in

Figure 6. The cumulative difference in annual average water level between Oswego and Rochester, N.Y. is plotted against time. It can be seen that between 1869 and 1907 a systematic error caused by the relative heights of the two gauges caused Oswego to record consistently higher water levels than Rochester. The change in the slope of the line occurring in 1883 indicates a change in the elevation of one of the gauges. A least squares regression to a straight line was computed for each segment as indicated on the diagram. These lines can be used to indicate that from 1869 through 1882 the Oswego station readings should be decreased by 0.21 foot to correspond to the Rochester station. From 1883 through 1907 the correction is only 0.14 foot. By applying these type of corrections to the water level data it is possible to attempt to evaluate very long term and aperiodic temporal changes in the water level of Lake Ontario.

As the time during which the level of Lake Ontario has been monitored is still relatively short compared with what may be extremely long periodic variations of water level, there are some doubts as to which variations are actually periodic and which are aperiodic. Veber (1960) postulated cycles of seven, eleven, and ninety years in the Great Lakes. In 1962 Laidly expressed that there was strong doubt by some as to the existance of any long term periodicities (Liu, 1972). Liu (1970) used spectral and autocorrelation analysis and found evidence of the existence of an eight year cycle.

A truly long term variation would be expected due to crustal movements of the earth. For thousands of years there has been a more or less continuous differential uplift of the Earth's crust in the basin of the Great Lakes. This upwarp is believed to be largely due to isostatic rebound since the retreat of the Wisconsin glaciation. Uplift of several hundred feet has occurred in some places on the shores of the Great Lakes since the glacial retreat (St. Lawrence-Eastern Ontario Commission, 1975). The land along the northern and eastern shore is rising with respect to the land along the southern and western shore as indicated on the map in Figure 7. The land along most of the shores of each of the Great Lakes is subsiding relative to the land at the lake's outlet. This is especially significant for Lake Ontario as the St. Lawrence River is rising relative to the southern end of the Ontario basin at about thirty centimeters per century according to Cohn (1973). This is causing the water level at Oswego, N.Y. to raise by approximately fifteen centimeters per century (Cohn, 1973).

The long term water level changes in the Great Lakes have many causes besides the crustal disturbance. The level will change in response to precipitation, runoff, evaporation, and retardation due to ice and aquatic growth. Although precipitation, runoff, and evaporation are relatively well documented, there is too little data to evaluate the effect of aquatic growth on Lake Ontario's level (St. Lawrence-Eastern Ontario Commission, 1975). Ice jamming occurs but is not easily predicted for any specific winter. It has been estimated that the outflow at the St. Lawrence River had a retardation prior to regulation of

about 200 m^3/sec (7000 cfs) or about three percent of the average annual flow of 6800 m^3/sec (239,000 cfs) obtained from 1860 through 1967 (St. Lawrence-Eastern Ontario Commission, 1975). The relatively low levels of Lake Ontario during 1964-66 and the high water levels experienced in 1972-74 primarily reflected the precipitation in the basin.

Since Lake Ontario gains inflow from the water which is effluent from the entire Great Lakes drainage basin, changes within this entire region can influence the level of Lake Ontario. The response is relatively slow however, and a "rule of thumb" indicated by the St. Lawrence-Eastern Ontario Commission (1975) is that it takes approximately three and one-half years for eighty percent of the change in the outflow from Lake Superior to reach Lake Ontario. They also state that "the recently released International Great Lakes Levels Board Study states that it takes two and one-half years for 50 percent of the total effect of a supply change to Lakes Michigan-Huron to reach Lake Ontario".

Due to the interconnected nature of the Great Lakes any man-made change which changes the level and outflow of any of the Great Lakes has an opportunity to alter the level of Lake Ontario. The significant factors which are already in existance include the Long Lake and Ogoki diversion into the Lake Superior Basin, the regulatory works on St. Mary's River, the diversions out of the Lake Michigan Basin via the Sanitary Canal at Chicago, the channel changes in the St. Clair/Detroit River system, the diversion of Lake Erie via the Welland Canal, the channel changes in the St. Lawrence River, and the regulatory works on the St. Lawrence River. The most direct of these, of course, is the control of the outflow of Lake Ontario through the 837 km (502 mile) long St. Lawrence River. This outflow has been controlled since the completion of the St. Lawrence Seaway in 1959. Prior to the construction of the Seaway the record discharge at Ogdensburgh, N.Y. was 9000 m^3/sec (318,000 cfs), since the Seaway the discharge at Cornwall-Massena, N.Y. was measured at 9950 m^3/sec (351,000 cfs) on July 11, July 21, and August 3 of 1974. The recorded outflow of the St. Lawrence River as of 1973 had a minimum value of 4400 m^3/sec (154,000 cfs) (St. Lawrence-Eastern Ontario Commission, 1975).

Despite the large variation in outflow rates, the maximum flow being more than double the minimum flow, the elevation of Lake Ontario has been comparatively consistent, varying only from 73.64 m (241.45 ft.) to 75.66 m (248.06 ft.) throughout the period from 1861 to 1972. This reflects the inherent ability of Lake Ontario to account for enormous changes in the quantity of water in storage with little effect on surface elevation. The rating curve of the river outflow prior to the St. Lawrence Seaway closely followed the relationship

$$F = 3.554852532 \times 10^{-51} h^{22.11490935}$$

where F = flow of the St. Lawrence River in thousands of cfs measured at the International Rapids section,
and h = height of Lake Ontario in feet measured at Oswego, N.Y.

The coefficient of correlation, r, for this relationship of monthly average outflows to the monthly average water level is 0.966. The graph shown in Figure 8 contains the data points for this rating curve for the period from 1861 through 1958. The points seem to form two distinct groups which parallel each other. The points of the upper group are primarily those which occurred after the beginning of the twentieth century. It may be more appropriate to consider this as two separate rating curves, one for the nineteenth century and one for the twentieth century prior to regulation of the St. Lawrence River. Figure 9 shows the rating curves as best fit to the data points by a least squares regression geometric curve fit. The three curves represent the best fit to the data from 1861 through 1899, from 1900 through 1958, and for all the data points.

An annual cycle of water levels in the lake is apparent from the water levels shown in Figure 4. Although the amplitude of the cycle differs from year to year a general description of this phenomena was given by Richards and Irbe (1969): "Rising water levels come in the spring and early summer: (i) after the snow-melt and spring floods, (ii) when precipitation is at its greatest, (iii) when groundwater levels are highest, and (iv) evaporation rates are lowest (due to the low water temperature). By contrast, falling water levels come in the fall and winter: (i) when evaporation rates are highest, (ii) when groundwater levels are lowest, (iii) when precipitation is at its lightest, and (iv) when most of the winter's precipitation on the watershed is locked up by winter snow."

These seasonal differences produce an average difference in water levels in Lake Ontario from a winter low to the summer high which averages 0.58 m (1.9 ft.). The maximum and minimum differences recorded are 1.07 m (3.5 ft.) and 0.21 m (0.7 ft.) respectively (St. Lawrence-Eastern Ontario Commission, 1975).

The long term volumetric changes in water level of the lake is generally considered responsible for the most serious flooding, (although many short term nonvolumetric changes in water level complicate this problem). As a result considerable effort has been devoted to both control of flooding through regulation and water level forecasting. The problem involved in regulation is that not only is there an effort to regulate the flow to protect the natural environment (sand dunes, beaches, bluffs, etc.) of Lake Ontario and also that along the St. Lawrence River, but at the same time the needs of navigation and power generation must also be served. The St. Lawrence-Eastern Ontario Commission (1975) observed that flooding occurs in the Lake St. Louis-Montreal section of the St. Lawrence River when the combined flow of the St. Lawrence River and the Ottawa River exceeds approximately 14,200 m^3/sec (500,000 cfs). The current burden of preventing this flooding is placed on the control of the approximately 8,500 m^3/sec (300,000 cfs) flow of the St. Lawrence River.

The ability to regulate the flow to produce desirable results are predicated on the availability of good hydrologic forecasts. Due to the limitations of the present techniques of long range meteorologic and therefore hydrologic forecasting, the ability to accurately predict long range water supply to Lake Ontario is likewise limited.

The Detroit District U.S. Army Corps of Engineers now employs a method of forecasting the water levels in the Great Lakes based on the concept of net basin supply. The net basin supply is defined as the algebraic sum of the change in the storage of the volume of water in the lake, the outflow volume through the natural outlet, the inflow volume from the lake above, and any diversions. By reference to the classical concept of the change in storage of a lake, the net basin supply embodies the precipitation on the lake's surface, the runoff from the lake's drainage area, the groundwater contribution, and any evaporation from the lake's surface. The forecast is developed for a six month period each month. The forecast for the first month's net basin supply of the period is determined by using a multiple linear regression model in which precipitation and temperature of the current and antecedent months are used as independent variables and the net basin supply as the dependent variable. The method employed for forecasting the net basin supply for the second through sixth month is based on a time series analysis of the recorded net basin supply. In developing this forecasting system it was assumed that the net basin supply for a given period is the result of two components: the persistence component which includes trend, seasonal, and cyclical subcomponents, and the random component which depends on seemingly chance factors. To make these forecasts possible the required antecedent temperature and precipitation prognosis for a thirty day period is supplied by both Canadian and U.S. weather services.

Comparing the forecasted Lake Ontario levels with the actual levels it is found that the one month predicted level for December 1972 was 0.20 m (0.65 ft.) less than the actual and the six month predicted level for March 1973 was 0.66 m (2.15 ft.) less than the actual. It appears that during periods of high mean water, peaks and troughs of water level were underestimated. During periods of low mean water the predicted levels were above those which occurred. The prediction by this method seems to consistently deviate from the average less than the actual levels do.

Another method of lake level forecasting is based on a climatological approach. Development of this method was started about three years ago by the Great Lakes Environmental Research Laboratory, NOAA. In this approach long term monthly net basin supplies are routed through the Great Lakes hydraulic response model to determine the beginning of the month lake levels for the following six months. The results of this method is compared with the forecast made by the U.S. Army Corps of Engineers and a coordinated six month lake level forecast is developed. The St. Lawrence-Eastern Ontario Commission (1975) noted that this forecast also suffers from problems similar to those previously noted

for the U.S. Army Corps of Engineers method. The forecast levels are too close to the mean and differences in lake level from the mean are underestimated.

Due to the interest in, and importance of, long term lake level variations, a list of hydrologic publications which include Lake Ontario data is included in Table I along with the publishers and other relevant information.

Table I
Hydrologic Publications Including Lake Ontario Data

Name	Publisher	Comments
Lake Ontario Data	U.S. Army Corps of Engineers	Published weekly. Includes daily mean elevation, daily outflow and average weekly inflow for Lake Ontario.
Water Levels of the Great Lakes, Weekly Data Summary	NOAA, Lake Survey Center, Water Levels Branch	Published weekly. Includes projected water levels for week and differences from stage recorded prior week, month, and year.
Monthly Bulletin of Lakes Levels	U.S. Department of Commerce	Published monthly. Includes recorded levels for previous years and current year to date with probable levels for next six months.
Monthly Water Level Bulletin	Department of the Environment, Canada	Published monthly. Includes mean for month, last years mean for month, maximum and minimum mean for month, mean for month for all years and for last ten years, and probable mean for next month.

Astronomical Tides

Astronomical tidal variations in water height caused by the gravitational attraction of the sun and moon acting upon the water mass of Lake Ontario has long been a topic of general public interest. The extent of this tide and its relative importance compared to the other forms of water level changes in the lake has been the subject of several different viewpoints for almost as long a period of time. Measurements of astronomical tides in the Great Lakes have been made for over a century. In 1860 Graham noted that the mean range of the astronomical tide in Lake Michigan at Chicago, Ill. was 0.045 m (0.15 ft.) (Graham, 1860). Harris (1907) found a similar mean range (0.043 m, 0.14 ft.) at both Chicago and Milwaukee. In 1964 Dohler recorded the mean range of astronomical tides

in the other four Great Lakes. Lake Erie showed a mean range of 0.030 m (0.10 ft.) at Port Colborne and 0.043 m (0.14 ft.) at Kingsville. Lake Superior at Saul Ste Marie was indicated to have a mean range of 0.030 m (0.10 ft.). Lake Huron at Port Huron showed a mean range of 0.012 m (0.04 ft.). Lake Ontario had a mean range of 0.018 m (0.06 ft.) at Toronto and 0.012 m (0.04 ft.) at Kingston (Dohler, 1964). This would indicate, at least for the stations recorded, that only Lake Huron has a smaller astronomical tide than Lake Ontario.

The relative importance of these tides to the lake have not been determined with absolute certainty. Liu (1972) considered them to be negligible when compared to the more pronounced effects of meteorological factors. Miller (1972) indicates that although there are numerous reports of water movement investigations for estuaries where astronomical tides are the principal method of water exchange, many of the results of these studies are not applicable to the Great Lakes harbors due to the negligible effect of the astronomical tides as well as the water not being saline. Platzman (1964) indicated that the relatively large astronomical tides on Lake Erie are the result of a near resonant coupling with the natural period of the basin (about fourteen hours). Although this might be of some importance in Lake Erie, Lake Ontario's natural period of about five hours would not be expected to exhibit similar resonance coupling. Simpson and Anderson (1967) considers several possible important effects of the astronomical tides in Lake Ontario, none of which seem to have been confirmed or denied with much certainty at the time of this writing. These proposed effects include: mixing action due to the tide at critical times and locations in the lake, possible influencing the thermal bar; frequent upwelling of cold subsurface water at Toronto during the summer, possibly related to tidal pumping coupled with the earth's rotation; and variations in flow through channels such as the Burlington Canal.

The dynamic theory of astronomical tides is well described by Proudman (1953) for the reader who is interested in a detailed treatment of the subject. A very brief description will be included in this monograph as an aid in understanding the rationale for some of the methods of analysis which has been used by Simpson and Anderson (1967) and others to study the astronomical tides in Lake Ontario. In the dynamic theory of tides as applied to lakes gravitational forces due to a body external to the earth, for example the sun or moon, is thought of as being composed of two components, one horizontal with respect to a line connecting the center of the earth with the center of the external body and one vertical or perpendicular to this line. Only the horizontal component is normally considered, the vertical component being treated as local variations in the earth's gravity. The forces acting on each unit of mass on the lakes surface is the earth's gravitation, gravitation due to the external body, and centrifugal force due to the earth's rotation about the center of mass of the earth and the external body. To simplify the problem several assumptions are normally made. The earth's gravity is usually considered uniform and consequently is neglected as one of the forces. The gravitational force at the center of

the earth due to the external body is assumed to be balanced by the centrifugal force due to the earth's rotation about the common center of mass of the earth-external body system. The variation of the gravitational force due to the external body is assumed to be negligible over the earth's surface when compared with the variations in the centrifugal force, (this is a better assumption for the earth-moon system than for the earth-sun system). These assumptions lead to maximum net tide producing forces at the point on the earth's surface nearest the external body and at the point opposite the external body. The rotation of the earth would then cause maximum tide producing forces to occur every 11.97 hours (one-half siderial day) for a location on the earth's surface if the external body was considered stationary. This is complicated by the sun and moon not being on the earth's equatorial plane and the moon not being exactly on the ecliptic. Also, relative to the stars, neither the sun or moon are stationary as seen from the earth. This has led to the usage of two somewhat ficticious tide producing bodies which allow the net tide producing force to be represented by the sum of a series of sinusoidal components with the three largest tide producing terms representing the lunar-semidiurnal, the solar-semidiurnal, and the luni-solar diurnal components. The relative magnitude of the amplitudes of these three tide producing terms are 1.0000, 0.4667, and 0.5844 respectively. The next largest amplitude term in the equation usually used is less than 0.41 on the same scale. The periods corresponding to the above three relative amplitudes are 12.42, 12.00, and 23.93 hours respectively.

In analyzing the astronomical tides of Lake Ontario, Simpson and Anderson (1967) utilized the general model outlined above. The hourly water level values used contain both larger term and shorter term variations in local lake level as well as motions, which although not due to astronomical tides, are strongly correlated with the apparent position of the sun in sky. (An example of the last type of water level variations would be those due to the diurnal variations in wind stress as discussed by Platzman (1966).) Simpson and Anderson (1967) describe the method used to eliminate the unwanted components as follows:

"Consecutive hourly lake observations commonly fluctuate 0.05 to 0.1 feet, consecutive daily means 0.1 to 0.6 feet, and the overall variation of monthly means for a year is of the order of 2.5 feet. Since the short term variations mask the tide in lake level readings and the long term changes affect averaging processes, two assumptions are made in the procedure: that the short term nontidal variations at a given point on a tidal cycle are randomly distributed with mean equal to the height of the tidal cycle at that point; that the long term changes can be regarded as occurring linearly for a period of a month."

To remove the long term changes the mean of hourly observations of lake level for the fifteen days preceding and following the first and last days of each thirty-two day "month" was used to extrapolate a linear change in water level during the month under consideration. The hourly observations during the month considered were corrected using this

prior to further analysis. The variation in water level remaining was expected to be comprised of a random component and the sum of a number of cycles, primarily 12.42, 12.00 and 23.93 hours. An averaging procedure was used in a harmonic analysis by the correct choice of "month" length. Semidiurnal and diurnal components were separated by averaging water heights twelve hours apart. The moon period which did not fit an averaging process from hourly observations exactly was approximated by making use of the anticipated 12.42 hour periodicity to indicate that observations 62 hours apart should be approximately in phase.

The resulting data corrected for long term changes and using an appropriate averaging period was plotted to show the residual astronomical tide components with the anticipated periods. Figure 10 shows graphs of mean hourly water level versus the hour of the day, adjusted for the lunar component. These are for Toronto during ten months of 1959. The curves drawn on the graphs are the best fit using a least squares regression to a sine curve. A similar graph for all of 1959 which depicts the solar component at Toronto is shown as Figure 11. Figures 12 and 13 are graphs of mean hourly water levels averaged over individual months versus hour of day for several stations on Lake Ontario.

From this analysis Simpson and Anderson (1967) concluded that the western basin of the lake behaves tidally as a simple unit. The averages of Port Weller were closely related to those of Toronto. Toronto records showed twelve twenty-four hour solar components, which like those of Port Weller, were 180° out of phase with those observed at Oswego. The lunar tide components were also present at these three stations. Both Rochester and Cobourg did not show an identifiable correlation with the solar components. This is believed due to their location near the central axis of the lake. The water levels at Cape Vincent appeared to be ambiguous with respect to the astronomical tide components. This may possibly be due to the shallowness of the eastern basin.

Evidence of the existence of the lunar and solar components of astronomical tides at several stations in Lake Ontario also exists in the form of analysis of energy spectrum of hourly water level data. Examples of graphs of relative spectral energy density versus frequency for Sackett's harbor (from Rao and Schwab, 1974) as well as for Cobourg and Kingston Ontario are shown in Figures 14, 15 and 16. Spectral energy density peaks occur at the frequencies anticipated for the solar and lunar components as well as several peaks which originate in seiche activity.

Simpson and Anderson (1967) from their study observed that there are several unexplained features in the astronomical tides of Lake Ontario. They noted that there appeared to be seasonal irregularities with the most regular tides in the spring and summer and the stations at the western end of the lake showing more regularity than Oswego did. It should be noted in this respect that only two years of water level data was analyzed and so there is some question whether this is also true in general. There was a change in phase of the luni-solar cycle which was not

explained but may be due to the interaction of the luni-solar force and the geometrical distribution of water in the lake. There appears to be a monthly variation in the amplitude of the diurnal sun cycle that has not yet been explained. There also is a number of apparently regular deviations from the fitted curves, as shown in Figure 10, which occur at more than one station at a given time in a given month's cycle. These remain unexplained although the possibility of a relationship to monthly average wind or other large scale meteorological effects have not been evaluated.

Wind Tides and Surges

Wind tides are forced oscillations which result from the action of wind only. These have a single wavelength with length double that of the fetch in the wind direction. They result in a rise in water level known as wind set-up.

There have been many attempts to predict the set-up and the inclination of the lake surface with known wind speeds and directions, both for the Great Lakes and for many other bodies of water. For a non-emperical treatment Liu (1972) indicates that for the simplest case of a wind tide with constant wind speed and direction and constant lake depth, the inclination of the lake surface would be:

$$(T_{xs} + T_{xb})/(\rho g (h + n))$$

where ρ is the density of water, g is the acceleration of gravity, h is the depth of the water, n is the height of the wave, and T_{xs} and T_{xb} are the surface and bottom stress respectively. This general formulation and its derivation is found in much of the literature available on wind tides (see for example Hutchinson, 1957) but suffers due to the stresses not being well understood. Consequently empirically obtained values generally are used to obtain the set-up and the form of the wind denivellated surface. Depending on the investigation chosen, the wind stress on the water surface is found from field observations to be approximately proportional to the wind speed raised to some power which may be 1.8 to 2.4 (Hutchinson, 1957). The slope of the wind denivellated water surface is not constant in the case of shallow basins but rather any longitudinal section is found to be convex. In real basins with non-uniform bottoms this form is further complicated. A mathematical treatment for lakes with non-uniform bottoms is given by Hellstrom (1941). Hellstrom has used his treatment to compute the form of the water surface under the influence of a wind tide in Lake Erie. His results have been criticized by Keulegan (1951) who has developed a semi-empirical equation which he has found to provide a fair approximation to the wind denivellations of Lake Erie during storms.

The wind tides of the Great Lakes have been studied more recently by Keulegan (1953), Harris (1954), Gillies (1959), Hunt (1959), Veber (1960), Irish and Platzman (1962), and Platzman (1963). Most of these studies have considered Lake Erie rather than Lake Ontario. This is not surprising

as the relatively shallow depth and the relatively long west-southwest to east-north-east orientation has made Erie much more vulnerable to wind tides. Set-ups as large as 4.2 m (13.8 ft.) have been recorded on Lake Erie and a set-up in excess of 3.0 m (9.8 ft.) could be expected once every two years. The author has found little detailed analysis of the wind tides of Lake Ontario although Bajorunas (1960) has estimated that for a given wind, the set-up excited on Lake Ontario would be only 17 percent of the set-up on Lake Erie.

A somewhat similar situation exists for the relative numbers of studies of surges on Lake Ontario versus the four Great Lakes. Surges are forced lake level oscillations which result from atmospheric pressure gradients combined with strong winds. The maximum energy transfer occurs when the atmospheric disturbance and the gravity waves are moving at nearly equal speeds. Harris (1957) concludes that the orientation of the strong pressure gradient will be at least as important as its speed when the topography of the lake bottom is taken into account. The studies of surges on Lake Ontario date at least to Denison's (1898) study although much of the more recent work has been on the other Great Lakes, particularly Lakes Erie and Michigan. The surge of 26 June 1964 on Lake Michigan, for example, has been studied by Freeman and Butes (1954), Ewing et al., (1954), Harris (1957), and Platzman (1958). Platzman (1958) made an important contribution to surge prediction studies in general by using numerical methods to solve linearized vertically integrated hydrodynamic equations and applying these results to observed surges on Lake Michigan. Another prediction model was developed by Harris (1962) and Harris and Angelo (1963). This model was applied to recorded surges in Lake Erie with fair agreement between the model and observations.

The purpose of studying surges is twofold: to explain the physical phenomenon, and to predict and to warn a threatened lake shore or harbor area of dangerous high waters. Perhaps since the damage caused by surges on Lake Ontario have not been as spectacular as that on some of the other Great Lakes much of the literature which deals with this phenomenon on Lake Ontario treats it along with the erosional damage resulting from wave action combined with unusually high water levels. As this appears to be a more logical method of treatment for this lake, further discussion of specific surges on Lake Ontario will be deferred until wave action is discussed in a later section.

Seiche

Wind tides persist as long as the wind stress is sufficient to maintain the water level gradient. As the wind stress decreases the relatively stable surface of the wind tide cannot be sustained. A seiche is the result of the set-up that was primarily caused by the wind tide. The seiche is a long, free oscillation with a period determined by the geometry and depth of the lake. In general several different modes of oscillation are possible and may occur concurrently. The graphs of hourly water level versus time shown in Figures 2 and 3 show the effect of seiche and wind tide on the waterlevel at individual stations.

These graphs are all for the month of June, 1972. These Figures show the water levels recorded at Kingston, Cobourg, and Burlington, Ontario. Kingston is at the northeastern end of the lake, Cobourg near the center of the lake along its northern shore, and Burlington is at the west end of the lake. Figure 2 is for the first half of the month and Figure 3 is for the second half. The large changes in water level which occur in phase at all stations over extended periods of time such as the change following 22 days on Figure 3 are long term volumetric changes in water level. Water level changes which last many hours or even for a day are due to wind tides. Notice that these generally show a depression of water level at one end of the lake and an increase at the opposite end. After this set-up free oscillations are generally prominent. By inspection of these graphs a periodicity of about five hours with opposite ends of the lake being about 180° out of phase can be noticed. Shorter periods are also evident, particularly at Cobourg near the center of the lake. These represent higher modes of oscillation, particularly the binodal and trinodal modes. As well as these major free oscillations which involve the entire lake, there are many shorter periods possible in restricted portions of the lake, cross lake seiche, and even seiche oscillations in harbor areas.

The seiche in Lake Ontario as well as the other four Great Lakes have been the subject of many studies. A good review of the knowledge up to the early 1960's can be found in papers by Bajorunas (1960) and Mortimer (1963). The studies may generally be divided in two principle types: empirical studies which attempt to establish relationships from observed data, and theoretical studies which endeavor to develop a quantitative understanding of the phenomena which can be verified by empirical data. In this section the author will treat the results of some of the empirical studies as these provide general information regarding the nature of the observed oscillations. Only the most recent theoretical work will be treated in detail due to the change in methods from analytical to numerical which has been made possible by modern computing machines and has made possible a more detailed treatment of standing wave motion in irregular basins than can be found in the earlier analytical treatments. Summaries of the analytical studies of free oscillations in enclosed water bodies of idea shapes originally done by Rayleigh, Jeffreys, Lamb, Hidaka, and others can be found in a paper by Rao (1965).

The earlier studies generally treat the equations of motion of the fluid in their continuum form and often provide simple closed solutions. To do this, several assumptions are normally necessary. Almost all existing theory has started with the assumptions of a wave with an amplitude which is small with respect to the depth of the lake and a horizontal scale which is large compared to the depth of the lake. These two assumptions have justified neglecting non-hydrostatic pressure forces and non-linear acceleration terms. The lake water is assumed incompressible and homogeneous, neglecting the density variations, in almost all cases. The resulting equations still involve the pressure gradients and the bottom and surface stresses. These stresses are not

easily determined and generally empirical approximations are used. This often results in still more assumptions and simplifications of the equations. A frequently used approximation for seiche motions is obtained from considering the region under study to be a long channel of uniform width and variable depth. This gives rise to the so-called channel calculations which are made using a linearized, one-dimensional form of the equations of motion in which the effect of the earth's rotation and external forces are usually neglected. Appendix I contains a brief treatment of these equations.

The channel approximations which have been often used in the past have generally proved satisfactory for obtaining the values of the periods of oscillation, but generally have not given the structure of the modes in good agreement with observation unless the lake is long and narrow. Proudman (1966) developed an analytical procedure for determining a two-dimensional free oscillation of a water body. This has been used by Rao (1965) and Longuet-Higgins and Pond (1970). In the original form the problem was discussed from a Lagrangian point of view but more recently Rao (1965) used a Eulerian reference frame. The original studies using this method considered only ideal geometry, but recently Rao and Schwab (1974) applied it to natural basins including Lake Ontario by the use of finite differences. In his treatment the frequencies and structures of the modes were computed as eigenvalues and eigenvectors associated with a Hermitian matrix. As would be anticipated from the method, which does not exclude the rotation of the earth, several of the lowest gravitational modes of oscillation which affect the entire lake as well as several rotational modes may be found. This is in contrast with solutions obtained from channel equations which generally yield only a standing wave solution with nodal lines fixed in space for all time. Observation by Mortimer and Fee (Rao and Schwab, 1974) indicates that the nodal lines tend to rotate around the basin with time. The lowest mode node may be caused to rotate in the framework of channel theory by using Kelvin wave dynamics as done by Defant (1954) and Platzman and Rao (1964). This gives satisfactory results for the lowest mode but the higher modes all have nodal lines which rotate counter-clockwise in the northern hemisphere. Both observations and theoretical calculations indicate that some of the higher modes have nodal lines which rotate clockwise (Rao and Schwab, 1974).

The most detailed theoretical treatments of seiche in Lake Ontario known to the author to date are those of Hamblin (1972) and Rao and Schwab (1974). Both of these treatments yielded both gravitational and rotational modes of oscillations. Most studies of seiche in the past, both theoretical and empirical, concentrated on the gravitational modes. These are undulations of the free surface of the lake which generally have frequencies larger than the local coriolis parameter. The existence of these modes is in no way related to the earth's rotation. The rotation has only a modifying influence on the properties of the gravitational modes. Platzman and Rao (1964) found that the effects of the earth's rotation had no significant effect on the period of any longitudinal gravitational mode. They agreed with the results of

Miles and Ball reported by Liu (1972) that the earth's rotation transforms the lowest longitudinal mode into an amphidromic wave, that is, the high water rotates about the lake. This amphidromic nature of the gravitational modes was apparently not detected in Hamblin's (1968) analysis of data from Lake Ontario.

The rotational modes correspond to low frequency oscillations with the frequency of rotation less than the local coriolis parameter. Their generation depends on the existence of a gradient of potential vorticity in the basic state of the fluid configuration. The potential vorticity gradient in the water of a lake is produced either by the variation in the coriolis parameter as a function of latitude or (assuming a homogeneous fluid) by variations in bottom topography. Rao and Schwab (1974) state that, "Even though it is difficult to resolve the properties of rotational modes in natural basins from water level data, these modes are nonetheless present in the system and their role would be important in the long period behavior of a lake."

Rao and Schwab (1974) developed a general method for determining the periods and structures of the normal modes of oscillation in any enclosed basin taking into account the basin shape and bathymetry as well as the earth's rotation. The general method is described in Appendix II. They used quasi-static dynamics for an incompressible homogeneous fluid on a rotating cartesian plane with a coriolis parameter which varies as the sine of the latitude angle. The equations were written in a linearized form with adiabatic boundary conditions for the enclosed basin. Harmonic solutions in time were sought. The transport vector was assumed independent of depth and prescribed as a function of the horizontal coordinates. The lake basin parameters were reduced to discrete points on a grid to allow a finite difference method of solution. This was represented as a single Richardson lattice with the boundary of the basin passing only through the points used for the computation of the stream function for the transport field. The algorithm, described more completely in Appendix II, was tested against some simple cases for which analytical solutions are available. Using a rectangular basin with a ratio of breadth to length of 1.01 (to avoid degeneracies in the spectrum of eigenvalues which would result if this ratio was 1.00) the stream functions and velocity potentials obtained for the first few modes of long and cross seiche differed by only 0.4 to 1.7% from those obtained from the analytical treatment.

Rao and Schwab (1974) applied this treatment to Lake Ontario, by imposing a grid with a 10.08 Km spacing between any two successive points for computation of the stream function or for the computation of the potential function for the transport field. This resulted in a total of 177 points for the velocity potential field and 137 points for the stream function field. The locations of these points as well as the boundary of the grid is shown in Figure 17. The bathymetric data used was that from the U.S. Lake Survey chart #2. The coriolis parameter was considered constant for the initial computations.

Figures 18 through 23 show the computed velocity potentials for the lowest six normal gravitational modes of oscillation if the earth's rotation is ignored. The velocity potential field can be thought of as similar to the height field of the displacement of the surface. These have been normalized so that the highest value is 100 units. This does not imply that under any given conditions these modes will all have this relative magnitude to each other. The relative vertical displacements seen for uninodal and binodal seiche for the stations shown on the graphs of hourly water level shown in Figures 2 and 3 demonstrate this, although they show general agreement with the calculated value in the relative magnitude of displacement of any one mode (uninodal or binodal) from one location to another.

The first mode shown in Figure 18 has one nodal line extending generally southward across the lake from Brighton, Ontario. The greatest displacement would be expected near the region of Kingston and Cape Vincent, with only slightly less displacement near Hamilton, Ontario.

The second mode as shown in Figure 19 is binodal showing maximum vertical displacement near Kingston with only about half as great of a displacement near Hamilton. The relative vertical maximum displacement near Brighton is out of phase with the other two regions of relative maximum displacement and exhibits a relative vertical displacement of only about 30% of that at Kingston.

The third mode as seen in Figure 20 is trinodal, most of the vertical displacement is isolated to the extreme western and northeastern ends of the lake, near Hamilton and the Kingston-Cape Vincent regions.

Figure 21 shows the fourth normal gravitational mode of non-rotating oscillation. This mode differs from what would have been expected if channel considerations had been used. It has four nodal lines and appears to be a combination of a longitudinal oscillation coupled with a strong transverse oxcillation which is primarily confined to the eastern end of the lake. This mode of oscillation was not found in the one dimensional non-rotating channel calculations done by Rockwell (1966). The first three modes have structures which agree well with those found by Rockwell.

The fifth mode, shown in Figure 22 corresponds to Rockwell's fourth mode. It has four vertical modes and is primarily longitudinal in orientation. The vertical oscillations are greatest in the eastern end of the lake.

Figure 23 shows the sixth gravitational mode which consists of five vertical nodal lines and has a structure which appears like that which might be considered the fifth longitudinal mode.

Computations of stream function for these modes were made and the results for the first four are illustrated in the form of contour plots of the stream function on maps of Lake Ontario in Figure 24 through 27.

The sense of circulation in each cell in the diagrams is such that higher stream function values are to the right of the direction of flow. Rao and Schwab (1974) used the stream functions to generate the vorticity component of the flow field in calculating the rotating cases for the gravitational as well as the rotational oscillations.

Figures 28 through 33 show the fluctuation of the free surface height of the lowest six gravitational modes computed by Rao and Schwab (1974). In these diagrams the solid lines indicate cotidal lines and the dashed lines represent the co-range lines. The high water propagates in the direction of increasing phase angular measurements from 0° through 360°. The points on these diagrams around which the cotidal lines are found represent the amphidromic points.

Figure 28 represents the first mode which has a single amphidromic point slightly to the east of the center of the basin. The high water propigates counter-clockwise around the point. The amplitude is always zero at the amphidromic point and increases away from it towards the boundaries of the basin. The co-range lines, which indicate the maximum vertical displacement which may occur at specific locations on the lake surface, are almost straight. This indicates that rotation has only a small effect on the amplitude distribution around the basin. Higher modes of gravitational oscillation show a somewhat increased influence of the earth's rotation on the amplitude distribution. This can be seen by comparing Figures 21 through 23 for the non-rotating case with the rotating cases depicted in Figures 28 through 30. The fourth gravitational mode displayed in Figure 31 has four amphidromic points which have counter-clockwise rotation around them. This mode appears not to have been found by Hamblin (1972) when he computed the seiche for Lake Ontario. Both the fifth and sixth modes show clockwise propogation around some of the amphidromic points.

Table II contains both computed and observed periods of oscillation noted by several investigators. It is suspected that the binodal seiche observed by Hamblin (1972) may have been a trinodal (third mode) seiche in light of the other observations of the third mode having a period which approximately agrees with this. In general it appears that the channel type computations underestimate the seiche periods on Lake Ontario with a greater degree of error apparent in the higher modes. The difference between rotating and non-rotating computations using a two dimensional approach does not seem great. This is probably due to the elongated nature of the basin and the relatively small value of rotation speed in comparison with the slowest non-rotating gravitational mode frequency.

Much of the empirical values of seiche periods have been obtained by the use of a spectral analysis of the water level records. Most of this known to the author has been done using hourly water level records and so cannot show the periods shorter than two hours. It is suspected that in the near future more data will be available, at least for selected locations, due to the ongoing analysis of the IFYGL data.

TABLE II

SEICHE PERIODS OF LAKE ONTARIO (HOURS)

MODE	CHANNEL CALCULATION ROCKWELL (1966)	NON-ROTATION 2 DIMENSIONAL RAO & SCHWAB (1974)	COMPUTED SIMPSON & ANDERSON (1964)	COMPUTED WITH ROTATION HAMBLIN (1972)	COMPUTED WITH ROTATION RAO & SCHWAB (1974)	OBSERVED HAMBLIN (1968)
1	4.91	5.10	5.41	4.86	5.11	5.40
2	2.97	3.11	2.48	2.96	3.11	2.38
3	2.15	2.31	-	2.21	2.31	-
4	-	1.87	-	-	1.87	-
5	1.63	1.78	-	1.63	1.78	-
6	1.29	1.45	-	1.36	1.46	-

MODE	OBSERVED RAO & SCHWAB (1974)	OBSERVED AT KINGSTON ONT. FROM HR H_2O LEVELS
1	5.00	5.33
2	3.12	3.10
3	2.30	2.25
4	-	-
5	-	-
6	-	-

Examples of relative energy density spectra of hourly water level measurements made at Sackett's Harbor, Kingston, and Cobourg, Ontario during 1972 are shown in Figures 14 through 16. Several apparent periodicities are indicated on each graph. Each also shows the effects of astronomical tides as well as seiche. The major peaks on the graphs represent frequencies of relative maximum energy per unit frequency and identify dominent frequencies of vertical oscillation in the two surfaces with periods greater than 2 hours observed at each station.

As well as gravitational modes of free oscillation of the water surface, which are also evident in the form of oscillating currents, there are also currents which correspond to the rotational modes of oscillation. These have periods which have been computed by Rao and Schwab (1974) to range from 52 hours to at least 14 years. Due to the low frequencies, these have not yet been definitely identified from observations. As Rao and Schwab (1974) believe these oscillations to possibly be of long term importance to Lake Ontario, their theoretical results for a few of these modes will be included in this monograph.

It is not possible to speak of the lowest rotational mode as one does of the lowest gravitational mode. The rotational modes which are probably the most important are those which have the largest space scale rather than time-scale. It is not possible to determine the space scale of the rotational modes by examing just the periods. Rao and Schwab (1972) examined the theoretical structure of forty modes of rotational oscillation of Lake Ontario, from those, the two modes they chose as being most important are the ones with periods of 229 hours and 464 hours.

Figure 34 shows the streamlines of the mass transport field of the mode with a period of 229 hours at a phase angle of 0. The phase angle is here to be regarded as the angular velocity multiplied by time and represents the oscillation at a time of zero hours. Figure 35 is of the streamline at a phase angle of $\pi/2$ or at about 57 hours after time zero. At phase angles of π and $3\pi/2$ (time about 115 and 172 hours after time zero, respectively) the magnitudes of the stream function are the same as at phase angles 0 and $\pi/2$ respectively; but the sign is reversed. In these diagrams higher values of the stream function lie to the right of the current direction.

At phase angle zero (time zero) the basin is dominated by clockwise propogation which would give rise to our easterly flow along the northern shore and a westerly flow along the southern shore. In the western part of the basin a counter-clockwise gyre would force the current northwards where it meets the westward flow along the southern shore. The clockwise propogation in the north and counter-clockwise in the south would cause a westward flow in the central part of the eastern basin. Where this flow meets the clockwise propogation in the central basin, southward flow would result.

At a phase angle of $\pi/2$ the main features are a counterclockwise gyre in the eastern basin and a clockwise cell in the east-central region. The current would be southward where these two circulations meet. At this time an eastward flow would be expected along the southern shore of the eastern basin and westward along the southern shore of the central region. In the western basin clockwise flow would be apparent. This mode of oscillation may correspond to the rotational mode computed by Hamblin (1972) with a period of 236 hours. This mode was compared to the cubic rotational mode of an elliptical paraboloid.

Figures 36 and 37 show the streamlines of mass transport computed for the rotational mode with a period of 464 hours. Figure 36 is for a phase angle of 0, and Figure 37 for a phase angle of $\pi/2$. Rao and Schwab (1974) indicate that this mode has the largest space scale of all the rotational modes that they computed for Lake Ontario and therefore it would be expected to be important in the low frequency response of this lake.

At phase angle zero (time zero) a clockwise cell is in the western half of the lake and a counterclockwise cell in the eastern half. The most vigorous currents due to this mode would be expected to be eastward in the northern part of the central basin and southwestward in the center of the lake. When the phase angle is $\pi/2$ (about 116 hours after time zero) the counterclockwise cell extends all the way across the northern half of the basin. The clockwise cell is at this time in the southern half of the basin. This implies that there would be strong currents from west to east in the central part of the basin and from east to west along the northern and southern shores. As this would be reversed in direction when the phase angle is $3\ \pi/2$ (approximately 348 hours after time zero) the flow from the west would be along the shores and a return flow from east to west in the center of the lake.

In the above cases, it must be remembered that the assumptions of constant density and an idealized shoreline may impose restrictions which are not realized in observed actual circulation. It should not be surprising if this exact current structure is not apparent from observations as, even if the representation is completely correct, it would constitute only one of many possible components of the total flow within the lake. The surface seiche of the gravitational modes are more easily observed. Even here, however, other periods of oscillation which may represent the free as well as forced surface elevation changes due to more localized geometry of somewhat isolated portions of the lake may become important.

When a periodic excitation, such as that caused by the seiche oscillations of the lake, is applied to one end of a bay or harbor at a period which is near the natural period of free oscillation of the bay or harbor, the motion will increase to an amplitude generally determined by the damping of the system. This resonance can have important effects on harbors but its extent will vary from harbor to harbor and consequently requires detailed analysis of each site separately.

A study of water level records from many of the harbors of the Great Lakes was made by Harris (1954). He found that many of the harbors exhibited short period oscillations with some generally similar characteristics. All the harbors within the same general area tend to become excited at approximately the same time but the characteristic periods varied from harbor to harbor as did the amplitude of the oscillations. He found that many harbor disturbances occur when no atmospheric disturbance is passing in the immediate area of the harbor and some occur as much as an hour or two prior or after the apparently associated atmospheric disturbances pass the harbor. This implied that the energy of the disturbance may be communicated to the lake some distance from the harbor and transmitted to the harbor in the form of a water-level disturbance in the lake.

If the harbor is considered to be open ended and having a reflecting boundary at the opposite end, a bay like free oscillation along the length of the harbor basin would be expected to result such that the long wave travel time is an odd-integer multiple of one fourth the wave period. Miller (1972) considers the resonant period to be reasonably approximated by using Merian's formula for open-ended basins. This indicates that the period of oscillation is equal to

$$\frac{4L}{n(g\bar{z})^{\frac{1}{2}}}$$

where n is the mode of oscillation, L the length of the basin, g the acceleration of gravity, and $\bar{z}$ the near depth of the basin.

When the harbor size is small the oscillations generally have short periods, but may respond rapidly to water level fluctuations as found in the study by Saylor (1966). The maximum flow rates of the reversing currents set up is usually at the harbor entrance. This is often enhanced due to the narrow restricted openings into many harbors. Although these provide protection from waves, periodic temporal changes in water level result in relatively large hydraulic heads. As would be expected these currents are most pronounced in harbors located near the vertical displacement antinodes of the seiche of the main basin of the lake (Miller, 1972).

It is frequently suspected that a combination of seiche-induced reversing currents through the harbor entrance and nearshore current flow across the entrance provide a good natural flushing mechanism. In this respect it is interesting to note that the construction of barriers to reduce waves and adverse currents in a harbor may be at odds with the interests of water quality. A change in water quality might occur if the barriers reduce the flushing rate and hence the rate of exchange of the water in some harbors with the water of the open lake.

Gravity Waves

The short period variations with periods between about one and thirty seconds are generally termed gravity waves as this describes the primary restoring force for these waves. Waves with much shorter periods require the consideration of surface tension forces in describing their dynamics. Waves with slightly longer periods, while still being primarily responsive to gravity as a restoring force are generally termed infragravity waves. These include long swell and surf beats. In this section the very short and long periods will not be treated in detail as the capillary waves are probably of little general interest to the study of large scale phenomena on Lake Ontario, and with the exception of some near shore and erosion connected observations, the longer periods between about thirty seconds and five minutes have not been studied in detail on Lake Ontario. In 1972 Liu (1972) observed that "there are few studies of wind waves in the Great Lakes". At the present this appears to be somewhat remedied by some of the waverider data taken as part of the IFYGL program, but much of this information is yet to receive complete analysis and be published. The occurrence of long swell is thought to be rare on the Great Lakes by Liu (1972). Swell is thought to be generated by the degeneration of wind generated gravity waves as they travel from the generating region into a relatively calm region. The lack of swell is believed due to the generating area generally covering the whole lake. During exceptional weather conditions such as those recorded by Project Mover during Hurricane Agnes on June 22, 1972, there seems to be indications that the uniformity of the generation of waves over much of Lake Ontario cannot always be expected. There is still, however, little published concerning swell on Lake Ontario.

The importance of a knowledge of waves on Lake Ontario is well understood. The waves are the primary agent responsible for shore erosion and deposition. Safe and economical navigation routes require the development of wave climate charts. Design criteria for lake vessels, harbor breakwaters, and offshore structures also require knowledge of waves.

Due to the recognized importance many theoretical studies of waves have been done. Between 1864 and 1875 the Kelvin-Helmholtz model of wave growth was developed. Since that time many additional models, none totally correct for all conditions have been developed. In 1957 Phillips (1957) developed a resonance model. The resonance mechanism in his model is intended for initial wave formation. Pressure fluctuations produced in turbulent air are assumed to be advected across the water surface by the wind. Waves are then initiated on a smooth water surface by resonance between pressure fluctuations in the air and free modes of oscillation of the water surface. Miles (1957) in the same year developed a shear flow instability model of wave maintenance and growth. This theory was formulated on the assumption that momentum and energy are transferred from the wind to the existing waves by the instability of the mean shear flow in the air. These two models are complimentary and

Phillips (1966) and Miles (1960) have reformulated the mechanism to provide essentially a combined Phillips-Miles model. Both laboratory tests and field measurements indicate that this model tends to underestimate the actual growth of waves by approximately one order of magnitude (Liu, 1970; Liu, 1972). A more recent treatment was done by Hasselmann (1968) who extensively discussed the theoretical derivations of the various wave related processes in the terms of nonlinear interactions.

It is apparent that some of the processes are still poorly understood and further advances in the theory of wind waves depend to a large extent on the further understanding of the physical environment. This understanding is in turn dependent upon further observations. The remainder of this section will concentrate on the recent observations related to gravity waves on Lake Ontario and some of the empirical results from these observations.

Much empirical work has focused on the practical problem of wave forecasting. As early as 1850 Stevenson formulated an empirical relationship between wave height and wind fetch from observations on several British lakes. Some of the earliest true forecasting methods were developed by Sverdrup and Munk (1947). Sverdrup and Munk's method was revised by Bretschneider (1951, 1952, 1957) and has evolved into the Sverdrup-Munk-Bretschneider method. Saville (1953) applied this method to Lake Ontario and produced hindcasts for the period 1948-1950 using synoptic weather charts.

The use of a wave spectrum concept was developed concurrently by Darbyshine, Lonquet-Higgins, Neumann, and Pierson in 1952 (Liu, 1972). A method of forecasting waves using the spectrum concept was further developed by Pierson, Neumann and Samos (1955). This method has been widely used since its development.

Although, in the absence of more realistic data hindcast wave data may be used as a source of Great Lakes Wave information, there is a growing amount of actual wave data from Lake Ontario. As of 1972 there were over 100 ships from both the U.S. and Canada participating in a program of making voluntary shipboard meteorological observations in the Great Lakes. These include both scientific and commercial vessels in Lake Ontario. The observations include wave observations and are generally made regularly at three hour intervals starting at 0000 GMT. The ships use the World Meteorological Organization definitions for wave height and period. The wave height is coded in half-meters and is the vertical distance between trough and crest. The wave period is coded in seconds and is the time between the passage of two successive wave crests over a fixed point. Both of these measurements are obtained from the "larger well-formed waves of the wave system being observed." These data are available on cards at the National Climatic Center in Ashville, North Carolina, U.S.A.

Another recent source of wave data has been through the use of the wave rider buoy systems during the IFYGL as well as from isolated wave recording stations near shorelines which have been used to access the erosional potential. Liu (1975) and Liu and Kessenich (1975) have analyzed some of the data from four of the wave rider buoys used during 1972. These were in proximity of the U.S. physical data collection system buoy stations 14, 17, 19, and 20. The location of these stations are shown on the map in Figure 38. The names indicated for the stations refer to the location of the recording station associated with each. In each case the buoys were in about 150 m of water and the analog data from each has digitized at a rate of 3 samples per second for the purpose of the studies conducted by Liu and Kessenich (1975).

Liu and Kessenich (1975) recognized that it would be important to be able to compare the relatively detailed wave data obtained from the automatic recording stations with the much less detailed but more widely distributed data from the ships. The shipboard observations are made visually and the accuracy depends on the ability, experience and subjectivity of the observer. To make the comparisons it was necessary to reduce the automatic buoy data to terms of wave heights and periods similar to those used for shipboard observations. Liu and Kessenich (1975) used ten minutes of the digitized data from each hour for comparison. The wave height used was the significant wave height which was defined as the average of the highest one-third of the recorded waves. The wave period was interpreted as the average wave period which was the average of all zero-upcrossing periods.

To test the often held idea that, aside from stations near shore, the wave field is essentially homogeneous over Lake Ontario, Liu and Kessenich (1975) compared the significant wave heights and average wave periods recorded at each of the buoy stations with that recorded at other buoy stations during the same ten minute period. The results for significant wave heights are plotted as Figure 39. The Oswego II station and Pultneville station corresponds well as indicated by the closeness of the least squares linear regression line to the line $x=y$. The scatter appears somewhat greater in the cases of Oswego II versus Oswego I and Brockport versus Pultneville. It would appear that Oswego II systematically recorded slightly smaller significant wave heights than recorded by Oswego I. In general Oswego II reported about 0.8 the significant wave height of Oswego I, although the correlation coefficient for the least squares linear regression line in this case in only 0.85. Figure 40 shows similar comparisons for the average wave period. Although the scatter is greater here, again Oswego II shows systematically lesser values than Oswego I. This would seem to imply that the larger waves more often occur at the Oswego I station, which was somewhat nearer shore than the Oswego II station (see Figure 38). Liu and Kessenich (1975) conclude that most of the scatter from a 1-1 correlation line is explainable by the effects of the fetch and duration of wind field and that the wave-pattern is homogeneous within the lake in a broad sense. For further comparison of locations within the lake away from shores, the shipboard observations in the middle part of Lake Ontario were compared with the

Brockport station and the shipboard observations in the eastern end of Lake Ontario were compared with the Oswego II station. Liu and Kessenich (1975) report that there is no distinguishable difference between the results of the two groups. There are, however, several differences between the visual observations made by ships and the results of the automatic recording wave rider buoy stations regardless of location.

Data from May through November 1972 was used to compare shipboard observation with automatically recorded wave data. Graphs with the recorded versus observed wave height and wave period are shown as Figure 41 and 42 respectively. For wave heights over 0.5 m and wave periods over three seconds, visually observed data tend to overestimate those recorded at a gradually increasing rate. The rate of overestimation for observed wave period is consistently higher than that of observed wave heights. Liu and Kessenich (1975) obtained an approximate linear relationship between the recorded and observed parameters. The best linear fit was $H_R = (0.25 + 0.6\ H_V)$ meters for recorded significant wave height and $T_R = (2.0 + 0.2\ T_V)$ seconds for the recorded average wave period. In each of the above equations the subscript R refers to recorded and V to the visually observed. A correlation coefficient of 0.79 was obtained for the relationship for wave height and 0.40 for wave period.

Using both shipboard observations and wave rider buoy data, Liu and Kessenich (1975) plotted the time a given wave height or wave period was exceeded on a probability paper, versus the logarithm of wave height or wave period. They obtained a linear relationship implying a log-normal distribution of each as shown on the graphs in Figures 43 and 44. Both the observed and recorded values each form a straight line on the graphs. This implies that each set of data is self-consistent but the visual data is somewhat an overestimate.

Using the same data, scatter diagrams that relate wave height and the corresponding wave period for both the recorded and visual observed data were produced. Figures 45 and 46 are contoured versions of these diagrams. The broken lines running from lower left to upper right on each represent the ratio of wave height to wave length (steepness) obtained using the relationship

$$\lambda = gT^2/2,$$

where λ represents the wavelength,
T represents the period,
and g the acceleration of gravity.

The majority of recorded waves lie around the steepness lines of 1:10 and 1:20. The most frequent conditions are those with a significant height of 0.5 m and an average wave period of 2.5 seconds. The visual observed waves show a broader scatter than the recorded data and a distribution around steepness lines of 1:10 and 1:30. In this case several of the data exceed the maximum theoretical steepness of 1:7 but

this is not meaningful as the height and period may not be of the same individual wave due to the methods of observation. The most frequently visually observed waves have a wave height of 0.5 meters and a period of 3.5 seconds.

The relationship of significant wave height to wind speed is of considerable interest. The wave rider buoy stations can yield much data in this respect due to their proximity to the meteorological recording stations used during IFYGL. Although much of this information is yet to be published, data obtained from Liu (1975) along with some earlier data obtained by the Great Lakes Institute, University of Toronto (Great Lakes Institute, 1964) is plotted on a graph of significant wave height versus wind speed in Figure 47. Although the scatter of the 1962 data points is greater than that from the Oswego I and Oswego II wave rider stations during June 22-23, 1972, they are in general agreement. The best linear fit to the wave rider data obtained by a least squares regression method is indicated on Figure 47. These stations were not near shore. For comparison Figure 48 is a similar graph of significant wave height versus wind speed plotted from data published by Coakley and Cho (1973). This station was just lakeward of the region of breaking waves off Von Wagners Beach, Lake Ontario. The data was collected between September 18 and October 31, 1972. The effect of fetch on wave height is apparent. The points plotted for an east or northeast wind is most similar to those of the open lake. Here the fetch was between 50 and 200 km. Progressively smaller significant wave heights for the same wind speed can be noted for winds from the north and from the northwest (having a fetch of about 8 km and much less than one kilometer respectively). The lines for each group of data represents the best fit obtained by linear regression.

Much more detailed analysis of data obtained from automatic recording stations such as the wave rider buoys used during the IFYGL is possible by using the methods of spectral analysis. The concept of the wave spectrum was originally derived from statistical analysis of stochastic signals. It is assumed that the apparently random sea surface at any instant can be considered as the sum of many sinusoidal waves having different wave lengths, heights, and directions of movement. Figure 49 graphically shows how an actual wave profile might be considered as being composed of component sinusoidal waves. The right hand side of this figure shows the graphical description of the component waves in terms of relative energy per unit frequency. A graph such as the one on the right hand side of Figure 49 may be thought of as a graphical representation of a relative energy spectrum.

Although most empirically derived wave spectra do not consider the direction of the waves due to the absence of this type of data, a more complete description would require a spectrum which is directional in nature. It is customary in theoretical work to represent the directional spectrum as the product of a scalar or one-dimensional spectrum and a directional wave-spreading function. There have been several attempts made to obtain theoretical or semi-empirical generalized wave spectra

which could be obtained from a minimum of data and therefore be useful in wave forecasting. The major recently developed spectral equations are those of Bretschneider, Pierson, Moskowitz and Liu. These are summarized by Liu (1972). Bretschneider's equation was obtained from an analytic function for the joint probability distribution of wave heights and periods. The equation requires a specific height and period statistic to determine the theoretical spectrum. Pierson and Moskowitz derived their equation for fully developed seas using the similarity theory of Kitaigorodski. This requires only the wind speed to estimate the theoretical spectrum. Liu used an empirical approach to develop a spectral equation for use on the Great Lakes. He used data taken at the Lake Michigan Research Tower near Muskegan, Michigan during the autumn of 1967 as well as oceanic observations in deriving his equation for fetch-limited conditions. Knowledge of fetch and friction wind velocity is needed to compute the wave spectrum from his equation.

In analyzing actual wave data the non-directional form of a spectrum is usually applied as there is often insufficient information to obtain the directional nature of the waves. Figure 50 is a graph of energy per unit frequency versus frequency showing the energy spectra of waves from data recorded in Lake Michigan during an episode of wave growth. This shows a rather typical pattern of increasing over all energy and a shift of peak energy to lower frequency as time increases.

Liu (1975) has used a method of analysis based on the Blackman and Tukey (1958) method to obtain estimates of wave spectra in Lake Ontario. He has applied this to study the development and growth of waves from data obtained from the wave rider buoys used during the IFYGL. One episode which Liu (1975) has treated in detail is that accompanying the storm of June 22-23, 1972, related to Hurricane Agnes. The data from the stations labeled Oswego I and Oswego II on the map shown in Figure 38 were used to obtain hourly spectra. The general weather pattern for this episode produced north and north-northeast winds which covered most of the lake. Figure 51 shows graphs of wind speed and direction for the period of study as well as a representation of the energy density spectra in the form of a diagram of frequency versus time, with the relative energy spectra for each hour in the form of a contour chart with the relative energy density in m^2s entered on each contour line. This is for the data obtained from the Oswego I station. That obtained for the Oswego II station is similar. Liu (1975) found that the patterns of variations of significant wave heights with respect to time followed the variation in wind speed quite closely at both stations. During the latter part of June 22 when wind speeds increased vigorously and the storm reached its peak, the wave heights grew almost linearly with time. After the storm peaked with significant wave heights of about two meters, wave heights decayed immediately. The decay of wave heights was also approximately linear with time. The period of initial growth from the relative calm conditions was quite abrupt and the growth rate during these early phases was not linear. This appears in conflict with Phillips (1957) resonance growth model which predicts that even the early stages of wave growth should be linear. The increase and decrease of wave

periods followed the variations of wind speed but at a much slower rate than wave heights. In a general overview Liu (1975) notes that the initial wave growth at Oswego I lagged that at Oswego II by about one hour. Both stations reached maximum energy concurrently, but Oswego II, the station farther from the southern shore, carried more energy content than Oswego I.

Before the storm began the relative calm was characterized by low energy and multiple low spectral peaks. The early stages of wave growth was characterized by a ridge of major spectral peaks migrating rapidly to lower frequencies as time progressed. Beyond the early stages of growth the wave energy was concentrated mainly on the low-frequency end of the spectrum (see Figure 51). The process of wave decay was characterized by reduced energy content. The frequency of the spectral peak remained the same as during maximum energy for quite some time before it migrated toward the higher frequency at a very slow rate. From the observations of this storm, Liu (1975) suggests that it would be useful to consider the wave spectra to consist of three spectral ranges, each having a different functional relationship to time. The low frequency range, which for the June 21-22, 1972, storm was less than about 1.26 rad/sec (wave periods greater than about 5 seconds), is sensitive to the wind field. These waves grow exponentially in energy concurrently when the wind speed is increasing and concurrently lose energy exponentially as soon as the wind speed is reduced. A high frequency range which in the storm studied would have frequencies greater than 2.51 rad/sec (wave periods less than about 2.5 seconds) was considered to be in equilibrium after a period of initial growth. All components in this range attain a relative maximum of energy concurrently and are insensitive to either increasing wind stress or time duration after being generated. The growth and decay characteristics at all frequencies in this range tend to parallel each other in time. A middle frequency range, which falls between the two previously defined ranges, covers the portion of the spectra which usually contains the spectral energy peak. These waves appear to have mixed properties and at a given instant in time, some components are growing, some have reached equilibrium, and some have started to decay. Liu (1975) notes that although this classification of waves may be useful, it is not precise. He indicates that if the intensity of the wind field continues to grow the middle range approaches the high range in frequency, the low range the middle range, and new lower frequency waves will be generated.

Analysis of waves in deep water far from shore are important to studies of transport and turbulent diffusion as well as to shipping. Analysis of the waves occurring near the shorelines are of more importance to those involved with nearshore transport, harbor safety and maintenance as well as erosional features.

Nearshore currents and those within harbors have been studied by Saylor (1964, 1966) and Keuleyan (1951). Part of their studies involve the effect of direct wind drift, but part of the near surface flow is generated through wave action. In general these wave-drift currents may be thought

of as being formed from the unclosed orbital motions of water particles during the passage of waves. This results in net current in the direction of wave propagation. This direction is altered when the waves approach a shoreline at an angle as the decreasing depth of the water leads to a change in the velocity, height, length, and direction of the waves. They are refracted and tend to conform very approximately to the bottom contours where the water becomes quite shallow. As they usually break at a slight angle to the shore, a longshore component of the motion causes a littoral or longshore current. Miller (1972) notes that these currents are effective in moving both masses of water and sediments along the shore. In deeper water the transport caused solely by waves is generally relatively small compared with other processes.

Along coasts wave action and its resulting currents, often coupled with longer period water level changes such as wind tides and surges, are the dominant cause of erosion. The water levels of the Great Lakes show long term variations discussed earlier in this monograph. Much of the recent coastal erosion has been facilitated by a rapid net increase in lake level. The high lake level, however, plays a passive role in that it allows erosion to take place by exposing higher regions of the coast. The actual initiator of the erosion is the wave in most cases. As onshore wind increases there is an increase in wave heights and energies. The turbulence caused by breaking waves causes much sediment to be placed into suspension. This makes it available for transport by longshore and rip currents. The longshore currents are induced by waves approaching the beach at an angle. The rip currents move lakeward approximately perpendicular to the shoreline and may be caused by the deflection of longshore currents by a sinuous shoreline or by the return of water piled up by breaking waves between shallow sandbars and the beach. During a storm the high winds and pressure changes can produce high waves, wind tides, and often a storm surge. The storm surge produces a temporary but sometimes dramatic local increase in water level, allowing the wave action to erode bluffs previously unexposed to wave action. Also the elevated water level will frequently allow waves to break over longshore sandbars and place great amounts of sand in suspension. Davis et al. (1973) states that, "Although storms are somewhat infrequent and seasonal, they cause virtually all of the erosion to the coastal areas."

Davis et al. (1973) has indicated that a generalized form of the nearshore bottom topography can be used to describe most of the beach regions in the Great Lakes where bedrock is not exposed. This form can then further be used to help understand the processes of erosion due to wave action and perhaps to develop methods of reducing the erosion where desirable. In his generalized form there are two major sandbars which generally show little modification after individual storms and can be thought of as essentially permanent. They tend to migrate at a rate comparable to the migration of the shoreline. The first is generally located in about two meters of mean water depth, and the second in about three meters. Somewhat closer to the shore is an ephemeral bar which may be in about one-half meter of water. These frequently are cut through by rip channels and are of a temporary nature. They migrate rapidly and may

form at the end of one storm only to be destroyed by the next storm. The beach profile itself, shoreward of the ephemeral bar, shows two distinct forms depending on the mean water level and the relative energy of the waves. During extended periods of low water and low energy waves there is an aceration stage which produces a relatively wide beach with a pronounced berm and rather steeply inclined foreshore. During periods of high water and storm periods erosion generally results in a more uniform slope with the absence of a berm. Behind the beach there is often a coastal bluff. In many cases this is of glacial outwash and during high water-storm periods this may be oversteepened by wave action at the base. This can result in a "gravity" collapse or a downslope movement causing a significant volume loss.

The effects of erosion of shorelines along the coasts of the Great Lakes has been well documented over the past several years. The combined effects of waves and a storm surge which locally raised water levels by 60 cm during the November 13-14, 1972 storm on Lake Erie was documented to have eroded an average of 5.5 m^3/m of beach length along at least the 10 km of shoreline studied by Coakley, et al. (1973). Although storm surge is generally less prominent in Lake Ontario, there is good documentation of the erosional effects of waves both at the eastern and western ends of the lake.

A study by Coakley and Cho (1973) has been of erosion at the western end of the lake at Van Wagners Beach, at the southeastern end of the Burlington Bar. Over the past 30 years the erosion of beaches along the southern end of Burlington Bar has averaged less than 0.2 m per year and at Van Wagners Beach only about 0.1 m/yr. The bottom topography at this site contains a parallel bar about 125 meters offshore with about one meter relief. The bottom offshore from the bar slopes at between 1:95 to 1:80. The bottom sediments are quite uniform and related to the depth of the water with fine sand (± 3 phi, ϕ) in the offshore area and course sand (± - 1 phi, ϕ) at the water line. In the study by Coakley and Cho (1973) during September and October 1972 the significant wave height outside of the zone of breakers exceeded 0.3 m only 19% of the time. The observed maximum significant wave height was 1.4 m during the period studied. The significant wave period had a maximum of 5.2 seconds with a median value of 2.5 seconds. The wave steepness varied from 0.005 to 0.05. The average longshore current speed was 15 cm/sec with a recorded maximum value of 33 cm/sec. No direct evidence of rip currents was found but periodic breaks in the continuity of the outer bar suggested their presence. Due to the effects of fetch, it was found that waves large enough to produce significant erosion occurred only when winds were from the north to southeast direction. Winds less than 5.3 m/sec (12 mph) had relatively minor effects. A review of wind records from April 1969 through December 1972 in this part of the lake revealed that winds from southwest to northwest occurred 53% of the recorded period, from the east to northeast for 25% and north and south winds accounted for only 9% of the record. The high intensity winds directed onshore occurred almost exclusively in the Autumn and early Winter. The expected refraction of wave paths and the relative anticipated longshore currents for waves with

a period of 7 seconds and a wind from N65E are shown on Figure 52 for the region studied by Coakley and Cho (1973). During their study they found that the subaerial beach zone, from the waters edge to the top of the beach, was stable. There was only slight changes in the form of scouring that were noted during higher energy wave action followed by rapid recovery and accretion during more quiescent periods. The result during the study was an average net accretion of 0.55 m^3/m of beach width in this zone. After a storm on November 14, 1972 an erosion of 3.6 m^3/m was observed by Coakley and Cho (1973). After this same storm the inner and outer sandbar converged somewhat with a net erosion in the general zone of bars of 5.9 m^3/m. During the previous September and October non-storm period these had been stable and shown little change. The regular gently sloping portion of the bottom beyond the outer bar which had also been stable during the period of study prior to the storm showed an erosion of 22 m^3/m resulting in an overall lowering of this zone by about 20 cm. Coakley and Cho (1973) found that when longshore components of wave energy were compared with the profile changes, "a distinct positive relationship is noted between northwestward wave energy flux and beach accretion and the converse for southeastward energy flux."

A study was done by Cohn (1973) from October 1971 through October 1972 at the Selkirk Shores region near Pulaski, N.Y., located near the eastern end of Lake Ontario. The measurements of shoreline erosion were made over a 2 km length of shoreline from the base of the dunes to 1.25 m of mean water depth. Here exists fine-grained sand with narrow barrier beaches backed by a stabilized dune complex and marshes. The wind during this study is shown in the form of a wind rose in Figure 53. On the same diagram is a wave rose for the same period as computed by Cohn (1973) using the method of wave hindcasting described by Bretschneider (1951). Beach erosion in this area was found to be a consequence of winds from the northwest. The erosional effectiveness of these winds were enhanced by their coincidence with the major fetch as shown on the inserted map in Figure 53. Here it was found that drift along the eastern shoreline was predominantly northward. Up to 25% of the material eroded from the beach face was found to be stored temporarily in the offshore zone in the form of ephemeral bars. During periods of low wave activity these bars were found to migrate landward and eventually become welded to the beach. During this study accretion occurred in the late summer and early autumn. This coincided with lower lake levels and winds blowing from the land. The upper part of the beach was beyond direct attack and the small amplitude waves approaching the beach were constructive in that they swept sand landward. During much of the winter large areas of the lake were covered with ice. This effectively shortened the fetch. The shoreline was protected by a thick shelf of ice which terminated with an ice ridge. Incoming waves during this period were unable to affect the beach itself. Zumberge and Wilson (1953) made similar observations concerning the winter conditions. During spring and summer when high lake levels and winds from the northwest occurred Cohn (1973) observed rapid erosion. During the 12 months studied the accretion was much less than the erosion along the beach. Profiles obtained by Cohn (1973) at the beginning and end of the study period are shown in Figure 54. For the 2 km of shoreline studied the beach experienced

a net average retreat of 4.5 m landward in 12 months. 8400 m^3 or over 9×10^5 kg (1000 tons) of sediment was removed. 65% of this occurred from the subaerial portion of the beach, the remainder was removed from the submerged nearshore zone.

Modifications of coastal erosion by several man-made factors have been locally introduced. Some of these are somewhat inadvertent such as large navigational channels which are maintained by large jetties that extend approximately perpendicular from the shoreline in the vicinity of harbors. These jetties act as a dam in that they interrupt the littoral flow of sediment. By retaining sediment on the updrift side the structure reduces the amount of material received on the downdrift beaches.

Davis et al. (1973) indicates that this reduction of beaches may allow the erosion of the bluff on the downdrift side. Small jetties or Groins may be used to retain beaches. If they are isolated they may protect one area and aggrevate shoreline change in another downdrift location.

Seawalls constructed of steel piling, wood, rock, etc., are usually located directly against the face of a slumping bluff. These are not expected to establish a beach, but to protect the bluff from further recession. They generally do not interrupt the littoral movements along the coastline. As beaches are generally absent in front of the seawalls the wave action often acts directly against the wall. This results in deeper water conditions to the front of the wall than would be normally anticipated. Davis et al. (1973) indicates that shoreline changes in adjacent unprotected areas may be aggravated by the presence of these walls.

Although Cole's (1973) study of the wave pressure caused by non-breaking waves against a vertical breakwater was done in Lake Erie rather than Lake Ontario, the results appear to be applicable to the problems involved in the construction of breakwaters and seawalls in Lake Ontario. Cole (1973) compared observed values of clapotis pressure with theoretical values obtained from formulations by Sainflou and by Minikin (both formulations are treated in some detail by Minikin (1963)). His measurements were made using strain-gage pressure transducers on a breakwater and with staff wave gauges on the breakwater and on a tower 488 m (1600 ft.) from the breakwater. Figure 55 shows his results for four different wave heights plotted on a graph of height versus pressure. The wave heights are those obtained from the "undisturbed" wave prior to reaching the breakwater. Figure 56 shows three similar graphs for three of the wave heights. The graph on the left side of the figure is for pressure values computed by Sainflow's formula, the middle one for values computed by Minikin's formula, and the graph on the right side for the observed values. Cole (1973) found a marked increase in wave pressure slightly below the mean water level which could not be explained in terms of an error. This is not predicted by either of the formulations used and also was a greater pressure than the predicted maximum pressure of either formulation. Below about 0.8 m the wave pressures decreased with depth. This decrease is predicted to some extent by Sainflou's formulation but not by Minikin's. Minikin's formula

also predicted a larger wave height on the breakwater than was observed. In general the measured wave pressures more nearly support the formulation of Sainflou except for the significantly higher wave pressure which is lacking in both theories. It is apparent that further work is needed in this area before the effect of a breakwater on waves is completely understood.

Remarks

Although this monograph has summarized only what appeared to the author to be the most useful recent information concerning temporal and spatial water level changes on Lake Ontario, it is hoped that the reader interested in obtaining more detailed information concerning any of the phenomena described in this monograph will find the references helpful.

The author recognizes that much information gained from the IFYGL related studies which was not available in a form which could be used for this monograph should soon be published. The interested reader is urged to seek this new material as it becomes available.

REFERENCES

Bajorunas, L., 1960: Water level disturbances in the Great Lakes and their effect on navigation. Proceedings, Princeton University Conf. on shipping and navigation problems of the Great Lakes on the St. Lawrence Seaway.

Blackman, R.B. and J.W. Tukey, 1958: The measurement of power spectra. Dover Publ., New York.

Bretschneider, C.L., 1951: Revised wave forecasting curves and procedures. Tech. Report He: 155047. Berkeley, California, Institute of Engineering Research.

Bretschneider, C.L., 1952: Revised wave forecasting relationships. Proc. 2nd Conf. on Coastal Engineering.

Bretschneider, C.L., 1957: Revision in wave forecasting: deep and shallow water. Proc. 6th Conf. on Coastal Engineering.

Coakley, J.P. and H.K. Cho, 1973: Beach stability investigations at Van Wagners Beach, western Lake Ontario. Proc. 16th Conf. Great Lakes Research. International Assoc. Great Lakes Res.

Coakley, J.P., W. Haras, and N. Freeman, 1973: The effect of storm surge on beach erosion, Point Pelee. Proc. 16th Conf. Great Lakes Res. Internat. Assoc. Great Lakes Res.

Cohn, B.P., 1973: Accretion and erosion of a Lake Ontario beach, Selkirk Shores, New York. Proc. 16th Conf. Great Lakes Res. Internat. Assoc. Great Lakes Res.

Cole, A.L., 1973: Experimental evaluation of wave pressure formulations for non-breaking waves. Proc. 16th Conf. Great Lakes Res. Internat. Assoc. Great Lakes Res.

Davis, R.A., Jr., E. Seibel, and W.T. Fox, 1973: Coastal erosion in eastern Lake Michigan--causes and effects. Proc. 16th Conf. Great Lakes Res. Internat. Assoc. Great Lakes Res.

Defant, F., 1954: Theorie der seiches des Michigansees und ihre abwendlung durch werkung der Corioleskraft. Archro. fur Meterologie, Geophysik unk Bioklimatologie, Vol. 6.

Dohler, G., 1964: Tides in Canadian waters. Canadian Hydrographic Service Marine Science Branch, Department of Mines and Technical Surveys.

Ewing, M., F. Press, and W.L. Donn, 1954: An explanation of the Lake Michigan Wave of 26 June 1954. Science, Vol. 120, No. 3122.

Freeman, J.C. and C.C. Bates, 1954: Present status of storm sorge research in the United States of America. U.S. Navy Hyprographic Office, Division of Oceanography.

Gillies, D.K.A., 1959: Winds and water levels on Lake Erie. Royal Meteorological Society, Canadian Branch Pub., Vol. 9, No. 1.

Graham, J.D., 1860: A lunar tidal wave in Lake Michigan. American Philosophical Soc., Proc. Vol. 7.

Great Lakes Institute, 1964: Great Lakes Institute data record 1962 surveys, Part I, Lake Ontario and Lake Erie. Report PR16, Great Lakes Institute, Univ. Toronto. November, 1964.

Hamblin, P.F., 1972: Some free oscillations of a rotating natural basin. Univ. Washington, Dep. Oceanography, Ph.D. Thesis.

Harris, D.L., 1962: The equivalence between certain statistical prediction methods and linearized dynamical methods. Monthly Weather Rev., Vol. 90.

Harris, D.L., 1954: Wind, tide, and seiches in the Great Lakes. Proc. 4th Conf. Coastal Engineering.

Harris, D.L., 1957: The effect of a moving pressure disturbance on the water level in a lake. Meteorological monographs, Vol. 2, No. 10.

Harris, D.L. and A. Angelo, 1963: A regression model for storm surge prediction. Monthly Weather Rev., Vol. 91.

Harris, R.A., 1907: Manual of Tides. U.S. Coast and Geodetic Survey Report.

Hasselmann, K., 1968: Weak-interaction theory of ocean waves. Basic Developments in Fluid Dynamics, Vol. 2, Holt, Maurice (ed.). New York Academic Press.

Hellstrom, B., 1941: Wind effect on lakes and rivers. Ingen Vetensk Acad. Handl.

Hunt, I.A., Jr., 1959: Winds, wind set-ups, and seiches on Lake Erie. U.S. Lake Survey, Corps of Engrs., Res. Rept. 1-2.

Hutchinson, E.G., 1957: A treatise on limnology, Vol. 1, John Wiley & Sons, Inc., New York.

Irish, S.M. and G.W. Platzman, 1962: An investigation of the meteorological conditions associated with extreme wind tides on Lake Erie. Monthly Weather Rev., Vol. 90.

Keulegan, G.H., 1951: Wind tides in small closed channels. J. Res. Nat. Bur. Stand., Vol. 46.

Keulegan, G.H., 1953: Wind tides in small closed channels. J. Res. Nat. Bur. Stand., Vol. 46.

Kinsman, B., 1965: Wind waves. Prentice-Hall, Inc., New Jersey.

Lonquet-Higgins, M.S. and G.S. Pond, 1970: Free oscillations of a fluid on a hemisphere bounded by meridians of longitude. Phil. Trans. Roy. Soc. London, Vol. 226.

Liu, P.C., 1970: Some features of wind waves in Lake Michigan. Limnology and Oceanography, Vol. 15, No. 2.

Liu, P.C., 1972: Water motion. Great Lakes Basin Framework Study, Appendix No. 4, Limnology of lakes and embayments, Chapter 4. Draft No. 2, Volume 1. Lake Survey Center, National Oceanic and Atmospheric Administration, Detroit, Michigan 48226, Dec. 1972 (The published version of this should be available shortly - GM).

Liu, P.C., 1975: Duration-limited wave spectra in Lake Ontario during the 1972 Hurricane Agnes. Great Lakes Environmental Research Laboratory, NOAA, Ann Arbor, Mich. (unpublished manuscript).

Liu, P.C. and T.A. Kessenich: IFYGL shipboard visual wave observations versus wave measurements. Great Lakes Environmental Research Laboratory, NOAA, Ann ARbor, Mich. (unedited manuscript).

Miles, J.W., 1957: On the generation of surface waves by shore flows. J. Fluid Mech., Vol. 3.

Miles, J.W., 1960: On the generation of surface waves by turbulent shear flows. J. Fluid. Mech., Vol. 7.

Miller, G.S., 1972: Water movement in harbors. Great Lakes Basin Framework Study, Appendix No. 4, Limnology of lakes and embayments. Draft No. 2, Volume 1. Lake Survey Center, National Oceanic and Atmospheric Administration, Detroit, Michigan 48226, Dec. 1972 (The published version of this should be available shortly - GM).

Minikin, R.R., 1963: Winds, waves, and maritime structures, 2nd ed., Charles Griffin, London.

Mortimer, C.H., 1963: Frontiers in physical limnology with particular reference to long waves in rotating basins. Proc. 6th Conf. Great Lakes Res., Great Lakes Res. Div., Univ. Michigan, Pub. No. 10.

Munk, W.H., 1962: Long ocean waves. The Sea, Vol. 1, M.N. Hill (ed.), Interscience Publishers, N.Y.

Phillips, O.M., 1957: On the generation of waves by turbulent wind. J. Fluid Mech., Vol. 2.

Phillips, O.M., 1966: The dynamics of the upper ocean. Cambridge Univ. Press.

Pierson, W.J., G. Neumann and R.W. James, 1955: Practical methods for observing and forecasting ocean waves by means of wave spectra and statistics. H.O. Pub. 603, U.S. Navy Hydrog. Office.

Platzman, G.W., 1958: A numerical computation of the surge of 26 June 1954 on Lake Michigan. Geophysical, Vol. 6, No. 34.

Platzman, G.W., 1963: The dynamical prediction of wind tides on Lake Erie. Meteorological monographs, Vol. 4, No. 26.

Platzman, G.W., 1964: Spectra of Lake Erie water levels. J. Geophys. Res., Vol. 69.

Platzman, G.W., 1966: The daily variation of water level in Lake Erie. J. Geophys. Res., Vol. 71.

Platzman, G.W. and D.B. Rao, 1964: The free oscillations of Lake Erie. Studies on Oceanography (Hidaka Volume), K. Yoshida (ed.).

Proudman, J., 1916: On the dynamical theory of tides. Part II, Flat Seas. Proc. London Math. Soc., 2nd ser., Vol. 18.

Proudman, J., 1953: Dynamical Oceanography. Methuen and Co., Ltd, London.

Rao, D.B., 1965: Free gravitational oscillations in rectangular basins. Univ. Chicago, Dept. Geophys. Sci., Ph.D. Thesis.

Rao, D.B. and D.J. Schwab, 1974: Two-dimensional normal modes in arbitrary enclosed basins on a rotating earth: application to Lakes Ontario and Superior. Special report No. 19, Center for Great Lakes Studies, Univ. of Wisconsin, Milwaukee. Milwaukee, Wisc. 53201. May 1974.

Richards, T.L. and J.G. Irbe, 1969: Estimates of monthly evaporation losses from the Great Lakes 1950 to 1968 based on the mass transfer technique. Int. Assoc. Great Lakes Res., Proc. 12th Conf. Great Lakes Res.

Rockwell, D.C., 1966: Theoretical free oscillations of the Great Lakes. Proc. 9th Conf. Great Lakes Res., Univ. Mich., Great Lakes Res. Div., Publ. No. 15.

Saville, T., 1953: Wave and lake level statistics for Lake Ontario. Tech. Memo. No. 38. Beach Erosion Board, U.S. Army Corps of Engineers. Washington, D.C.

Saylor, J.H., 1964: Survey of Lake Michigan hrabor currents. Proc. 7th Conf. Great Lakes Res. Internat. Assoc. Great Lakes Res.

Saylor, J.H., 1966: Modification of nearshore current by coastal structures. Proc. 1966 Army Science Conf.

Simpson, R.B. and D.V. Anderson, 1964: The periods of the longitudinal surface seiche of Lake Ontario. Proc. 7th Conf. on Great Lakes Res. Publ. No. 11, Great Lakes Res. Div., Univ. of Mich.

St. Lawrence-Eastern Ontario Commission, 1975: Lake Ontario and the St. Lawrence River: analysis and recommendations concerning high water levels. State of New York St. Lawrence-Eastern Ontario Commission, 317 Washington St., Watertown, N.Y. 13601. March 1975.

Sverdrup, H.V. and W.H. Munk, 1947: Wind, sea and swell; theory of relations for forecasting. H.O. Publ. 601, U.S. Navy Hydrog. Office.

Veber, J.L., 1960: Long and short period oscillations in Lake Erie. Ohio Dept. Nat. Res., Div. Shore Erosion.

Zumberge, S.H. and J.T. Wilson, 1953: Effect of ice on shore development. Proc. 4th Conf. Coastal Engineering. Univ. California Press, Berkley, California.

FIGURE CAPTIONS

Figure 1 Classification of waves by frequency.

Figure 2 Hourly water levels at three stations on Lake Ontario during first half of June 1972.

Figure 3 Hourly water levels at three stations on Lake Ontario during second half of June 1972.

Figure 4 Mean monthly water levels of Lake Ontario for the period from July 1971 through June 1974.

Figure 5 Mean annual water level of Lake Ontario at Oswego, N.Y. since 1861.

Figure 6 Cumulative difference in mean annual water level observed at Oswego and Rochester, N.Y. versus time. Least squares linear regression lines are fit to the data points for the period 1869-1883 and 1883-1907.

Figure 7 Relative uplift of the Lake Ontario region with time. Contours in feet rise per century.

Figure 8 Elevation of Lake Ontario at Oswego, N.Y. versus the discharge of the St. Lawrence River at the International Rapids section. Mean monthly values are plotted for the years 1861 through 1858.

Figure 9 Rating curves for the St. Lawrence River at International Rapids section with respect to lake levels measured at Oswego, N.Y. Mean monthly values used for data points. Curves obtained by using least squares geometric fit to data points for the periods 1861-1899, 1900-1958, and 1861-1958.

Figure 10 Mean of reduced hourly water levels during month versus hour of day. Water levels for Toronto, Ontario during 1959. Curves represent best fit using least squares regression to a sine curve. Lunar tide component obtained by using means plus superposition of 12 hour Fourier component.

Figure 11 Average of reduced water levels versus hours of day to show effect of solar component of tide at Toronto, Ontario during 1959.

Figure 12 Average of reduced water levels versus hours of day for May 1958, Oswego, N.Y. and November 1958, Port Weller, Ontario.

Figure 28 Computed fluctuation of free surface height for first mode of oscillation considering earth's rotation. Solid lines represent cotidal lines and dashed lines represent co-range lines.

Figure 29 Computed fluctuation of free surface height for second mode of oscillation considering earth's rotation. Solid lines represent cotidal lines and dashed lines represent co-range lines.

Figure 30 Computed fluctuation of free surface height for third mode of oscillation considering earth's rotation. Solid lines represent cotidal lines and dashed lines represent co-range lines.

Figure 31 Computed fluctuation of free surface height for fourth mode of oscillation considering earth's rotation. Solid lines represent cotidal lines and dashed lines represent co-range lines.

Figure 32 Computed fluctuation of free surface height for fifth mode of oscillation considering earth's rotation. Solid lines represent cotidal lines and dashed lines represent co-range lines.

Figure 33 Computed fluctuation of free surface height for sixth mode of oscillation considering earth's rotation. Solid lines represent cotidal lines and dashed lines represent co-range lines.

Figure 34 Computed streamlines of mass transport for rotational mode with 229 hour period at a phase angle of 0.

Figure 35 Computed streamlines of mass transport for rotational mode with 229 hour period at a phase angle of $\pi/2$.

Figure 36 Computed streamlines of mass transport for rotational mode with 464 hour period at a phase angle of 0.

Figure 37 Computed streamlines of mass transport for rotational mode with 464 hour period at a phase angle of $\pi/2$.

Figure 38 Location of wave rider buoys used by Liu and Kessenich (1975) for analysis of Lake Ontario gravity waves.

Figure 39 Significant wave heights recorded at one wave rider buoy versus significant wave heights recorded at a second wave rider buoy. The dashed line indicates the line $x = y$ that the data would be expected to follow if significant wave heights were the same at both stations. The solid lines is the best fit obtained by least squares linear regression. The equation below each graph refers to this line. r is the correlation coefficient.

Figure 40 Average wave period recorded at one wave rider buoy versus average wave period recorded at a second wave rider buoy. The dashed line indicates the line x = y that the data would be expected to follow if the average periods were the same at both stations.

Figure 41 Recorded versus observed significant wave height on Lake Ontario.

Figure 42 Recorded versus observed average wave period on Lake Ontario.

Figure 43 Percent of time a given significant wave height was exceeded from wave rider buoy measurements of Liu and Kessenich (1975) and by shipboard visual observation.

Figure 44 Percent of time a given average wave period was exceeded from wave rider buoy measurements of Liu and Kessenich (1975) and by shipboard visual observation.

Figure 45 Scatter plot of shipboard observations of wave heights versus periods. The numbers represent number of points. Dotted lines represent contours of frequency of occurrence. Dashed lines represent steepness of waves.

Figure 46 Scatter plot of recorded significant wave height versus average zero crossing wave periods. The numbers represent the number of points. Dotted lines represent contours of frequency of occurrence. Dashed lines represent steepness of waves.

Figure 47 Significant wave heights from Oswego I and II wave rider buoys and Great Lakes Institute shipboard data versus wind speed. Line represents best fit by least squares linear regression. r is the correlation coefficient.

Figure 48 Significant wave heights from station just lakeward breaking waves off Van Wagners beach versus wind speed. The three lines represent best fit by least squares linear regression to data points with three different ranges of fetch. r is the correlation coefficient.

Figure 49 Representation of actual wave profile as the sum of 14 sinusoidal component waves. The relative energy density spectrum for a wave profile formed from the 14 sinusoidal waves shown on the left side of the figure is represented on the right side of the figure.

Figure 50 Relative energy density spectrum versus frequency plotted for an episode of wave growth.

Figure 51 Wind speed and direction and frequency of waves versus time for the storm of June 22-23, 1972 at wave rider buoy Oswego I. The upper diagram of time versus frequency is contoured in terms of relative spectral energy density.

Figure 52 Computed refraction of wave paths initially from N65E near Van Wagners beach, Lake Ontario.

Figure 53 Wind rose and hindcasted wave rose obtained by Cohn (1973) for October 1972-October 1972 at Selkirk Shores region of Lake Ontario near Pulaski, N.Y. Insert map shows fetch for several directions of wind.

Figure 54 Beach profiles at Selkirk Shores region of Lake Ontario for October 1971 and October 1972.

Figure 55 Clapotis wave pressure vs. height on a vertical breakwater for four different wave heights measured by Cole (1973).

Figure 56 Clapotis wave pressure vs. height on a vertical breakwater for three wave heights. Left graph is for computed values using Sainflou's method. Center graph is for computed values using minikin's method. The right graph is for values measured by Cole (1973).

APPENDIX I

The linearized, vertically integrated hydrodynamic equations of motion often used in theoretical seiche studies take the form

$$\frac{\partial(hu)}{\partial t} - fhv = -gh\,\frac{\partial n}{\partial x} - \frac{h}{\rho}\,\frac{\partial p}{\partial x} + \frac{1}{\rho}\,(\tau_{x_s} - \tau_{x_b}),$$

$$\frac{\partial(hv)}{\partial t} - fhu = -gh\,\frac{\partial n}{\partial y} - \frac{h}{\rho}\,\frac{\partial p}{\partial y} + \frac{1}{\rho}\,(\tau_{y_s} - \tau_{y_b}),$$

and

$$\frac{\partial n}{\partial t} + \frac{\partial(hu)}{\partial x} + \frac{\partial(hv)}{\partial y} = \zeta$$

where x and y are horizontal rectangular coordinates,
u and v are the corresponding velocity components,
ρ is the density of water,
p is the atmospheric pressure,
h is the depth of the lake,
g is the acceleration of gravity,
τ_{x_s} and τ_{y_s} are the horizontal components of surface stress,
τ_{x_b} and τ_{y_b} are the horizontal components of bottom stress,
f is the coriolis parameter,
and h is the height of the free water surface above the mean lake level.

These equations are the basic equations applicable to the processes of a long period wave, already incorporating the usual long wave assumptions. When obtaining the one-dimensional channel equations from these the external forces and earth's rotation are neglected, yielding

$$\frac{\partial(hu)}{\partial t} + gh\,\frac{\partial n}{\partial x} = 0,$$

and

$$\frac{\partial(hu)}{\partial x} + \frac{\partial n}{\partial t} = 0,$$

which upon cross differentiation produces the equation of continuity in the form

$$\frac{\partial}{\partial x}\left\{h\,\frac{\partial n}{\partial x}\right\} - \frac{1}{g}\,\frac{\partial^2 n}{\partial t^2} = 0$$

When harmonic oscillations of the free surface is assumed

$$\frac{d}{dx}\left[h\,\frac{dn}{dx}\right] + \frac{\omega^2}{g}\,n = 0,$$

where ω is the angular velocity or the oscillation frequency multiplied by 2π.

APPENDIX II

The general method used by Rao and Schwab (1974) in developing the two-dimensional rotating model for seiche in Lake Ontario represents an interesting application of Proudman's (1916) procedure in a discretised form. This method has recieved rather limited attention in the past but represents a reasonable approach to modeling seiche with the aid of modern computing machines. For this reason the author has chosen to include a brief summary of the method as this appendix.

The method is concerned with the quasi-static (or shallow water) dynamics of an incompressible fluid on a rotating Cartesian plane with a local Coriolis parameter defined as

$$f = 2\,\Omega \sin\theta$$

where Ω is the angular rotational speed of the earth,
and θ is the latitude angle.

The velocity, V, is represented by components u, and v in the x and y directions respectively. Although the x-axis is normall aligned with the long axis of lake, for Lake Ontario this results in the x-axis being almost toward the east and the y-axis being almost toward the north.

The linearized shallow water equations can be written in terms of a transport-vector $\vec{M}$ as

$$\frac{\partial \vec{M}}{\partial t} = -f\,[\vec{M}] = -g\bar{H}h\nabla\eta$$

and

$$\frac{\partial \eta}{\partial t} + \nabla\cdot\vec{M} = 0.$$

In these equations the transport-vector, $\vec{M}$, is equivalent to $H\vec{V}$, where H is the depth of fluid in equilibrium and is a function of x and y. η represents a departure of the water level from the mean. g denotes the gravitational force per unit mass. $\bar{H}$ represents some constant depth and h is a dimensionless depth parameter such that

$$h \equiv H/\bar{H}$$

As these equations are for a plane the ∇ operator is considered as the horizontal gradient operator and the brackets, [], represent a rotation of a vector through a right angle in the clockwise direction on the horizontal plane.

Since one is dealing with an enclosed basin the adiabatic boundary condition at the shoreline is

$$\vec{M}\cdot\hat{n} = h\vec{V}\cdot\hat{n} = 0,$$

where $\hat{n}$ is the unit normal drawn outward from the shoreline.

One could now seek harmonic solutions in time in the form $e^{i\omega t}$, where ω is the angular frequency of oscillation.

The approach which might seem most straightforward would be the elimination of two of the dependent variables (the transport components) in terms of η. Although such an approach would result in single equation with relatively simple boundary conditions, it was not chosen by Rao and Schwab (1974) due to difficulties that would be introduced in the resulting eigenvalue problem by ω appearing both in the boundary conditions and in the tidal operator. They chose instead to follow Proudman's (1916) general method and attack the equations in their primitive form.

The general method of solution assumes that the transport vector $\vec{M}$ is independent of depth and may be separated into two parts, $\vec{M}^{\phi}$ and $\vec{M}^{\Psi}$, such that $\vec{M} = \vec{M}^{\phi} + \vec{M}^{\Psi}$.

$\vec{M}^{\phi}$ is defined as $-h\nabla\phi$ and $\vec{M}^{\Psi}$ as $-[\nabla\Psi]$ where ϕ is the scalar potential function for the transport field and Ψ is the stream function. As $\vec{M}^{\Psi}$ is the solenoidal part of $\vec{M}$ and $h^{-1}\vec{M}^{\phi}$ is the irrotational part, $\nabla\cdot\vec{M}^{\Psi} = 0$ and $\nabla\cdot[h^{-1}\vec{M}^{\phi}] = 0$.

The boundary condition $\vec{M}\cdot\hat{n} = 0$ is satisfied if $\vec{M}^{\phi}\cdot\hat{n} = 0$ and $\vec{M}^{\Psi}\cdot\hat{n} = 0$, or in terms of the stream function and potential

$$h\frac{\partial\phi}{\partial n} = 0, \quad \Psi = 0 \quad \text{at the boundary.}$$

To proceed to determine $\vec{M}$ one now examines the divergence of the mass field and the vorticity of the velocity field,

$$\nabla\cdot h\nabla\phi = -\nabla\cdot\vec{M},$$

and

$$\nabla\cdot h^{-1}\nabla\Psi = \nabla\cdot[h^{-1}\vec{M}].$$

Although $\vec{M}$ is an unknown, it satisfies the dynamical equations so the procedure is now to convert the governing equations into conditions on ϕ and Ψ and reconstruct $\vec{M}$ in terms of $\vec{M}^{\phi}$ and $\vec{M}^{\Psi}$. A method which may be used for this purpose is to represent ϕ and Ψ in terms of the spectra of the elliptic operators which appear in the above equations for the divergence of the mass field and the vorticity of the velocity field.

$$\nabla\cdot h\nabla\phi_{\alpha} = \lambda_{\alpha}\phi_{\alpha}, \quad h\frac{\partial\phi_{\alpha}}{\partial n} = 0 \quad \text{at the boundary}$$

and

$$\nabla\cdot h^{-1}\nabla\Psi_{\alpha} = -\mu_{\alpha}\Psi_{\alpha}, \quad h^{-1}\Psi_{\alpha} = 0 \quad \text{at the boundary.}$$

α represents a binary index used for the enumeration of the spectral components.

λ_{α} and μ_{α} are characteristic values which are real and the associated functions ϕ_{α} and Ψ_{α} each form a complete and internally orthogonal set. The orthogonality condition may be chosen as:

$$\int h^{-1}\underset{\sim}{M}_\alpha^\phi \cdot \underset{\sim}{M}_\beta^\phi dA = \lambda_\alpha \int \phi_\alpha \phi_\beta dA = AC^2\bar{H}^2\delta_{\alpha\beta}$$

$$\int h^{-1}\underset{\sim}{M}_\alpha^\Psi \cdot \underset{\sim}{M}_\beta^\Psi dA = \mu_\alpha \int \Psi_\alpha \Psi_\beta dA = AC^2\bar{H}^2\delta_{\alpha\beta}$$

Here C^2 is defined as $g\bar{H}$ and A is the surface area of the basin. $\delta_{\alpha\beta}$ is 1 if $\alpha = \beta$ and 0 if $\alpha \neq \beta$. In accordance with our manner of partitioning $\underset{\sim}{M}$,

$$\underset{\sim}{M}_\alpha^\phi \equiv -h\nabla\phi_\alpha$$

and

$$\underset{\sim}{M}_\alpha^\Psi \equiv -[\nabla\Psi_\alpha].$$

The non-dimensional expansion coefficients P_α and Q_α used to represent $\underset{\sim}{M}^\phi$ and $\underset{\sim}{M}^\Psi$ can be defined as

$$P_\alpha \equiv \frac{1}{C^2A\bar{H}^2}\int h^{-1}\underset{\sim}{M}_\alpha^\phi \cdot \underset{\sim}{M}^\phi dA = \frac{1}{C^2A\bar{H}^2}\int h^{-1}\underset{\sim}{M}_\alpha^\phi \cdot \underset{\sim}{M} dA,$$

and

$$Q_\alpha \equiv \frac{1}{C^2A\bar{H}^2}\int h^{-1}\underset{\sim}{M}_\alpha^\Psi \cdot \underset{\sim}{M}^\Psi dA = \frac{1}{C^2A\bar{H}^2}\int h^{-1}\underset{\sim}{M}_\alpha^\Psi \cdot \underset{\sim}{M} dA.$$

With the orthogonality condition chosen the sums

$$\underset{\sim}{M}^\phi = \sum_\alpha P_\alpha \underset{\sim}{M}_\alpha^\phi$$

and

$$\underset{\sim}{M}^\Psi = \sum_\alpha Q_\alpha \underset{\sim}{M}_\alpha^\Psi$$

spanning the complete spectra are least squares approximations of $\underset{\sim}{M}^\phi$ and $\underset{\sim}{M}^\Psi$.

To obtain a representation of the height field η one may define $\eta_\alpha \equiv C^{-1}(\lambda_\alpha)^{\frac{1}{2}}\phi_\alpha$, as η is governed by the divergent part of $\underset{\sim}{M}$ and hence ϕ_α form a sufficient basis for η. $\int \eta_\alpha\eta_\beta dA = AH^{-2}\delta_{\alpha\beta}$ describes the orthonormality among the η_α. Letting R_α be the expansion coefficients for the η-field,

$$R_\alpha = \frac{1}{A\bar{H}^2}\int \eta_\alpha \eta dA, \text{ then } \eta = \sum_\alpha R_\alpha \eta_\alpha.$$

Spectral prediction equations can be obtained by substituting the expansion sums for $\underset{\sim}{M}^\phi$, $\underset{\sim}{M}^\Psi$, and η into the dynamical equations yielding

$$\frac{dP_\alpha}{dt} - \sum_\beta A_{\alpha\beta}P_\beta - \sum_\beta B_{\alpha\beta}Q_\beta - \nu_\alpha R_\alpha = 0,$$

$$\frac{dQ_\alpha}{dt} - \sum_\beta C_{\alpha\beta}P_\beta - \sum D_{\alpha\beta}Q_\beta = 0,$$

and $$\frac{dR_\alpha}{dt} + \nu_\alpha P_\alpha = 0,$$

where $\nu_\alpha \equiv (C^2\lambda_\alpha)^{\frac{1}{2}}$, the frequency of oscillations in the non-rotating case (f=0),

$$A_{\alpha\beta} \equiv \{\overleftarrow{M}^{\phi}_{\alpha}, [\overleftarrow{M}^{\phi}_{\beta}]\},\ B_{\alpha\beta} \equiv \{\overleftarrow{M}^{\phi}_{\alpha}, [\overleftarrow{M}^{\Psi}_{\beta}]\},$$
$$C_{\alpha\beta} \equiv \{\overleftarrow{M}^{\Psi}_{\alpha}, [\overleftarrow{M}^{\phi}_{\beta}]\},\ \text{and}\ D_{\alpha\beta} \equiv \{\overleftarrow{M}^{\Psi}_{\alpha}, [\overleftarrow{M}^{\Psi}_{\beta}]\}.$$

The notation $\{\overleftarrow{A}, \overleftarrow{B}\} \equiv \frac{1}{C^2AH^2}\int fh^{-1}\overleftarrow{A}\cdot\overleftarrow{B}dA.$

It is necessary in working towards a solution of the above spectral-dynamical equations to order the wave number vector index α with respect to a single scalar index. If such indices are indicated by i and j, then letting $P_i \equiv P_{\alpha i}$, $Q_i \equiv Q_{\alpha i}$, $R_i \equiv R_{\alpha i}$, and $\nu_i \equiv \nu_{\alpha i}$ the column vectors can be defined as $\bar{P} \equiv \mathrm{col}(P_i)$, $\bar{Q} \equiv \mathrm{col}(Q_i)$, $\bar{R} \equiv \mathrm{col}(R_i)$ and

$$\bar{S} \equiv \begin{pmatrix} \bar{P} \\ \bar{Q} \\ \bar{R} \end{pmatrix}.$$

If matrices are defined as $A \equiv [A_{ij}]$, $B \equiv [B_{ij}]$, $C \equiv [C_{ij}]$, $D \equiv [D_{ij}]$ and $\langle\nu\rangle \equiv$ diagonal ν_i, the spectral-dynamical equations may be written in the form

$$\frac{d\bar{S}}{dt} + \xi\bar{S} = 0$$

where ξ is defined as

$$\xi \equiv \begin{bmatrix} -A & -B & -\langle\nu\rangle \\ -C & -D & 0 \\ \langle\nu\rangle & 0 & 0 \end{bmatrix}$$

If a solution is sought where $\bar{S} \sim e^{i\omega t}$, then

$$i\omega\bar{S} + \xi\bar{S} = 0$$

or using the identity matrix π,

$$(\omega\pi - i\xi)\ \bar{S} = 0.$$

This indicates that ω represents characteristic values of the matric $i\xi$ and since this matrix has Hermitian symmetry the values of ω are real. These values of ω represent the angular frequencies of free oscillation of the basin considered. Rao and Schwab (1974) determined these

frequencies by a numerical procedure after choosing an appropriate size for truncation of the matrix. The associated eigenvectors $\bar{S}$ could be computed yielding the structure of the various normal modes of oscillation. To apply this to the Lake Ontario basin numerical methods using a finite difference system were applied to construct the orthogonal functions.

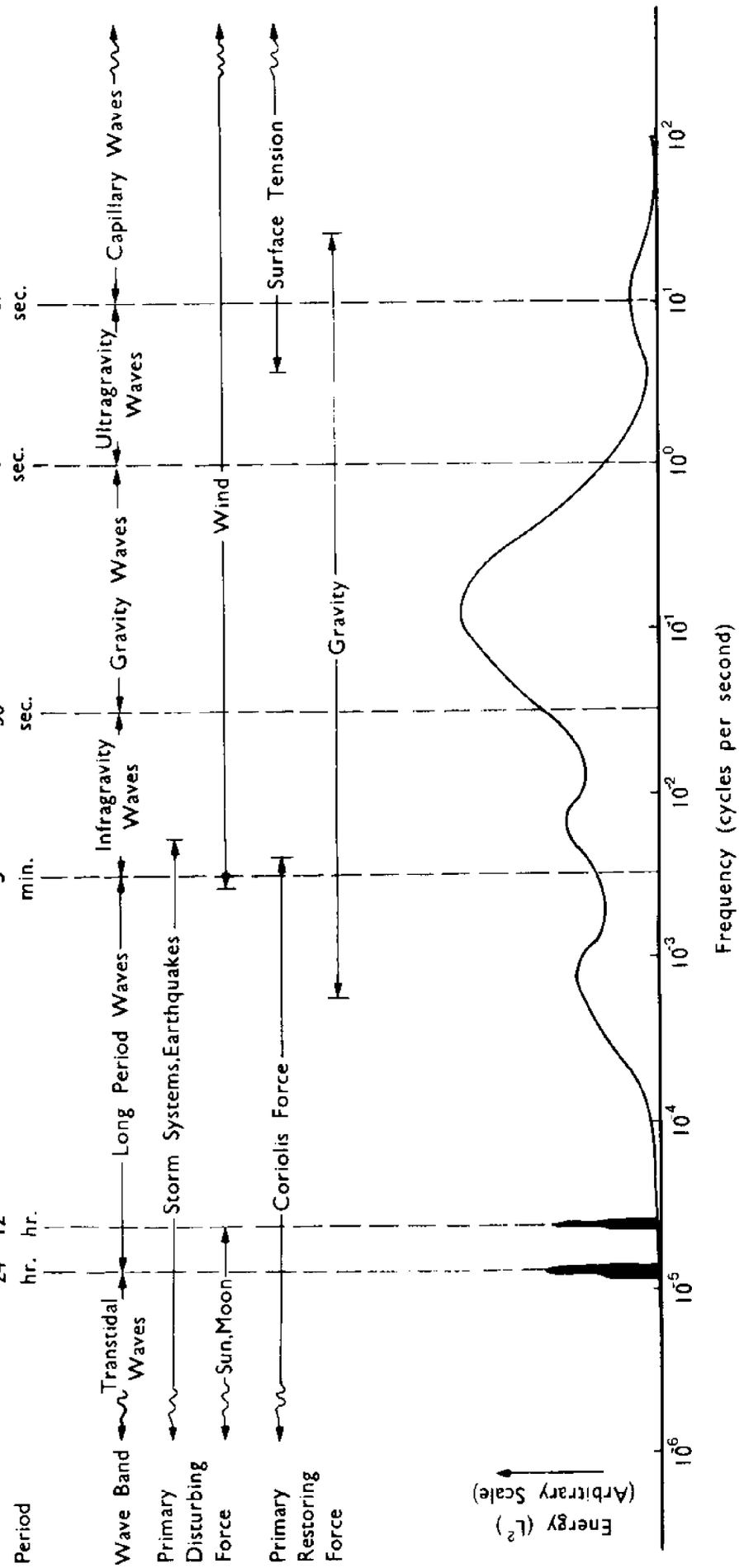

Figure 1 Classification of waves by frequency.

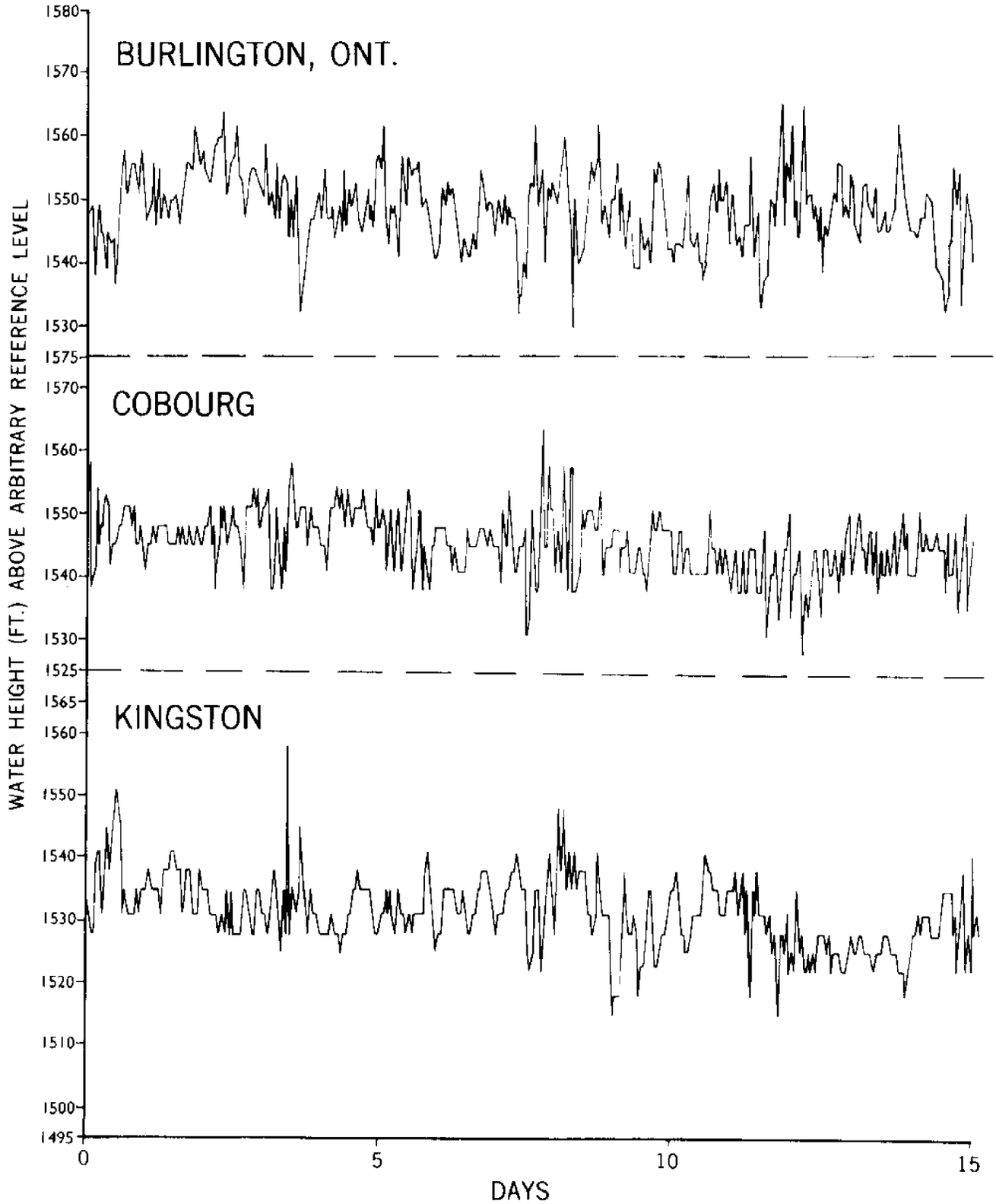

Figure 2 Hourly water levels at three stations on Lake Ontario during first half of June 1972.

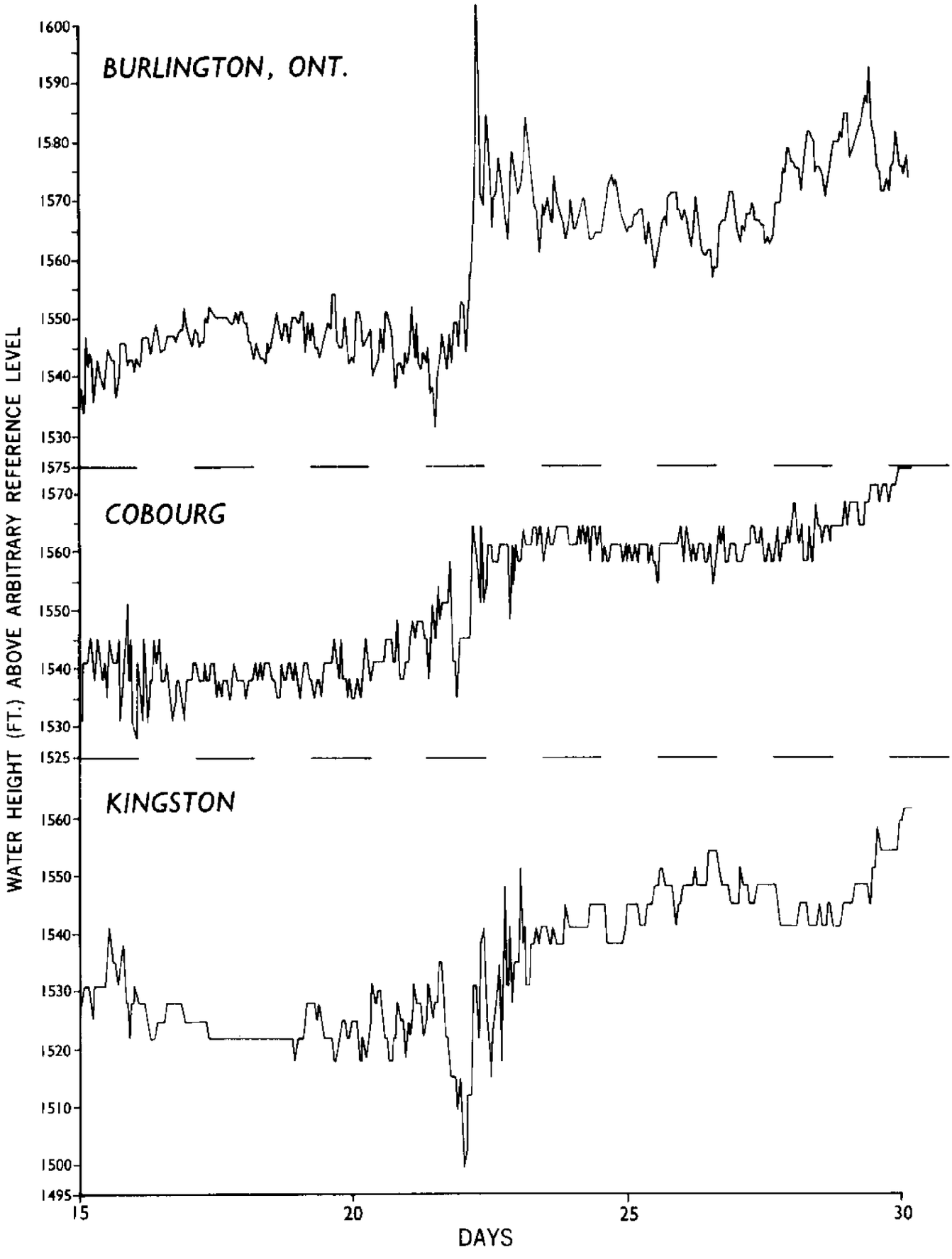

Figure 3 Hourly water levels at three stations on Lake Ontario during second half of June 1972.

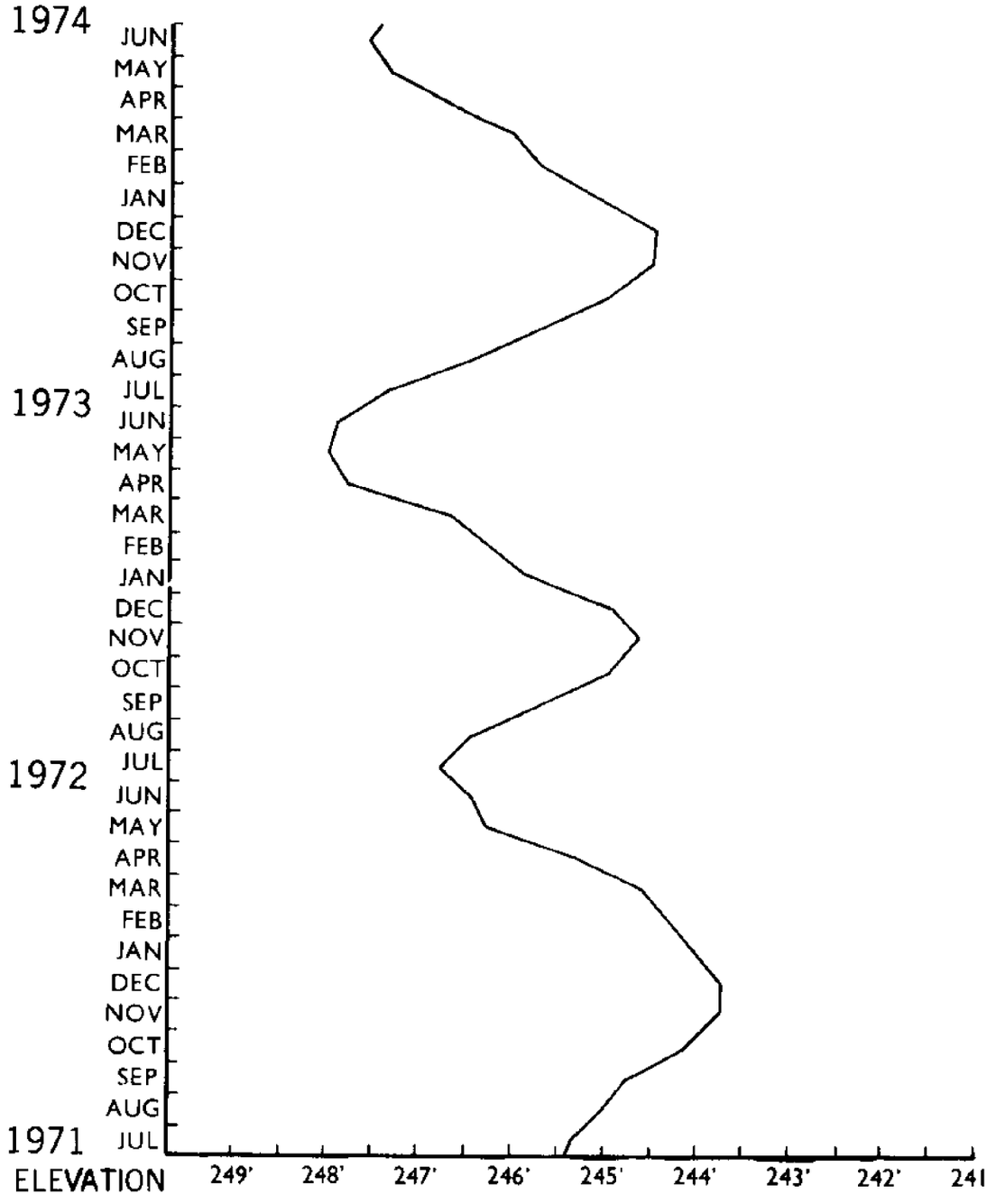

Figure 4 Mean monthly water levels of Lake Ontario for the period from July 1971 through June 1974.

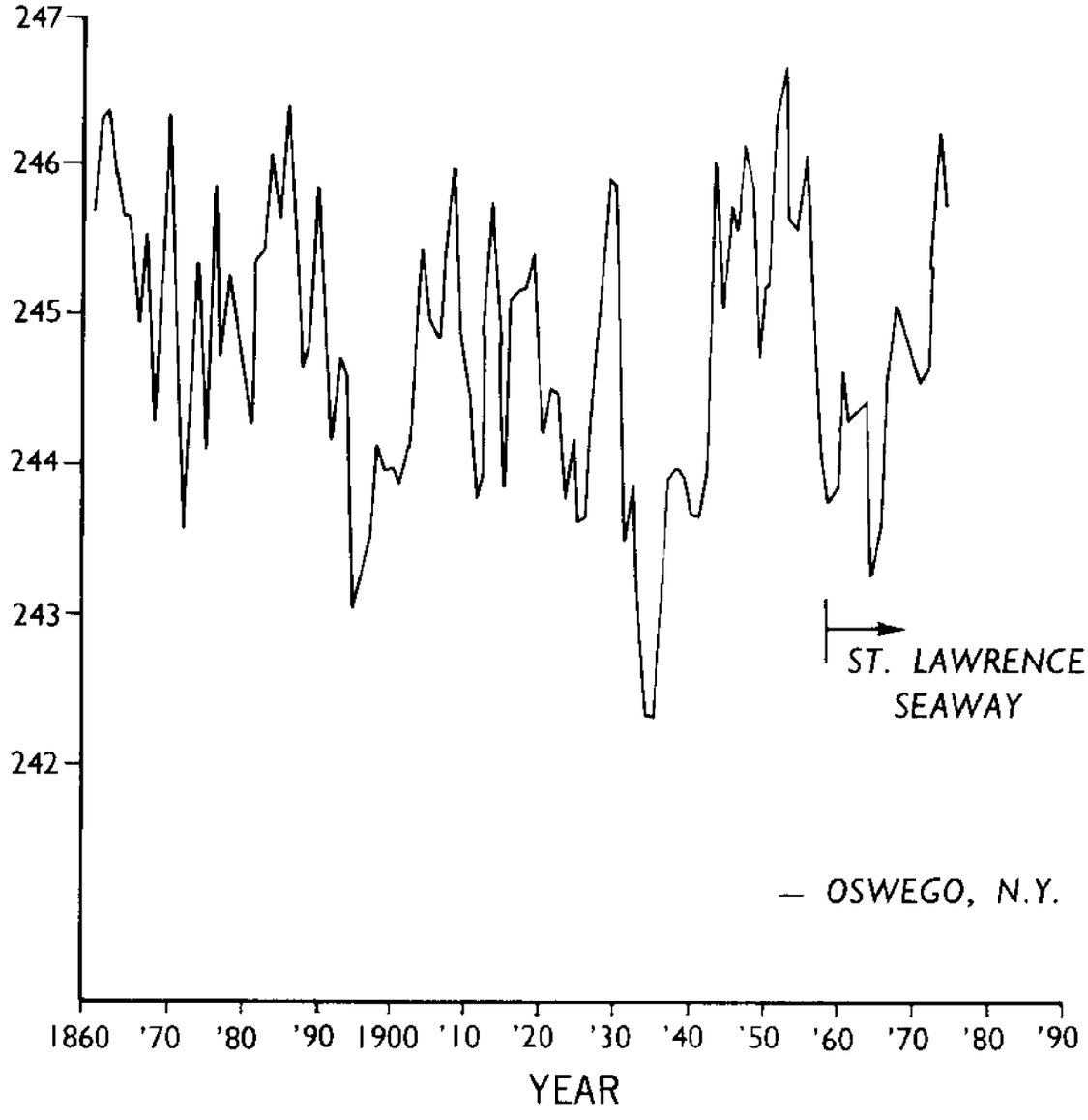

Figure 5 Mean annual water level of Lake Ontario at Oswego, N.Y. since 1861.

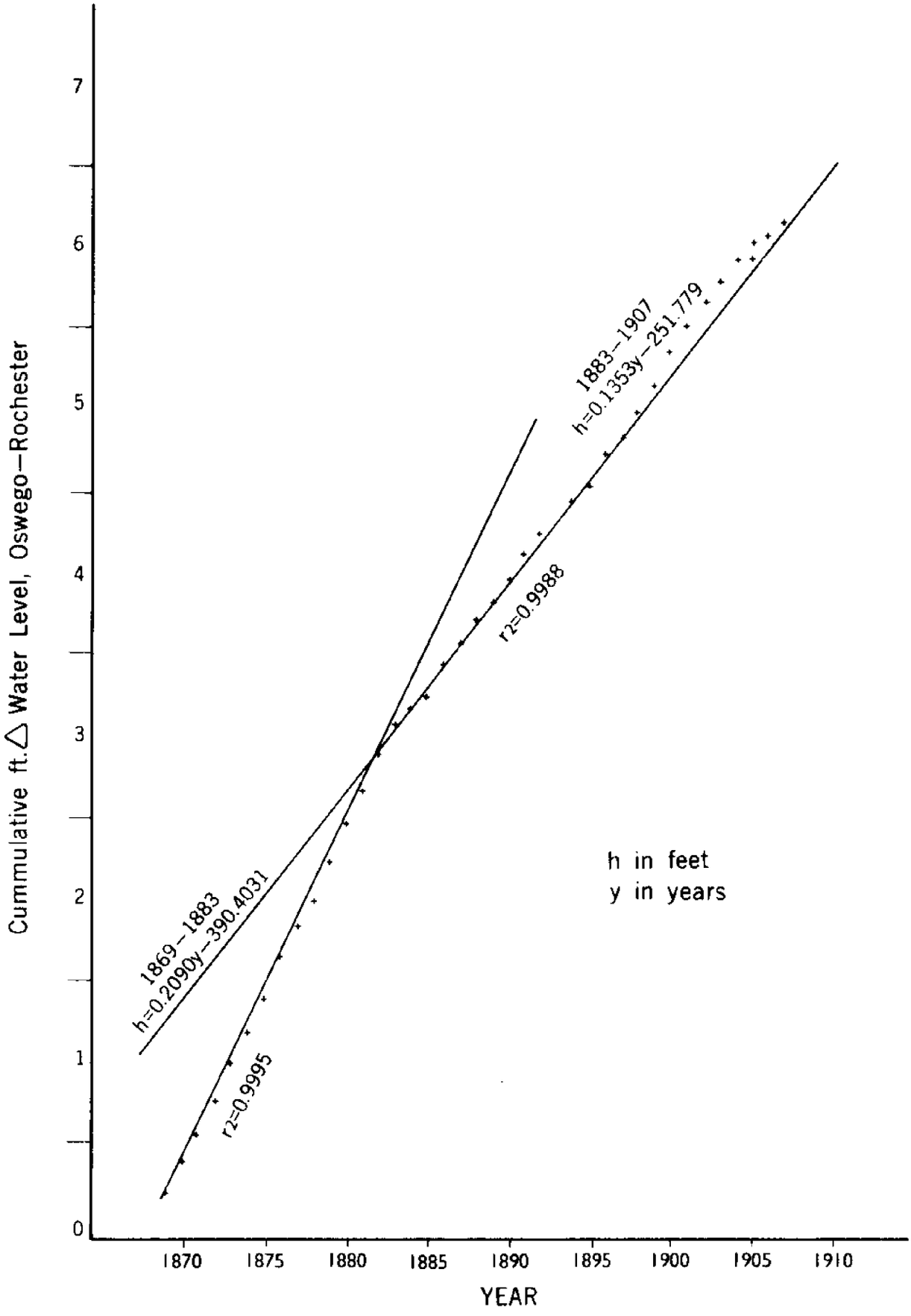

Figure 6 Cumulative difference in mean annual water level observed at Oswego and Rochester, N.Y. versus time. Least squares linear regression lines are fit to the data points for the period 1869-1883 and 1883-1907.

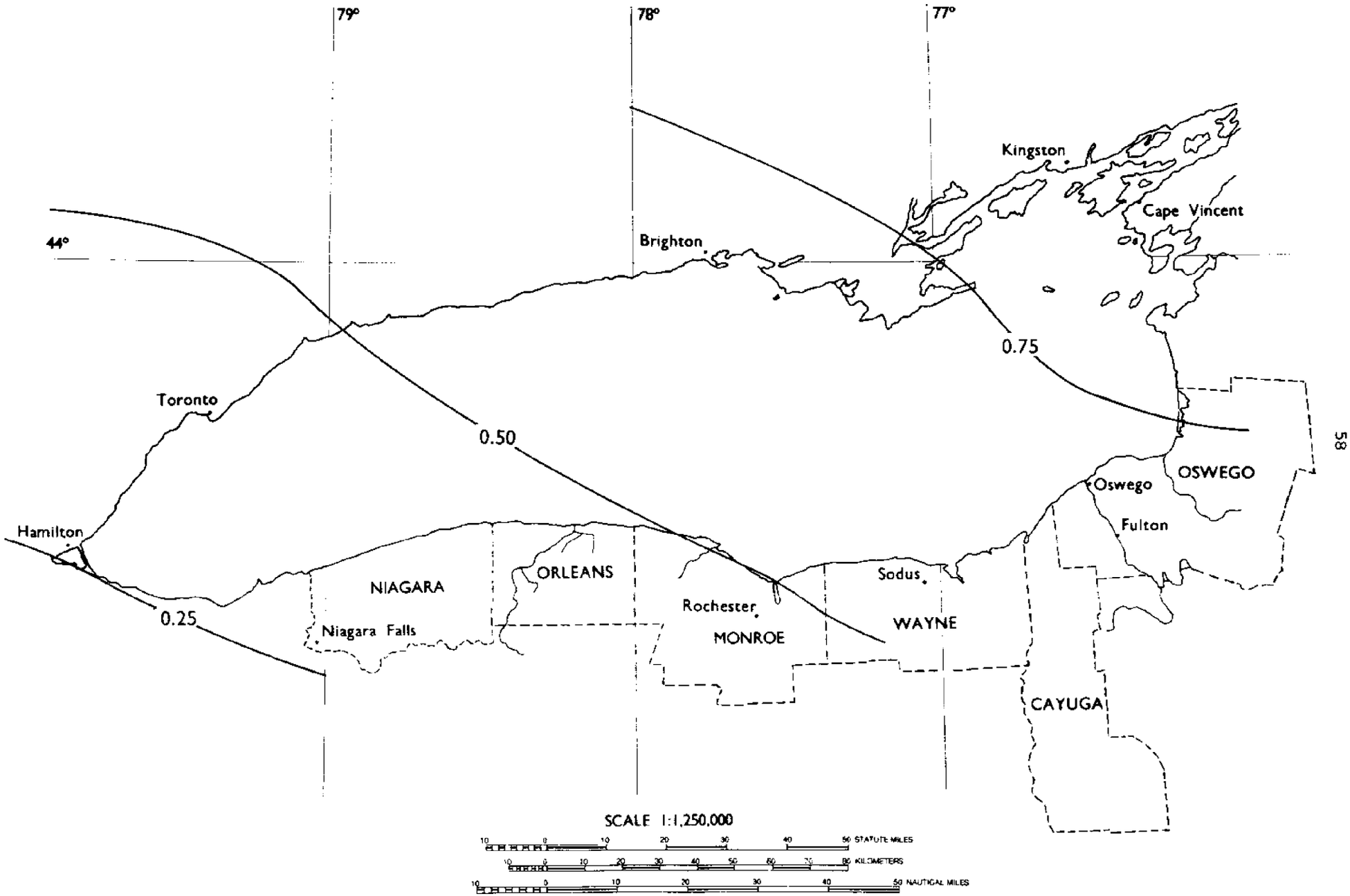

Figure 7 Relative uplift of the Lake Ontario region with time. Contours in feet rise per century.

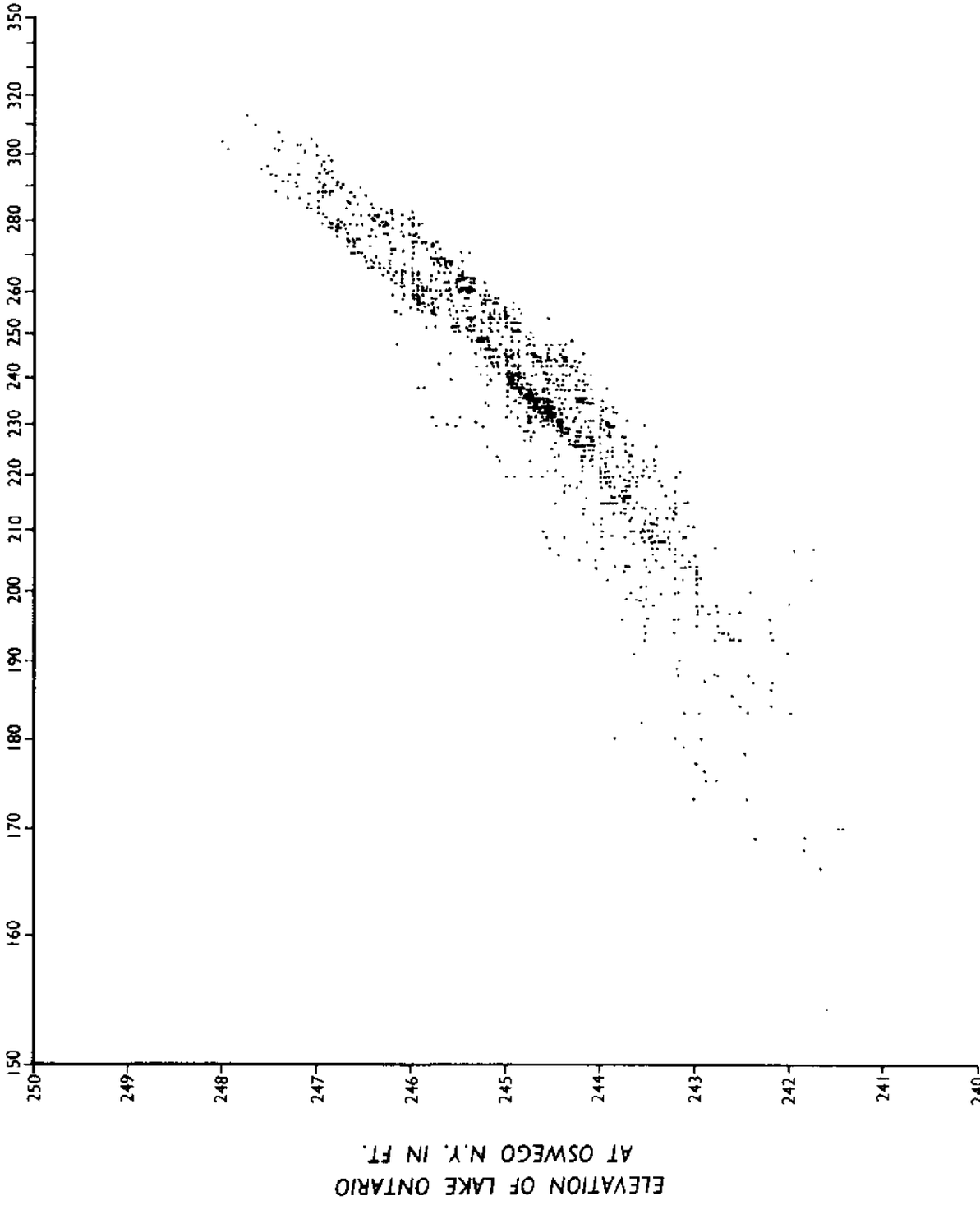

Figure 8 Elevation of Lake Ontario at Oswego, N.Y. versus the discharge of the St. Lawrence River at the International Rapids section. Mean monthly values are plotted for the years 1861 through 1858.

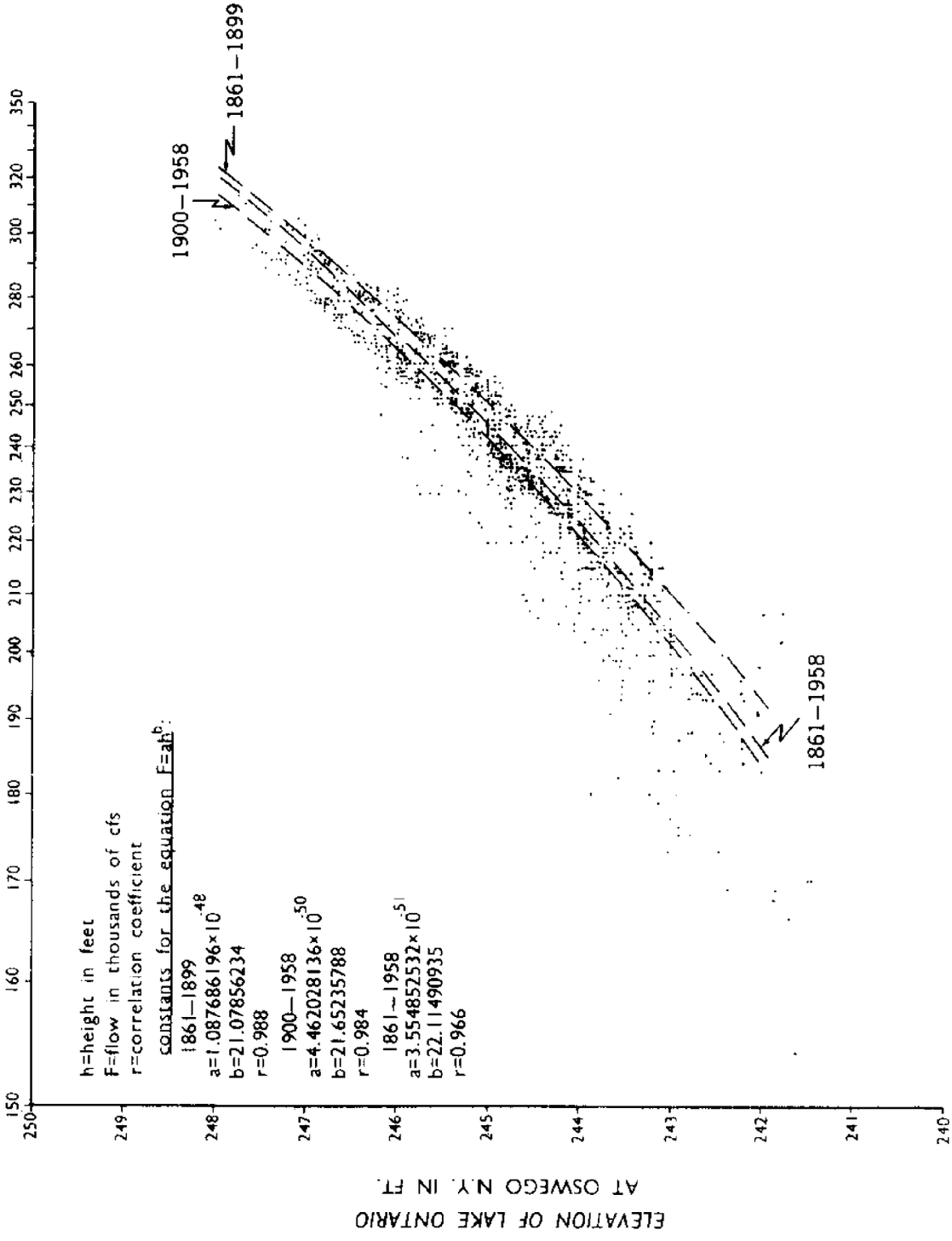

Figure 9 Rating curves for the St. Lawrence River at International Rapids section with respect to lake levels measured at Oswego, N.Y. Mean monthly values used for data points. Curves obtained by using least squares geometric fit to data points for the periods 1861-1899, 1900-1958, and 1861-1958.

MOON TIDE—TORONTO 1959

Means Plus Superposition of 12 Hour Fourier Component

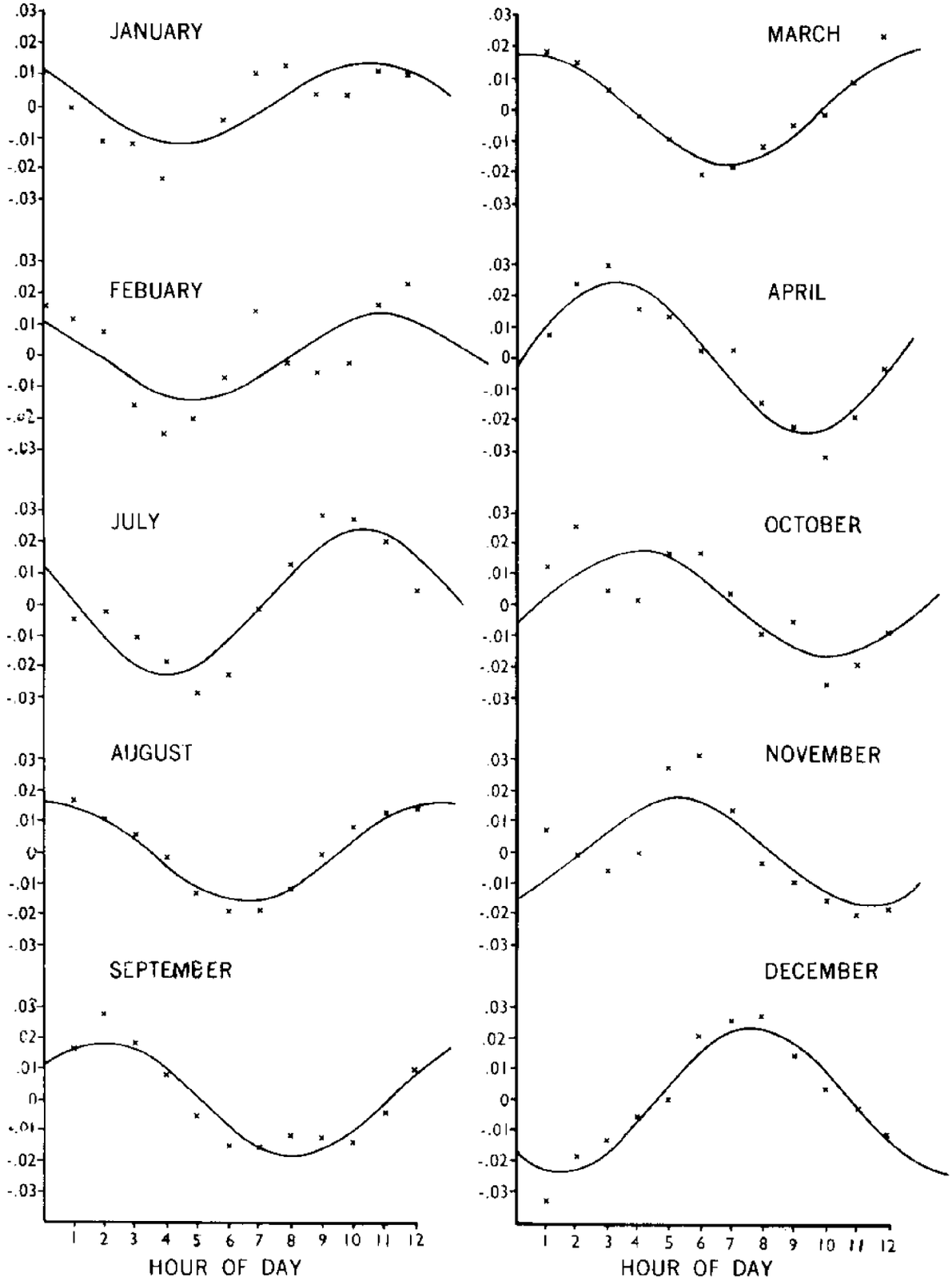

Figure 10 Mean of reduced hourly water levels during month versus hour of day. Water levels for Toronto, Ontario during 1959. Curves represent best fit using least squares regression to a sine curve. Lunar tide component obtained by using means plus superposition of 12 hour Fourier component.

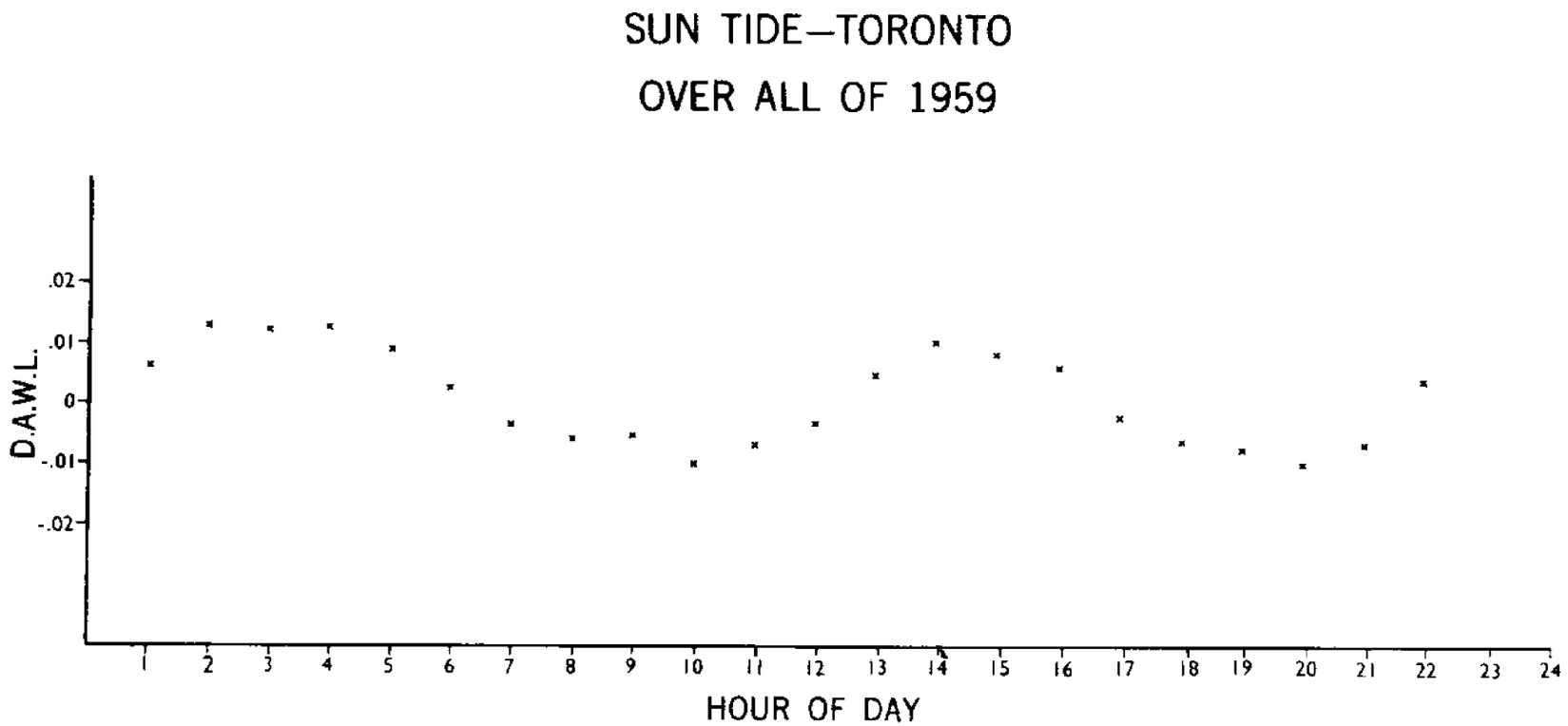

Figure 11 Average of reduced water levels versus hours of day to show effect of solar component of tide at Toronto, Ontario during 1959.

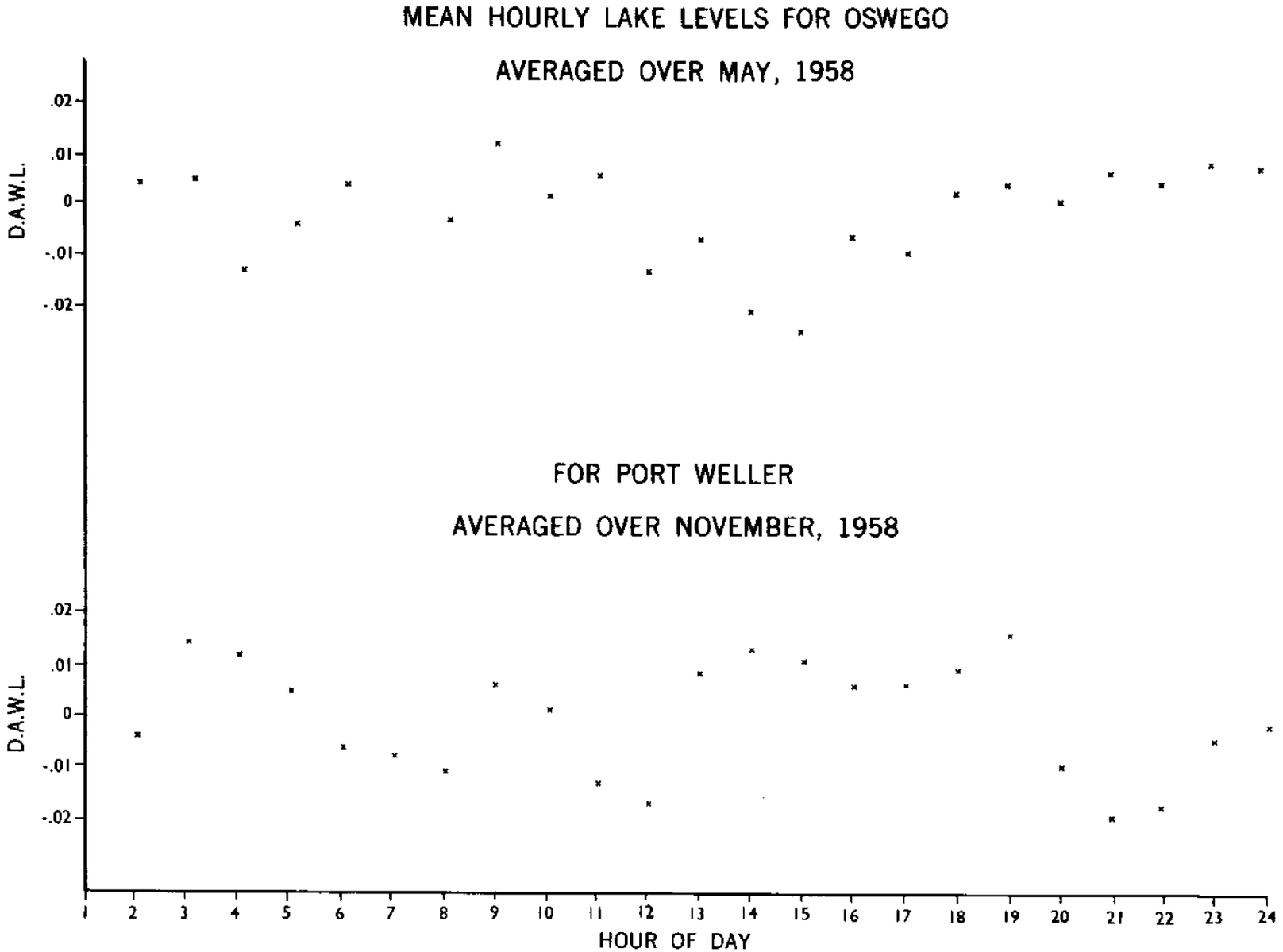

Figure 12 Average of reduced water levels versus hours of day for May 1958, Oswego, N.Y. and November 1958, Port Weller, Ontario.

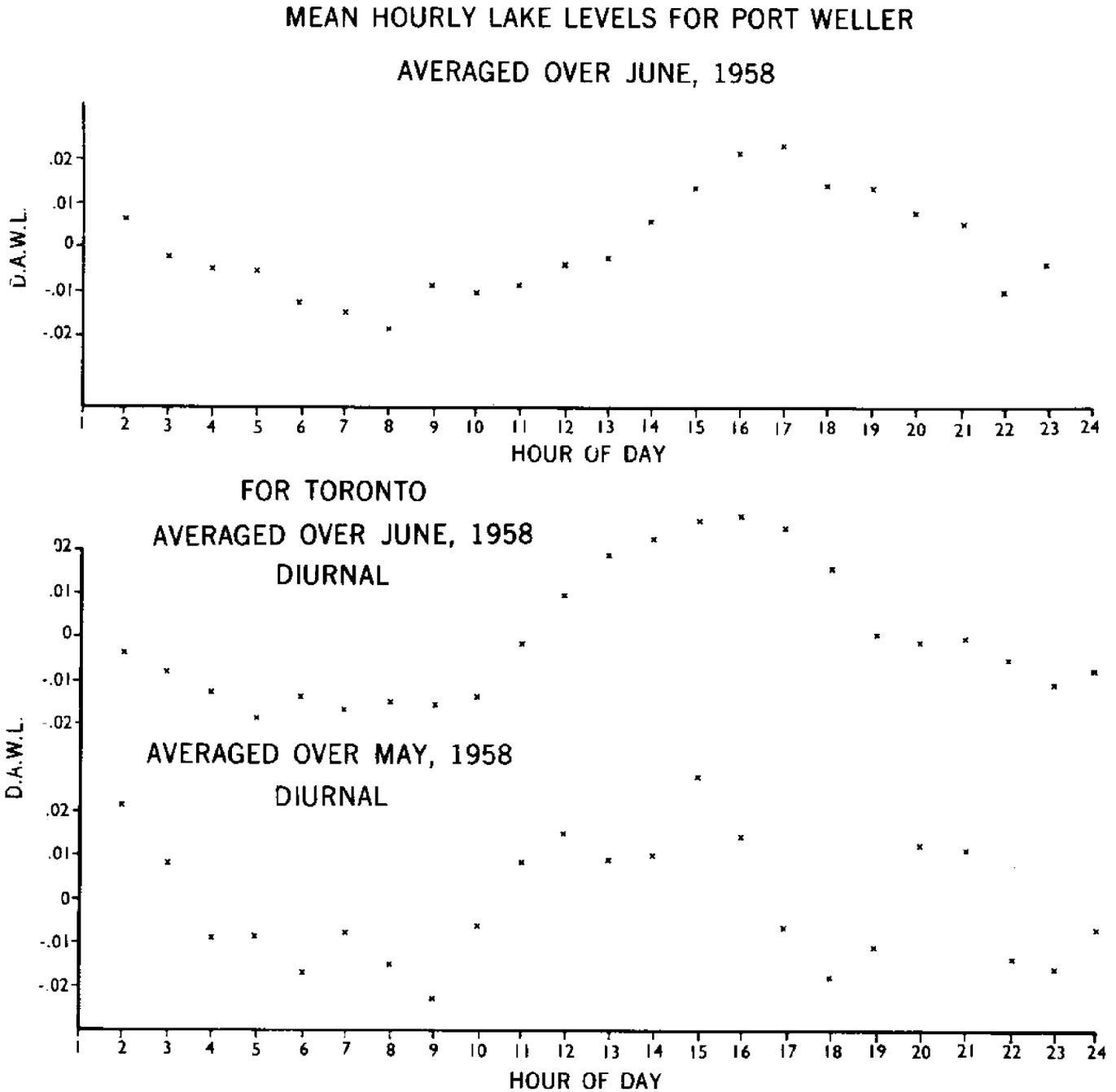

Figure 13 Average of reduced water levels versus hours of day for June 1958, Port Weller, Ontario, June 1958, Toronto, Ontario, and May 1958, Toronto, Ontario.

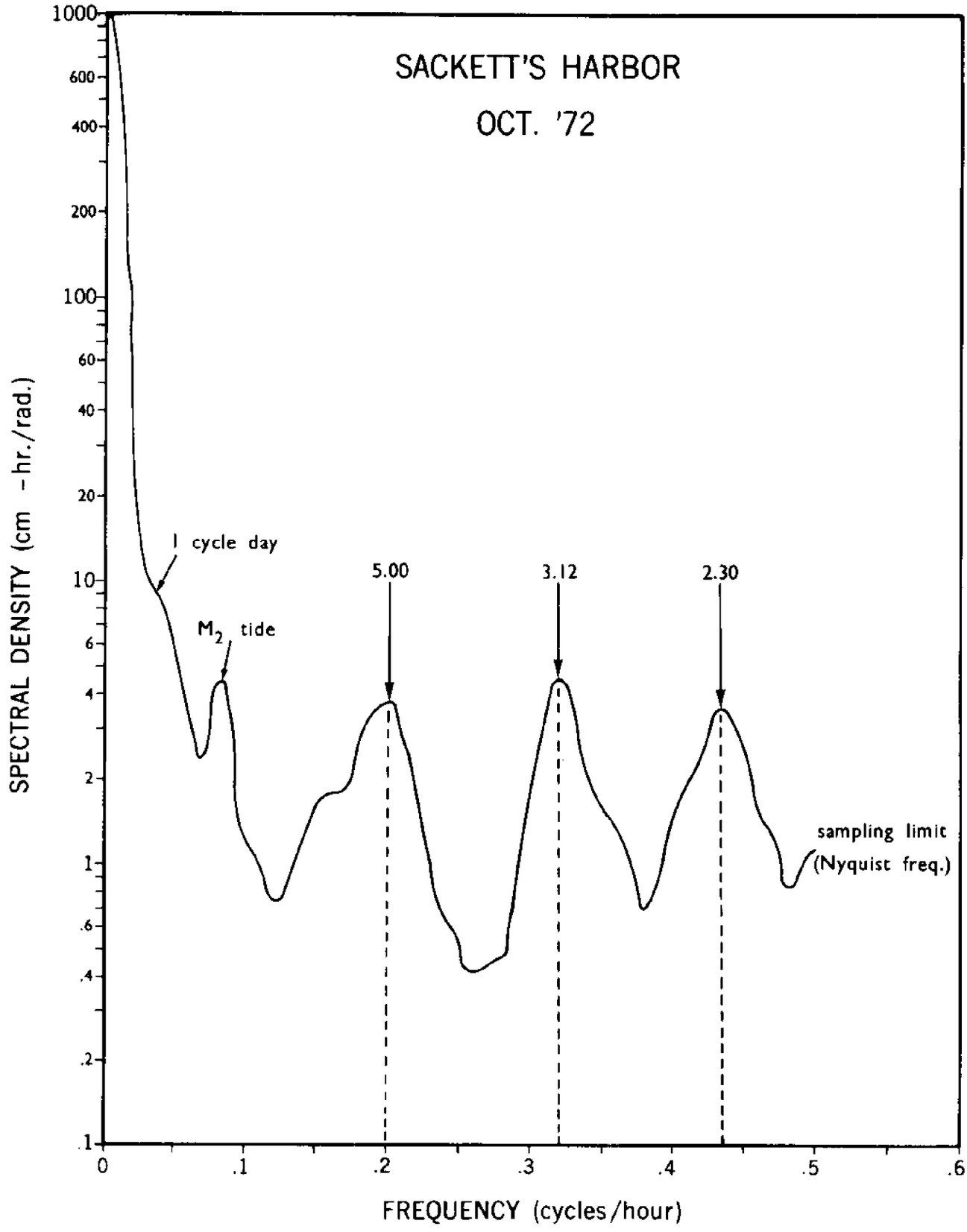

Figure 14 Relative spectral energy density versus frequency for hourly water levels from Sackett's Harbor, Lake Ontario, October 1972.

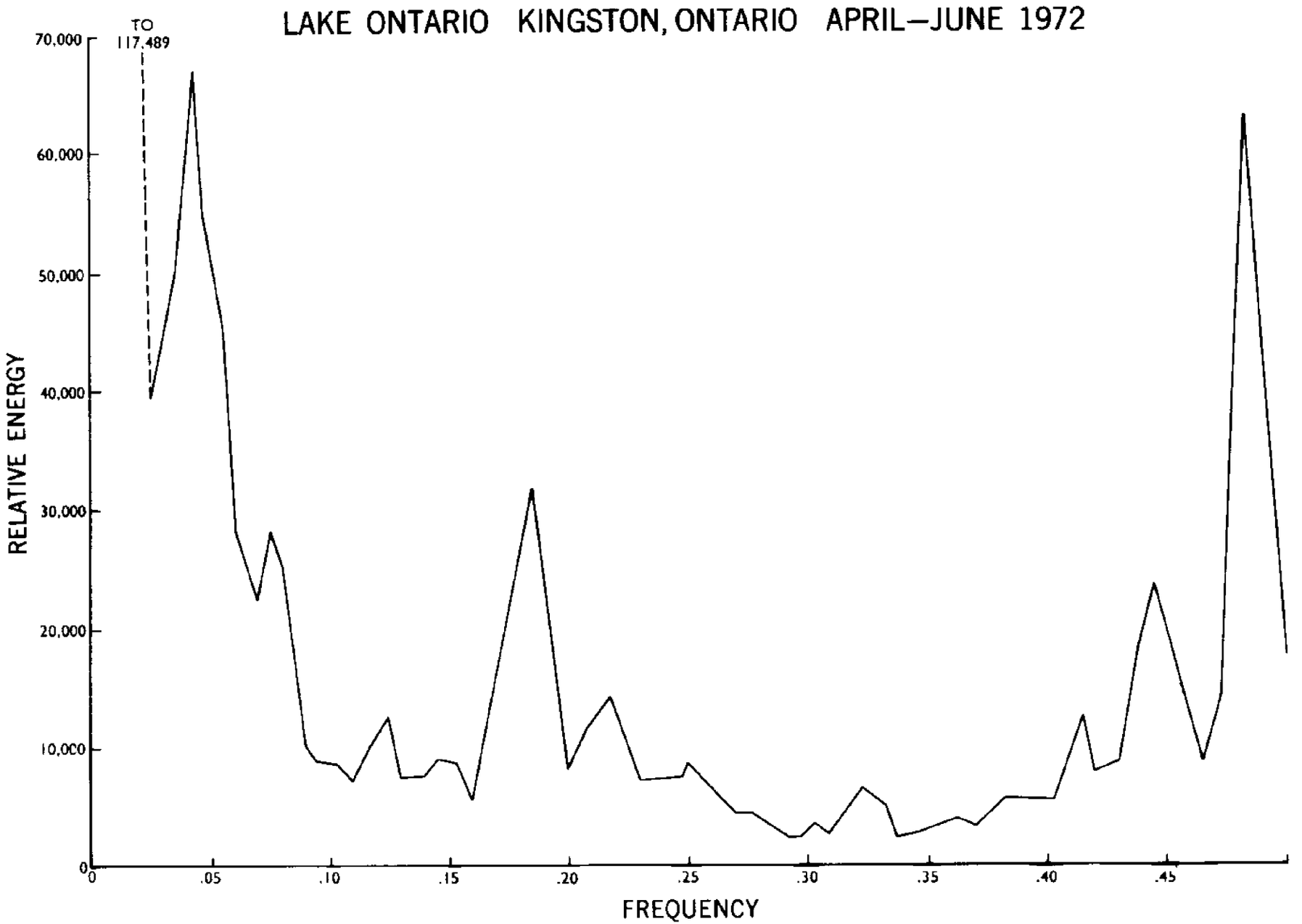

Figure 15 Relative spectral energy density versus frequency for hourly water levels from Kingston, Lake Ontario, April-June 1972.

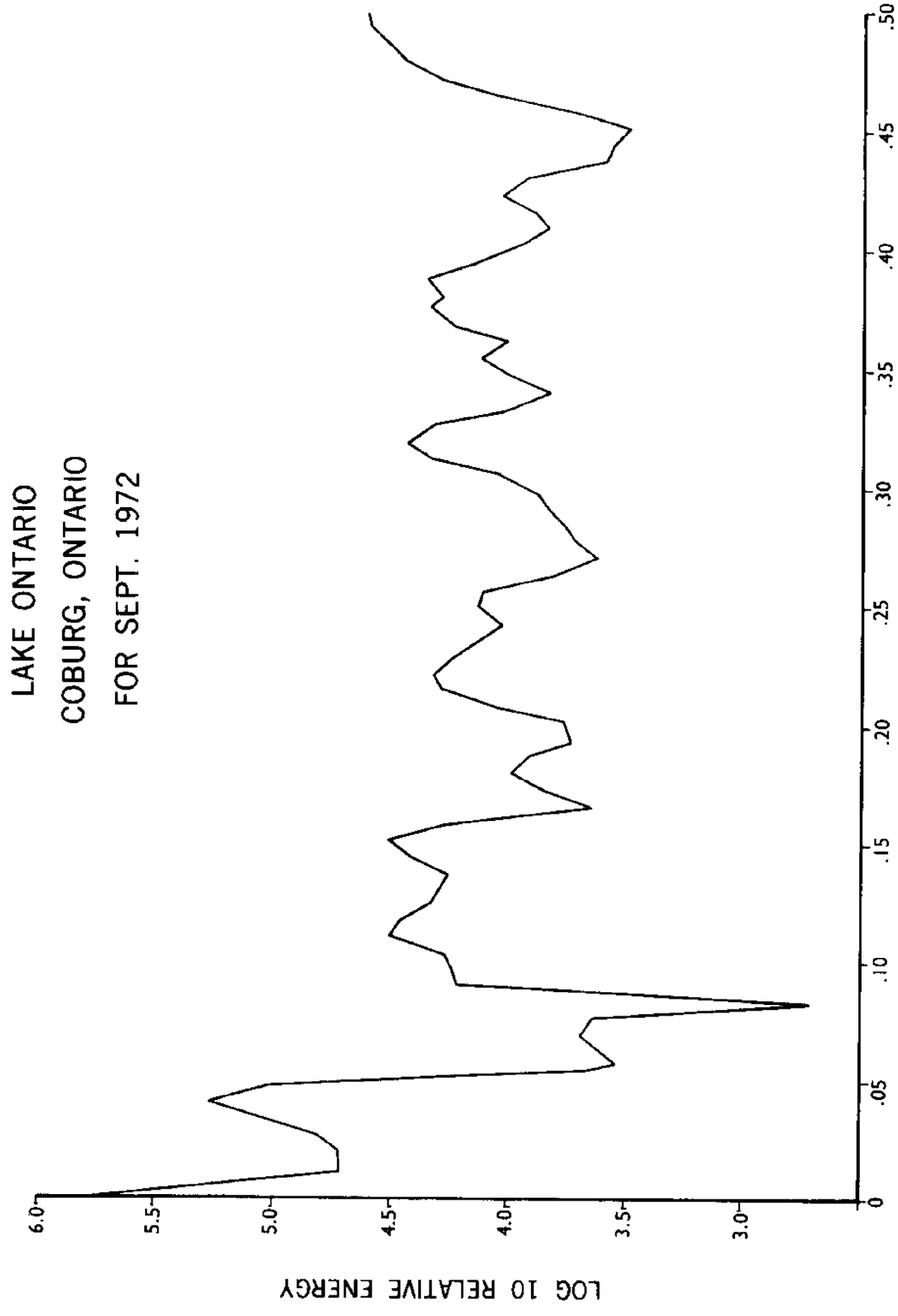

Figure 16 Relative spectral energy density versus frequency for hourly water levels from Cobourg, Lake Ontario, September 1972.

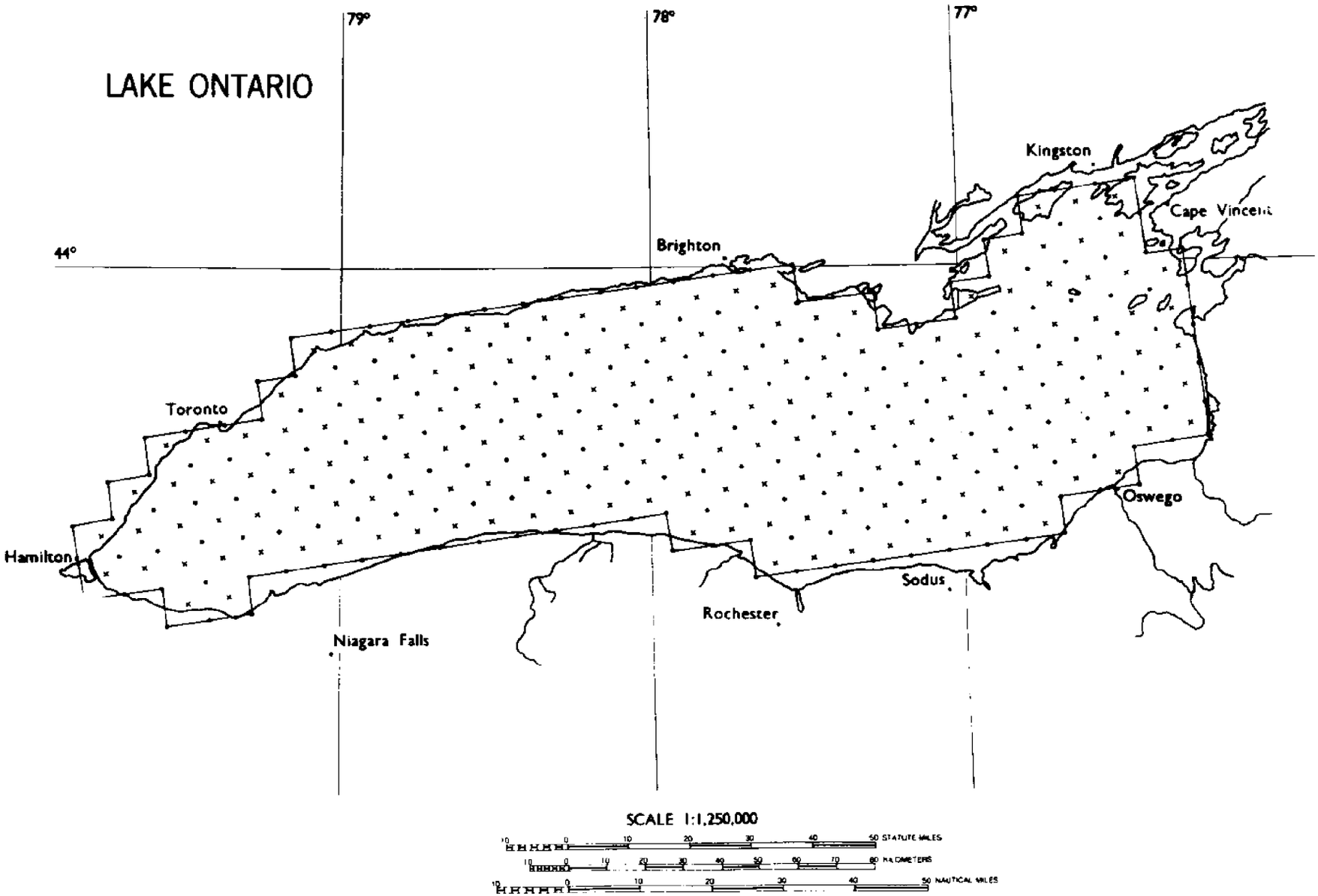

Figure 17 Location of points used by Rao and Schwab (1974) to compute stream functions and potential functions used in theoretical computation of seiche of Lake Ontario. The solid line indicates the assumed boundary used for the purposes of computation.

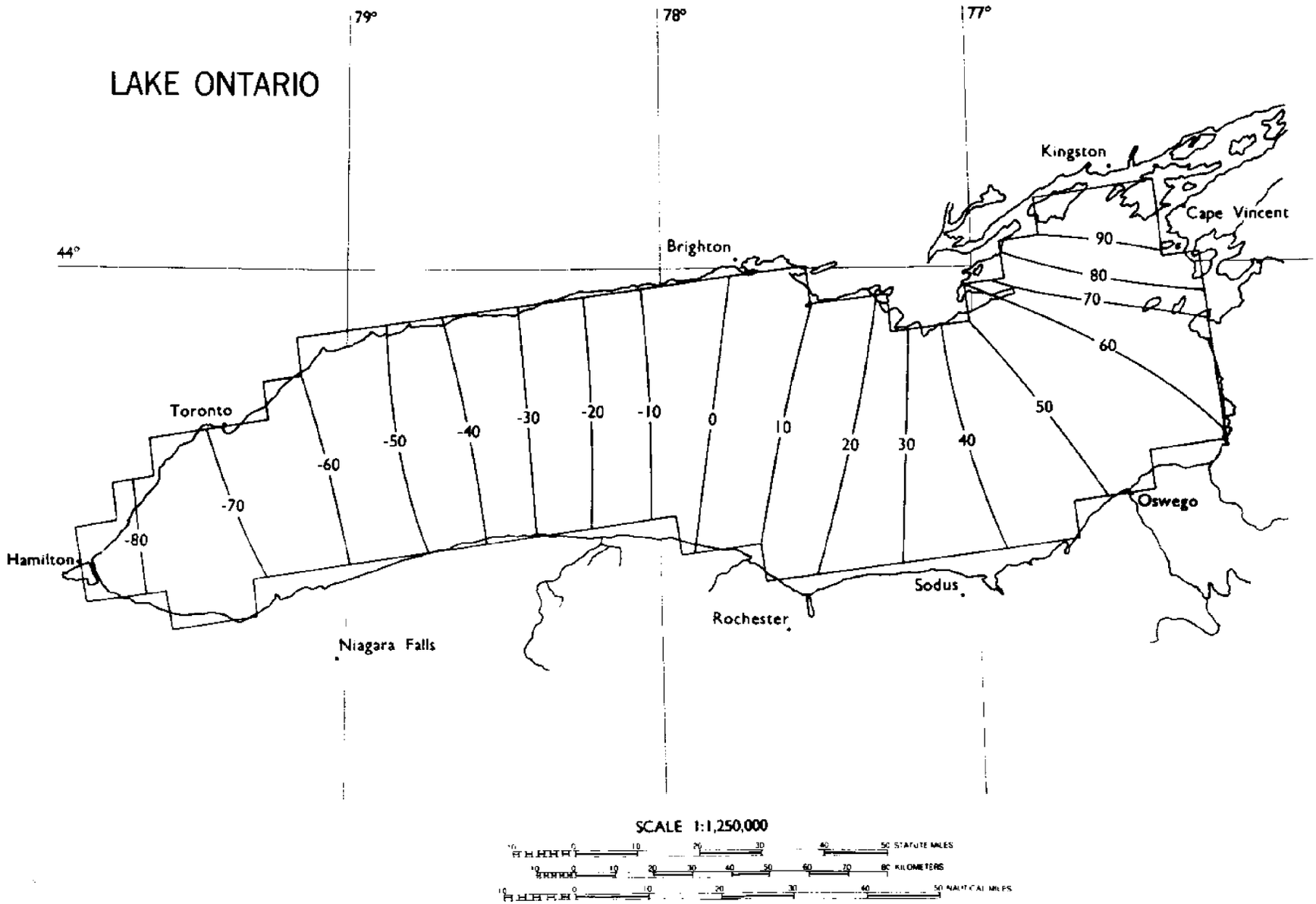

Figure 18 Computed velocity potentials for first mode of oscillation of Lake Ontario neglecting rotation of earth.

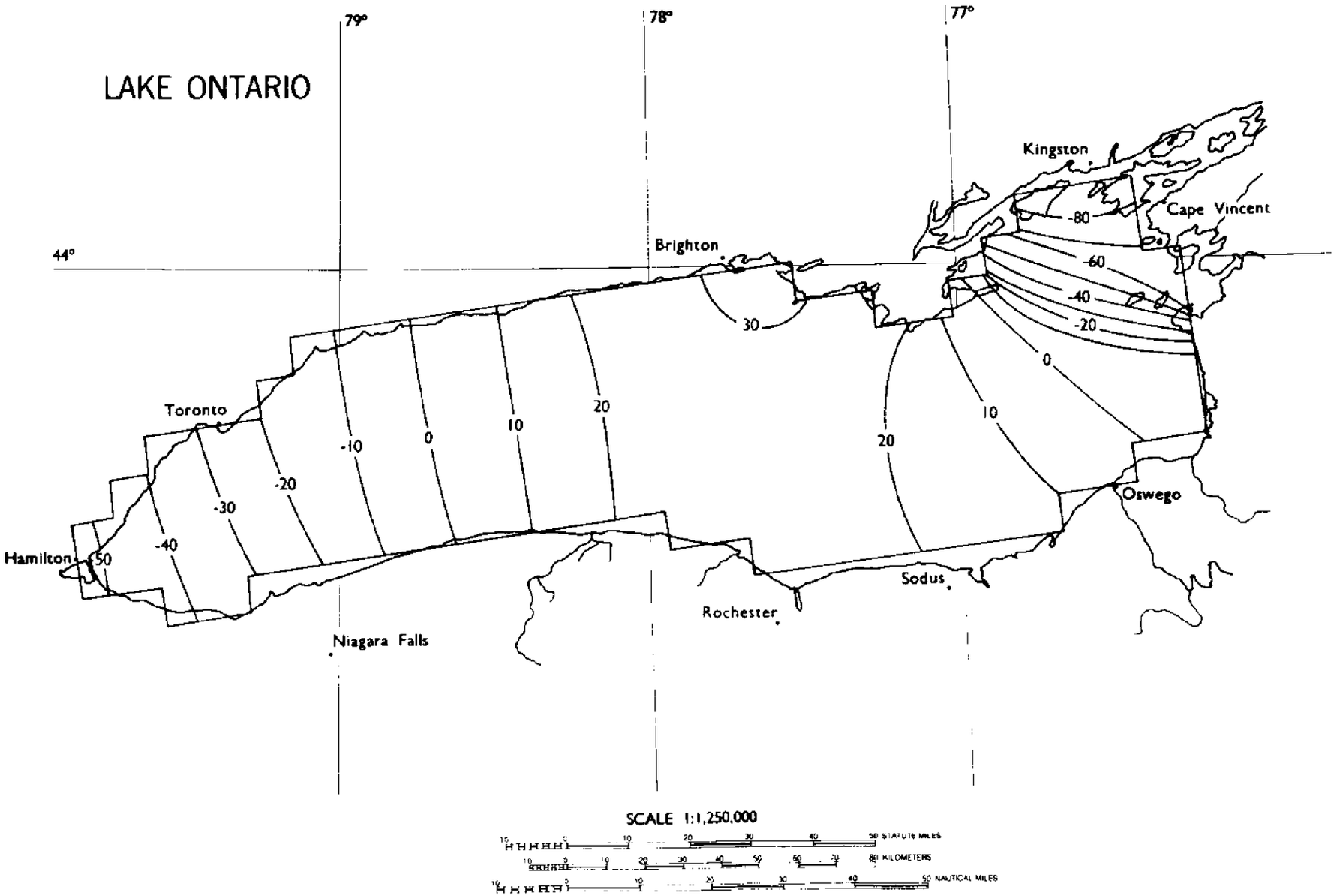

Figure 19 Computed velocity potentials for second mode of oscillation of Lake Ontario neglecting rotation of earth.

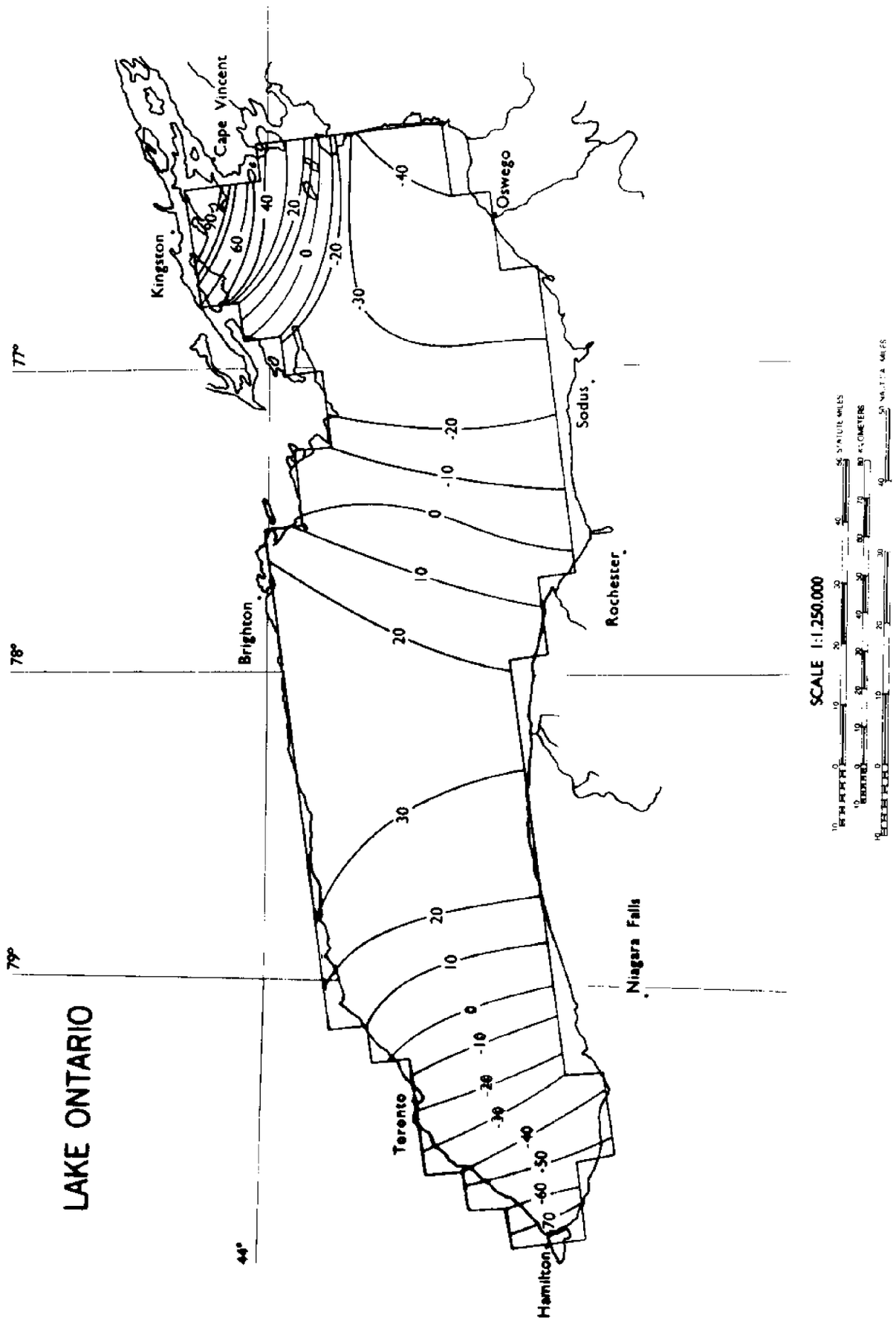

Figure 20 Computed velocity potentials for third mode of oscillation of Lake Ontario neglecting rotation of earth.

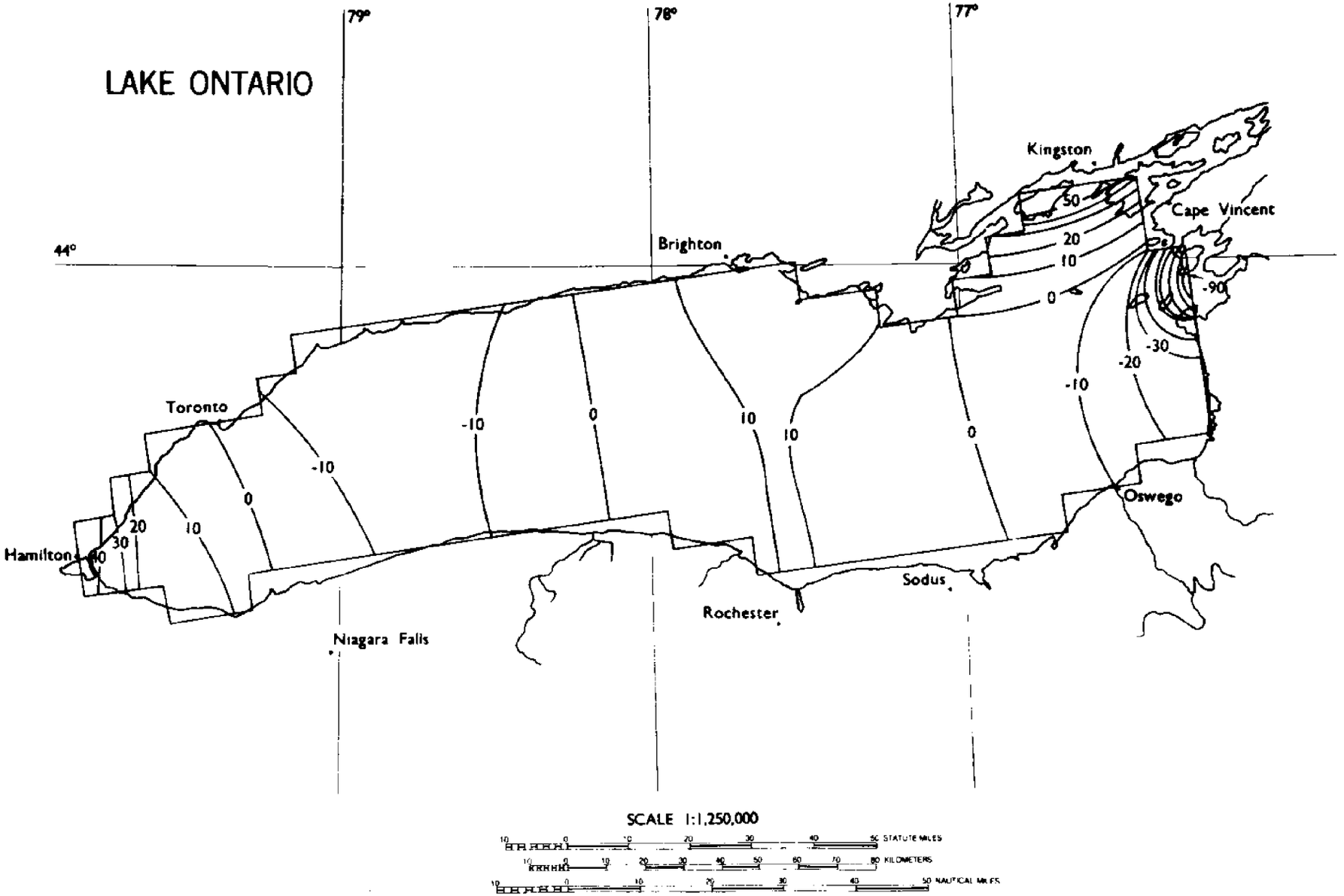

Figure 21 Computed velocity potentials for fourth mode of oscillation of Lake Ontario neglecting rotation of earth.

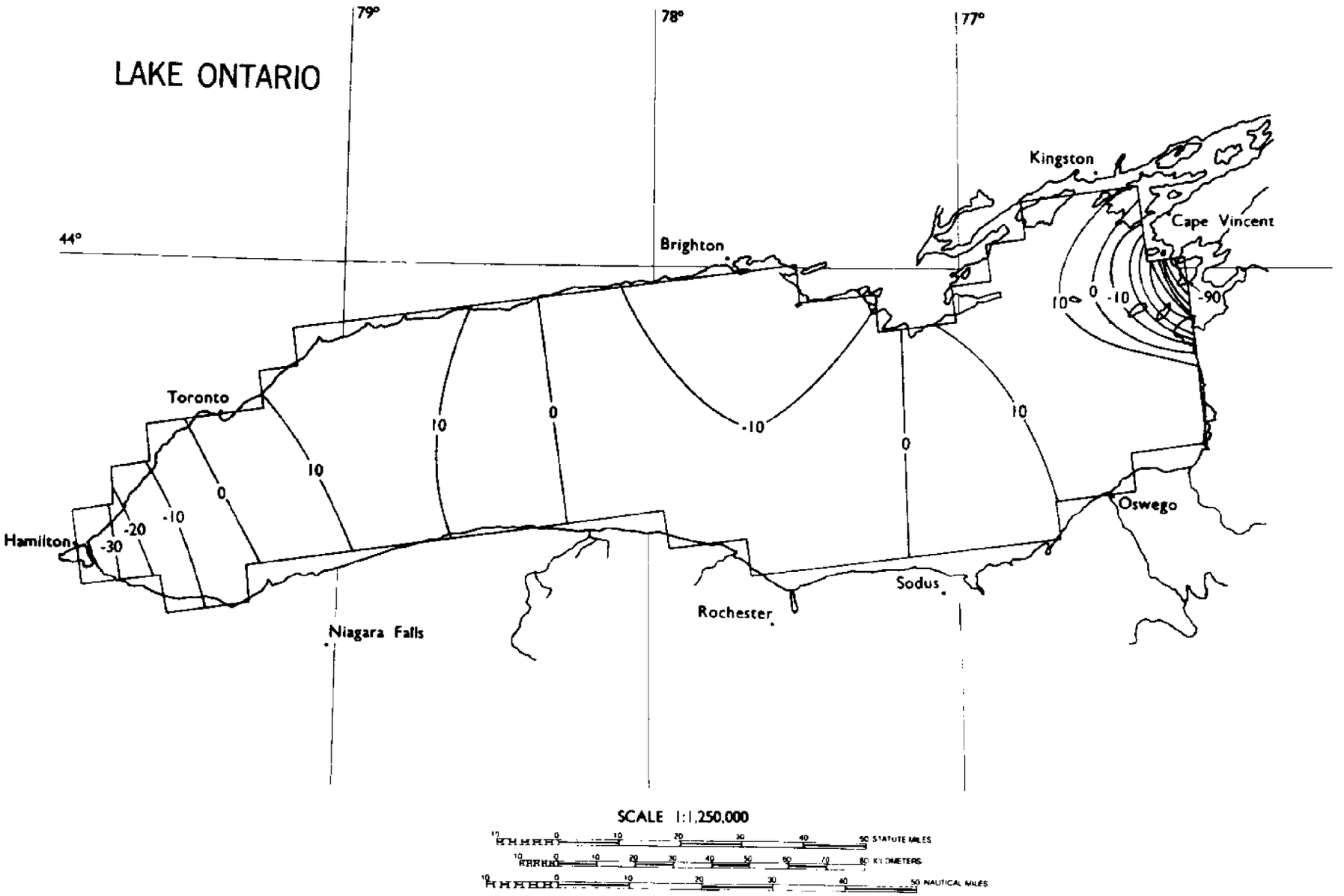

Figure 22 Computed velocity potentials for fifth mode of oscillation of Lake Ontario neglecting rotation of earth.

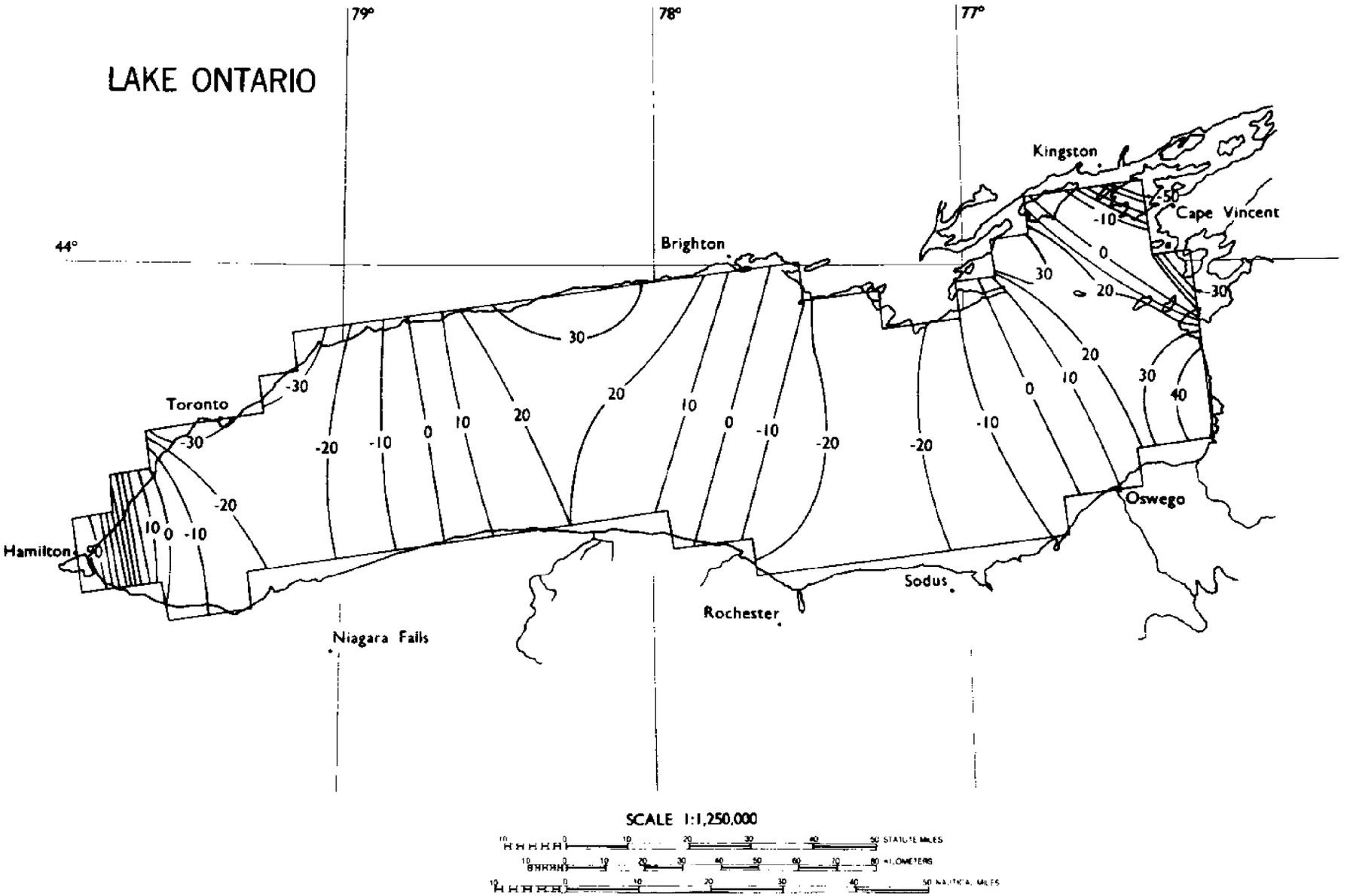

Figure 23 Computed velocity potentials for sixth mode of oscillation of Lake Ontario neglecting rotation of earth.

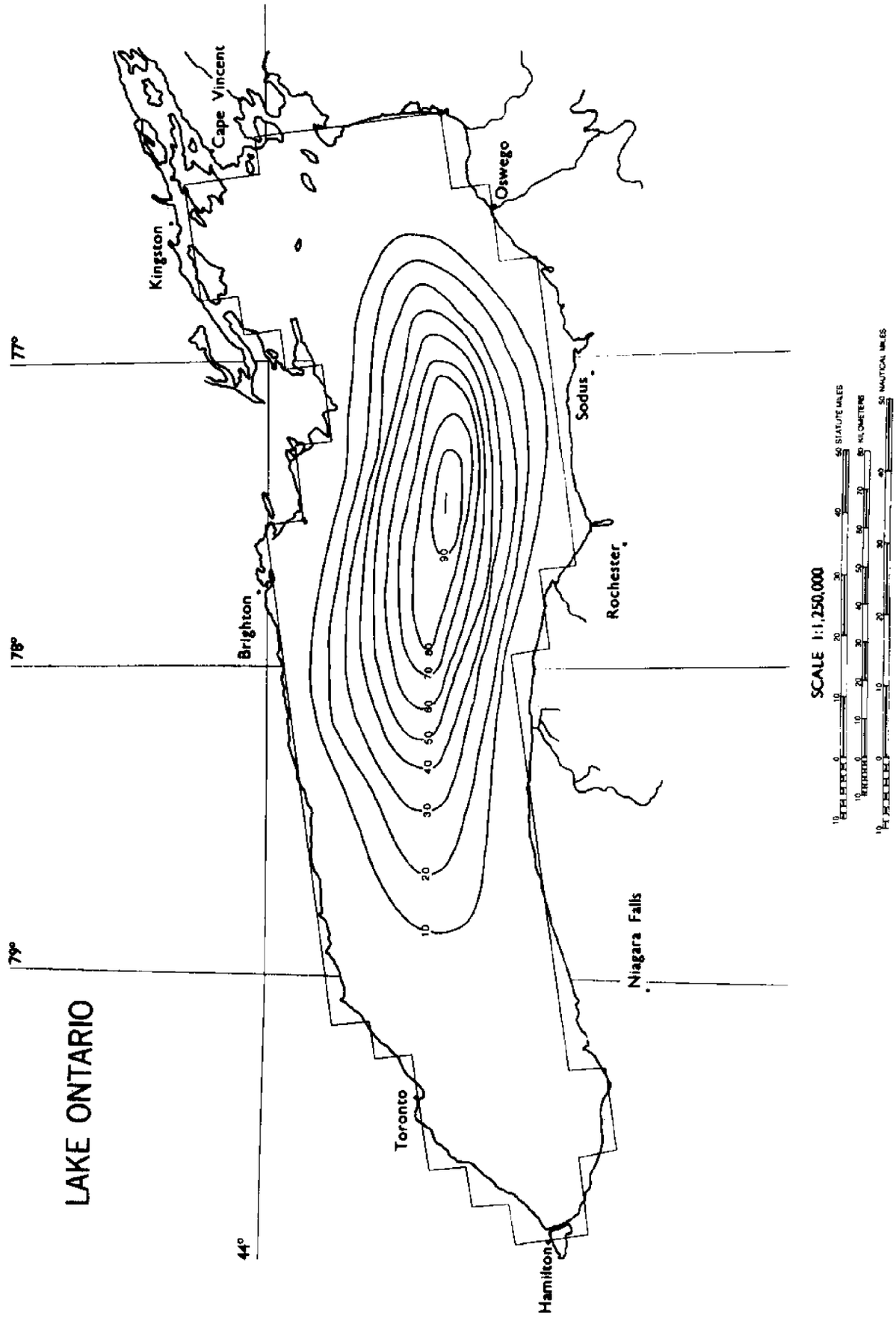

Figure 24 Computed stream function used to generate vorticity component of flow for first mode of oscillation.

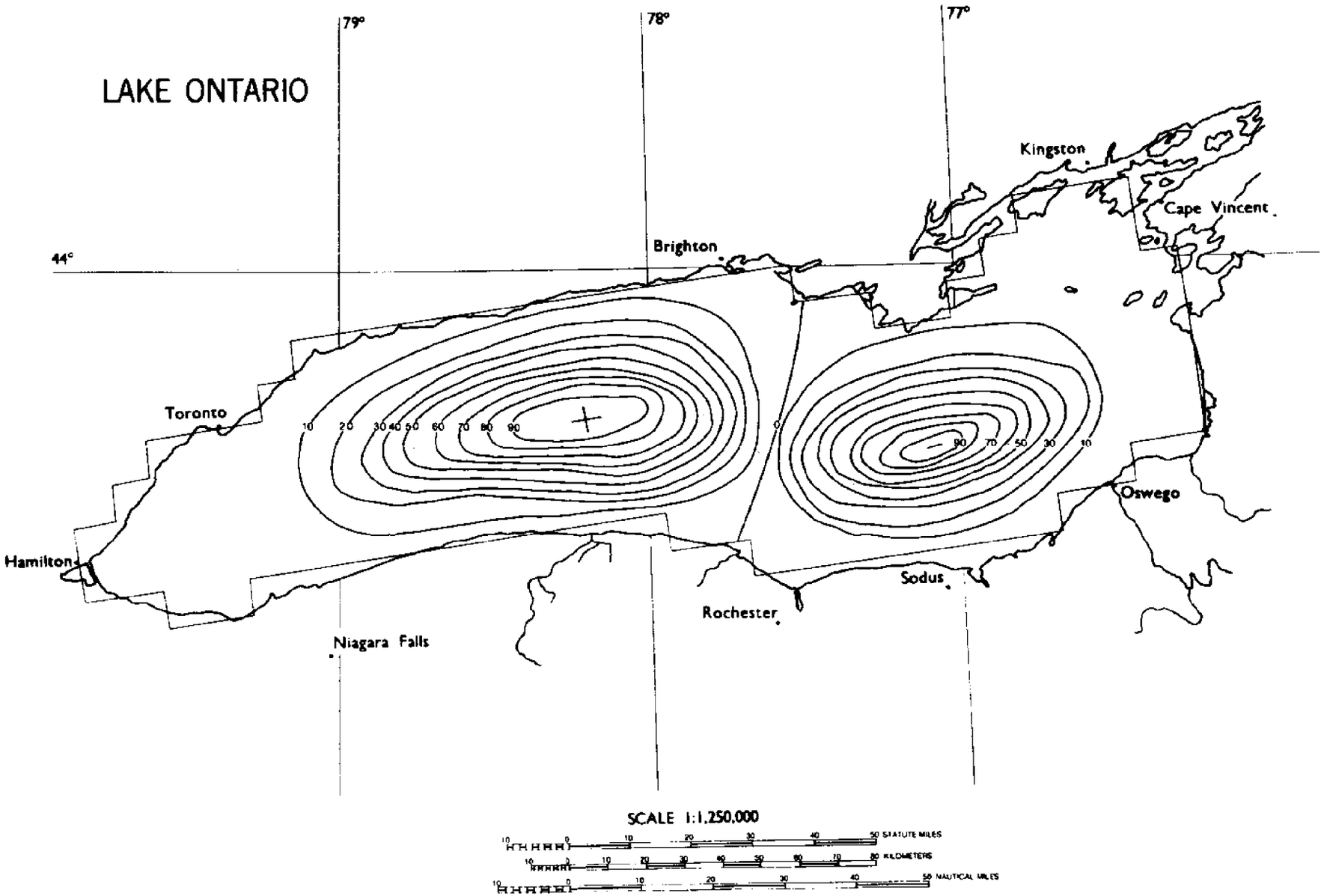

Figure 25 Computed stream function used to generate vorticity component of flow for second mode of oscillation.

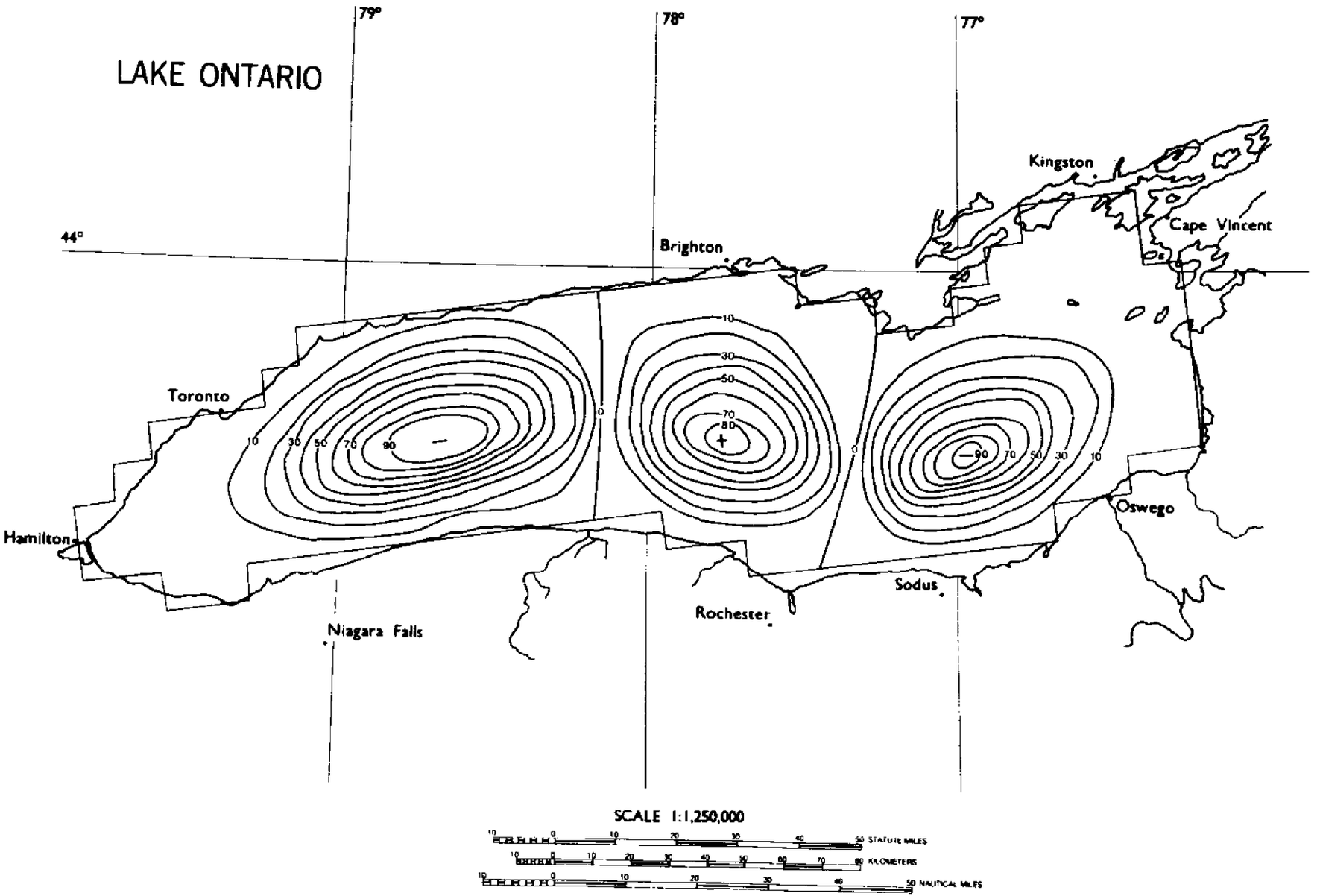

Figure 26 Computed stream function used to generate vorticity component of flow for third mode of oscillation.

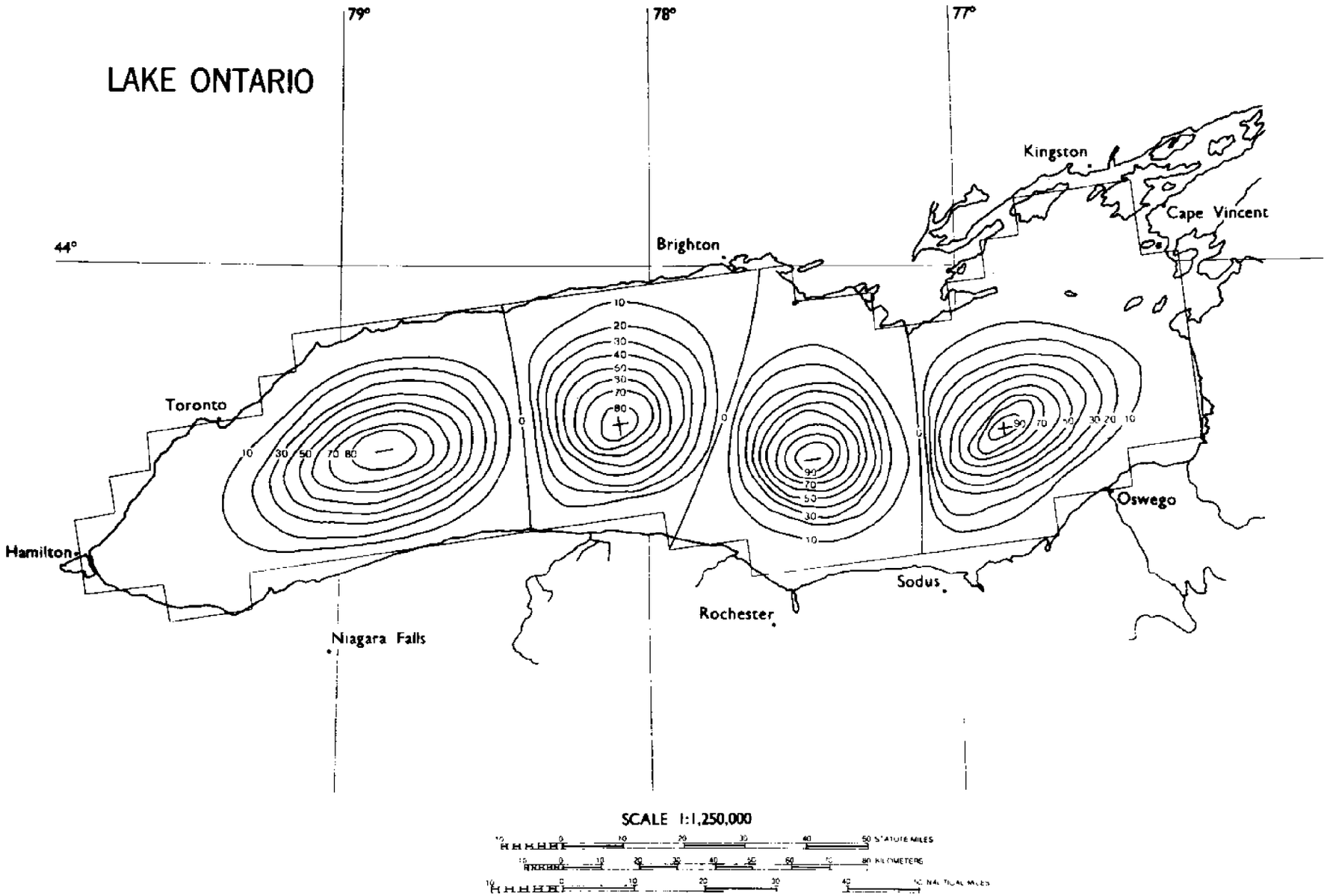

Figure 27 Computed stream function used to generate vorticity component of flow for fourth mode of oscillation.

Figure 28 Computed fluctuation of free surface height for first mode of oscillation considering earth's rotation. Solid lines represent cotidal lines and dashed lines represent co-range lines.

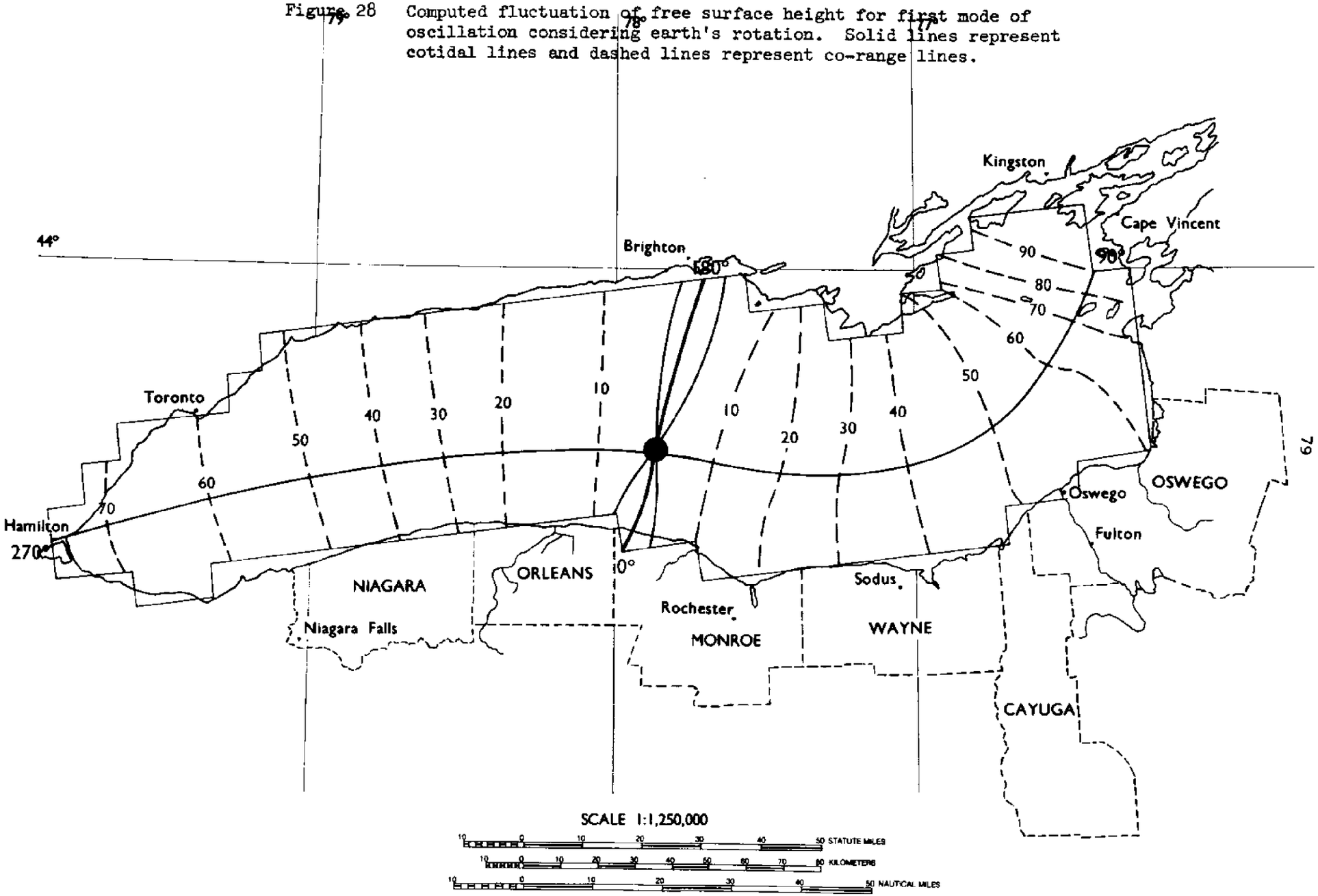

Figure 29 Computed fluctuation of free surface height for second mode of oscillation considering earth's rotation. Solid lines represent cotidal lines and dashed lines represent co-range lines.

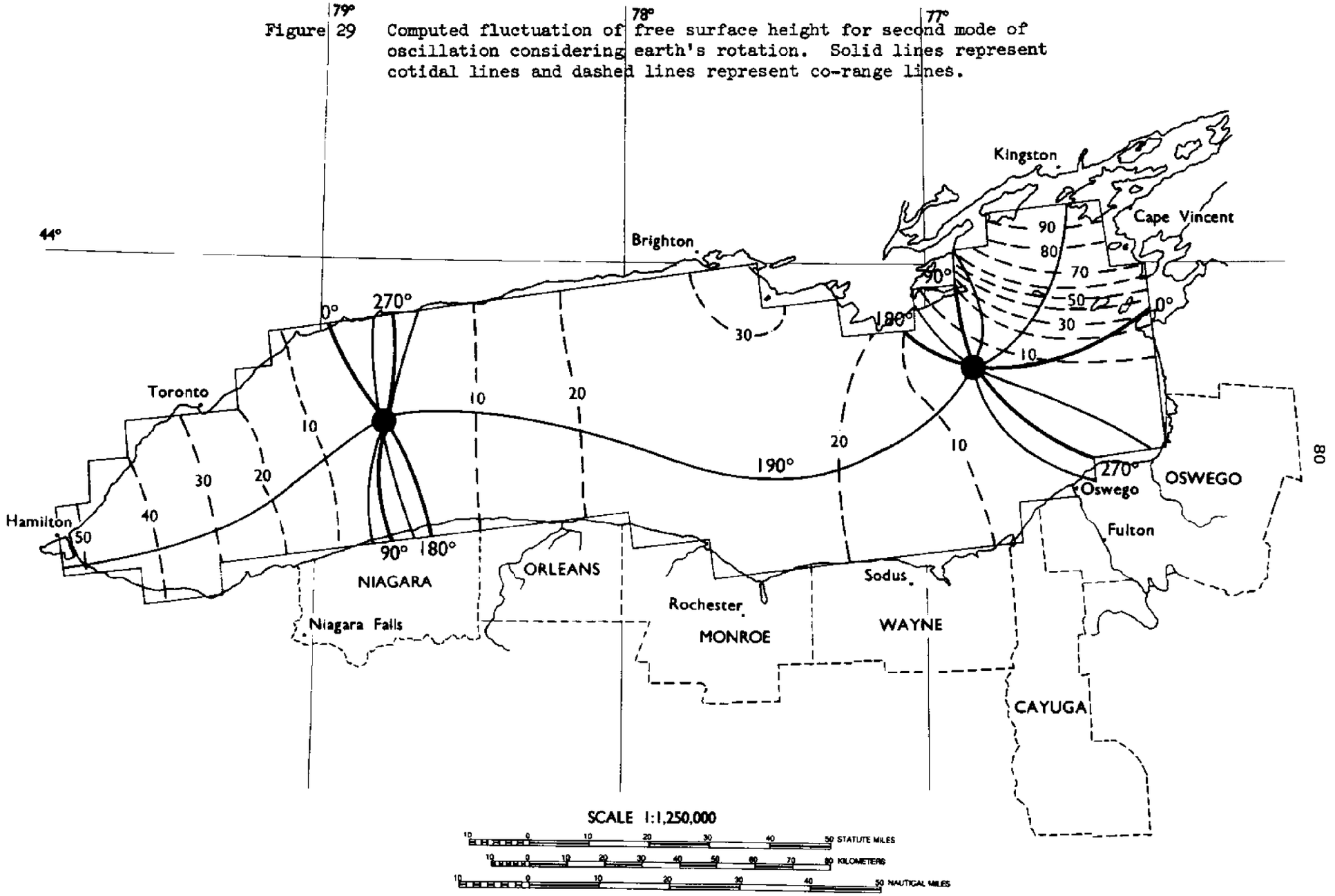

Figure 30 Computed fluctuation of free surface height for third mode of oscillation considering earth's rotation. Solid lines represent cotidal lines and dashed lines represent co-range lines.

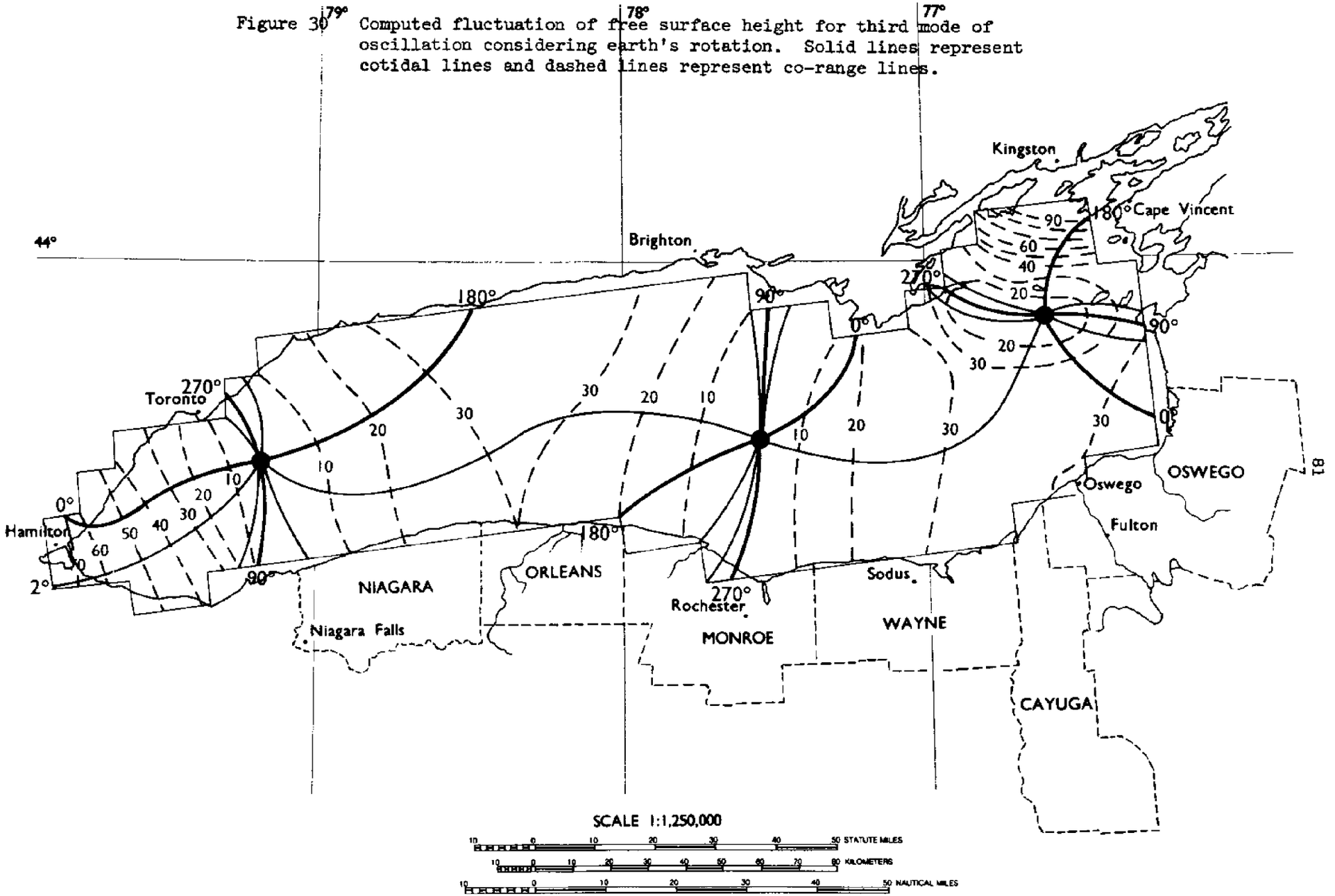

Figure 31 Computed fluctuation of free surface height for fourth mode of oscillation considering earth's rotation. Solid lines represent cotidal lines and dashed lines represent co-range lines.

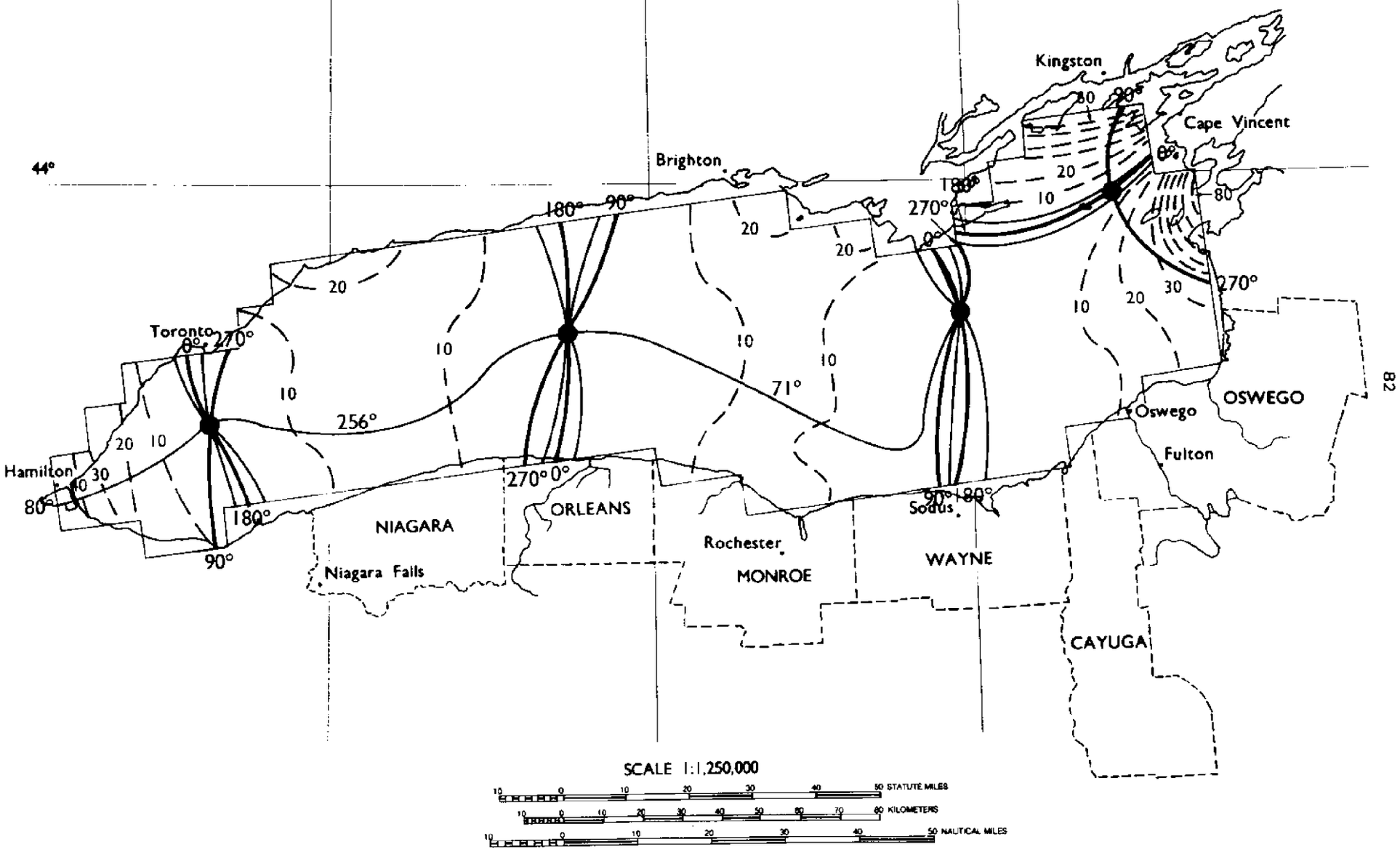

Figure 32 Computed fluctuation of free surface height for fifth mode of oscillation considering earth's rotation. Solid lines represent cotidal lines and dashed lines represent co-range lines.

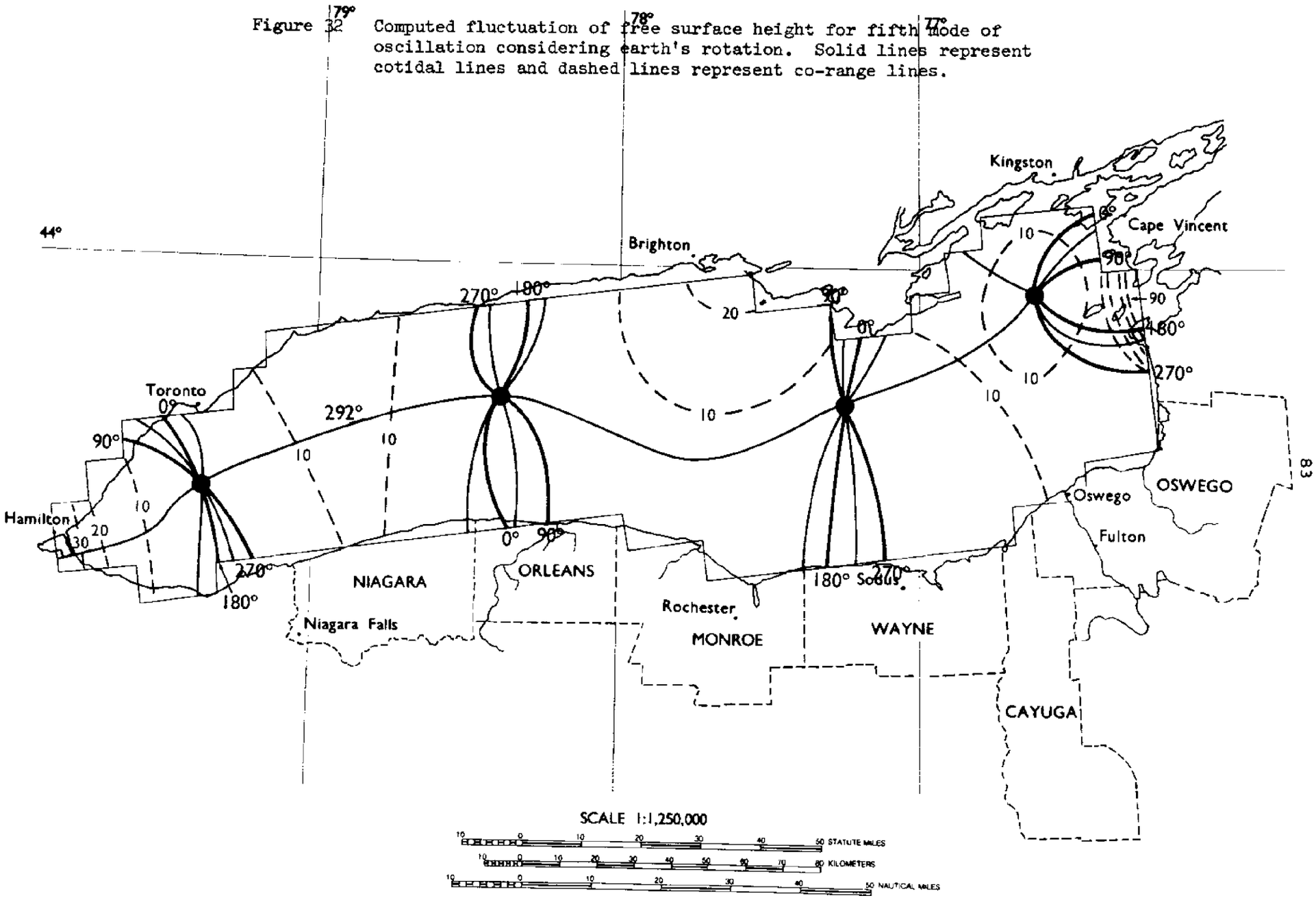

Figure 33 Computed fluctuation of free surface height for sixth mode of oscillation considering earth's rotation. Solid lines represent cotidal lines and dashed lines represent co-range lines.

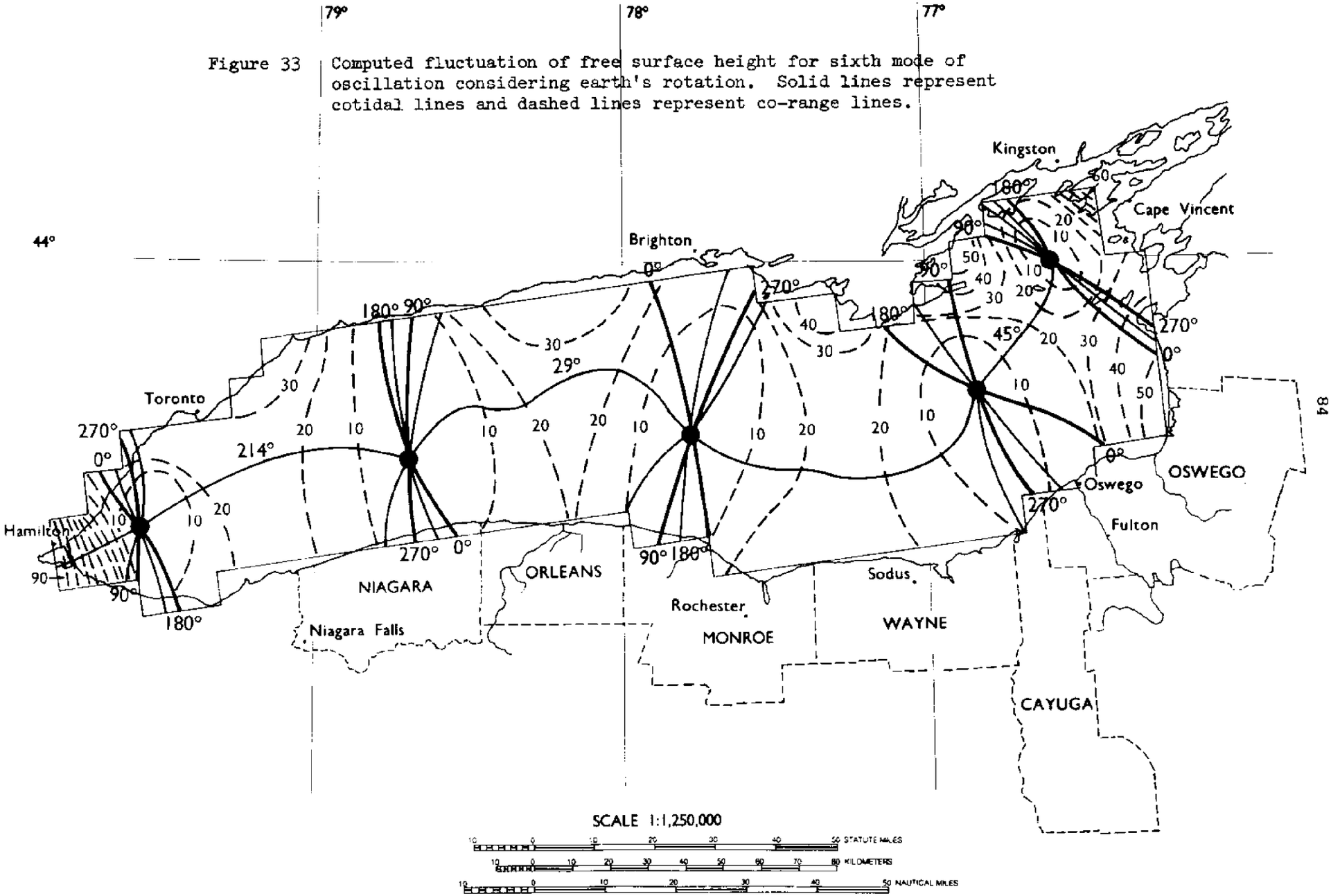

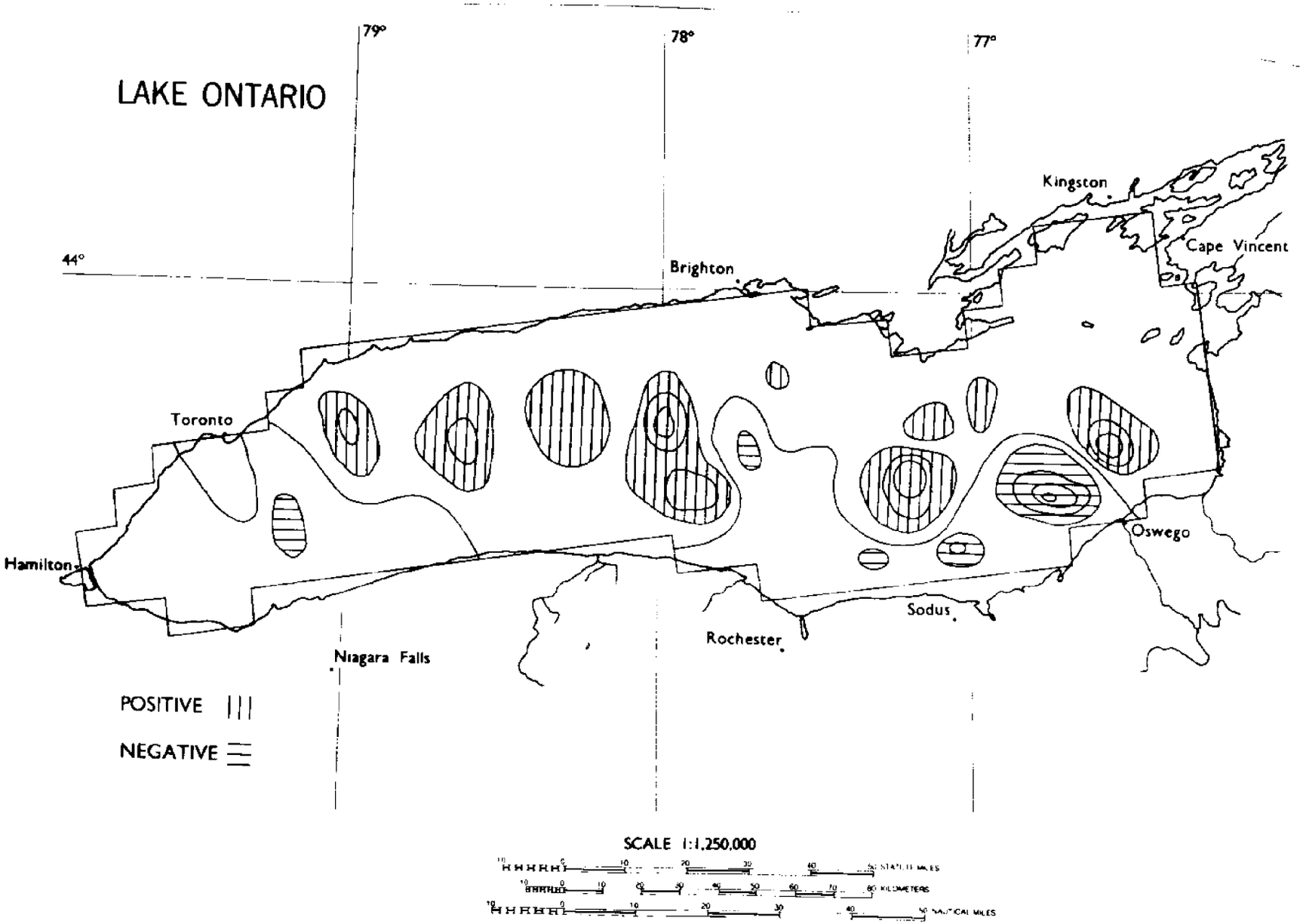

Figure 34 Computed streamlines of mass transport for rotational mode with 229 hour period at a phase angle of 0.

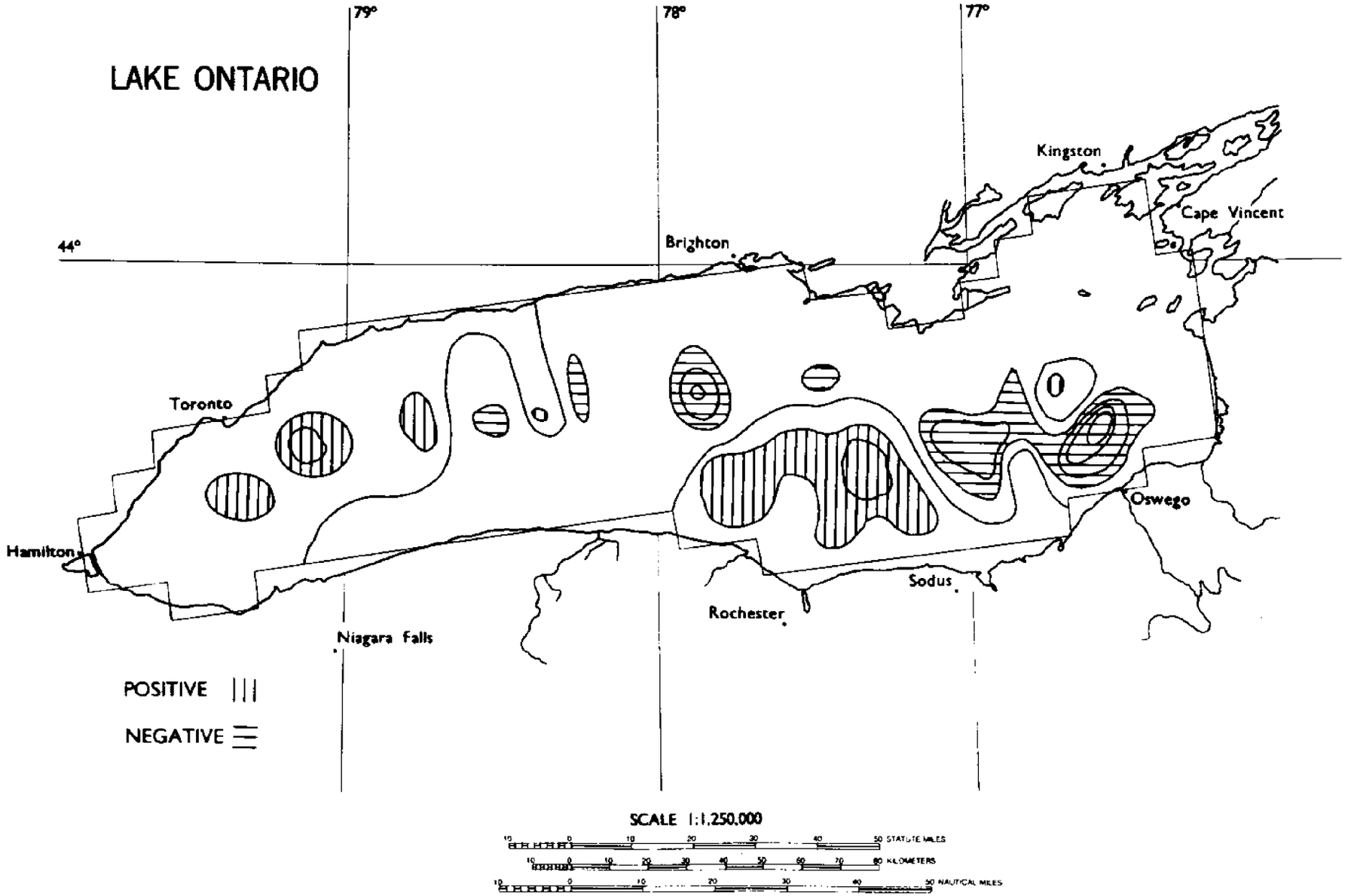

Figure 35 Computed streamlines of mass transport for rotational mode with 229 hour period at a phase angle of $\pi/2$.

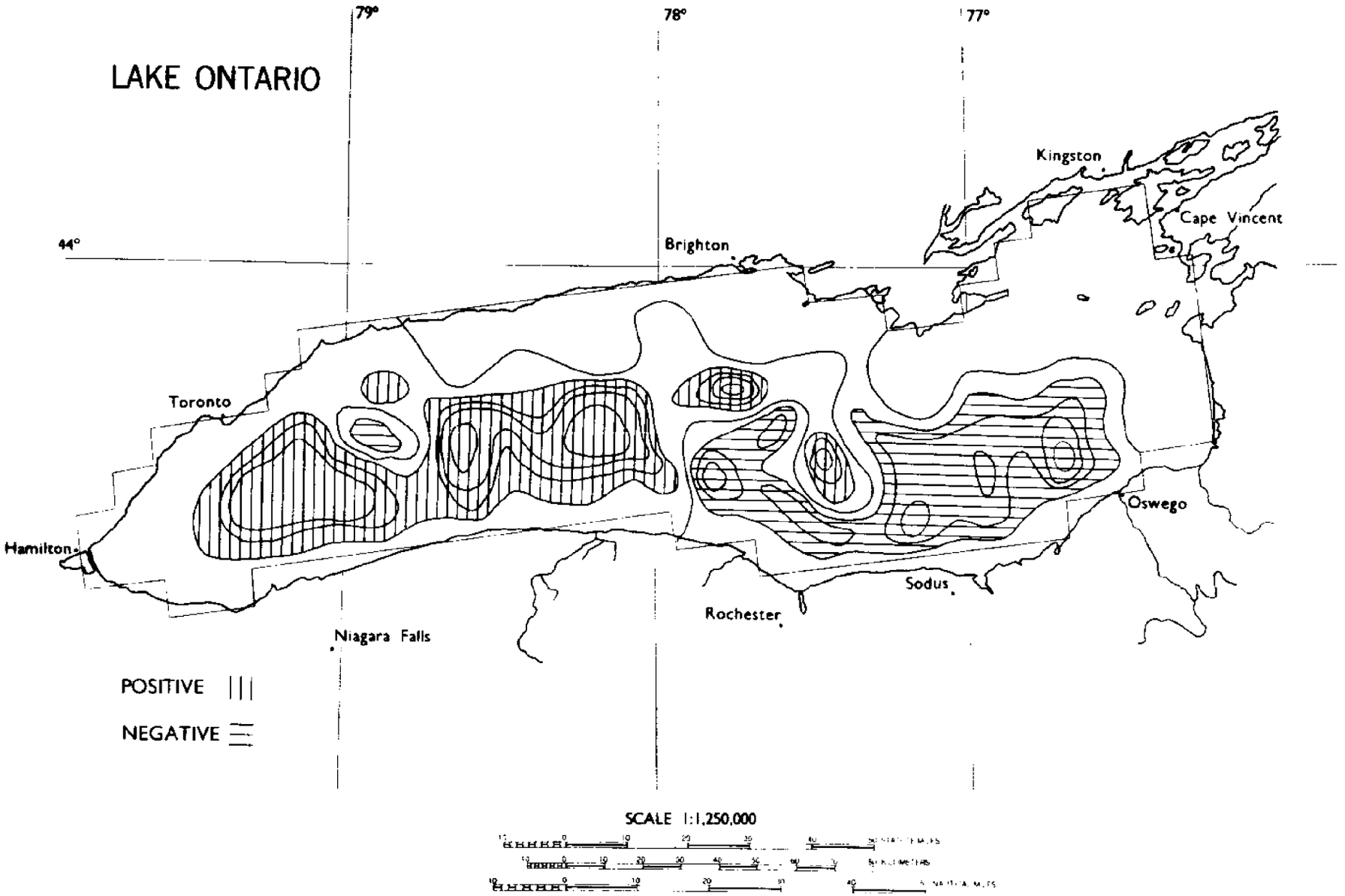

Figure 36 Computed streamlines of mass transport for rotational mode with 464 hour period at a phase angle of 0.

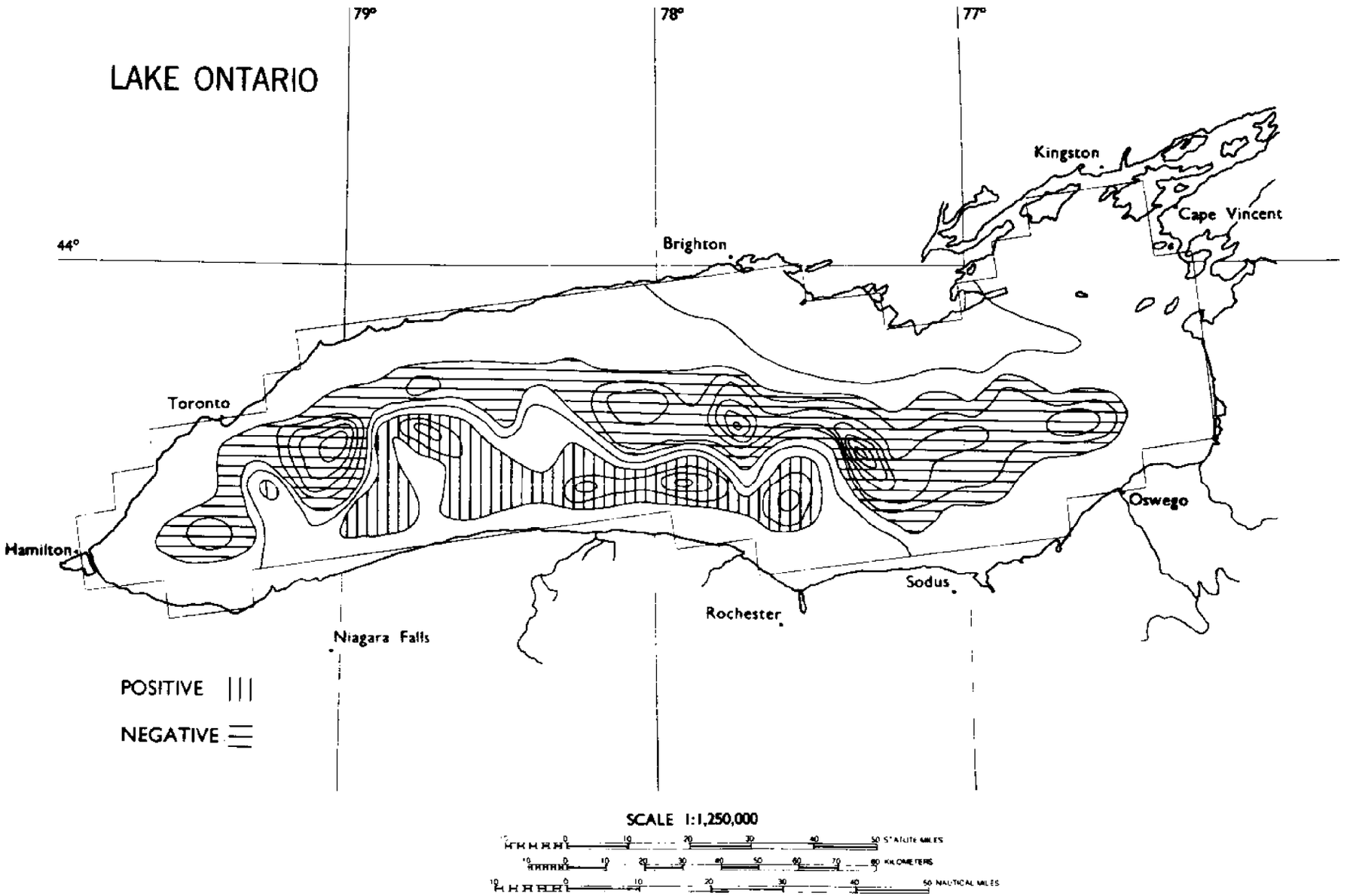

Figure 37 Computed streamlines of mass transport for rotational mode with 464 hour period at a phase angle of $\pi/2$.

Figure 38 Location of wave rider buoys used by Liu and Kessenich (1975) for analysis of Lake Ontario gravity waves.

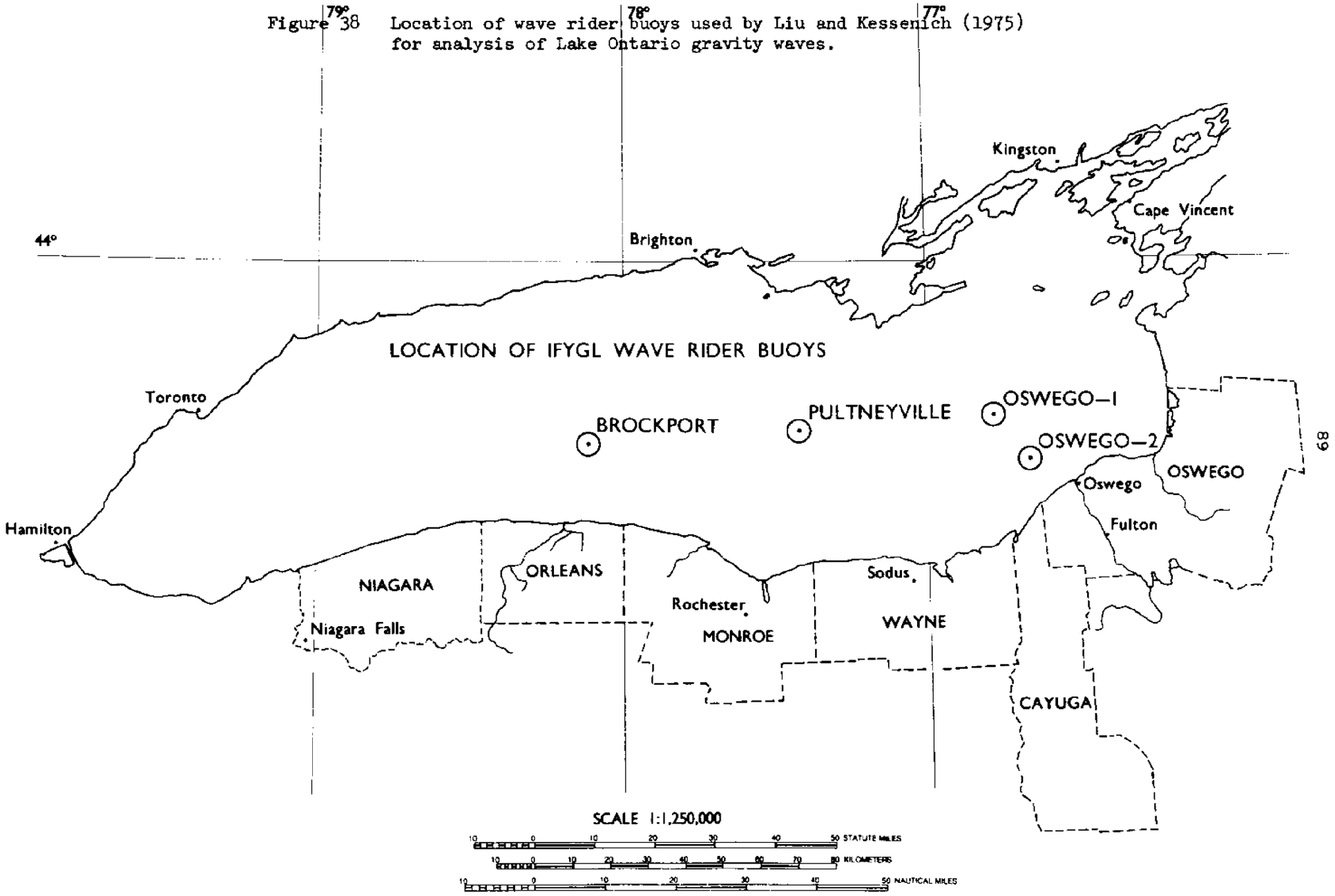

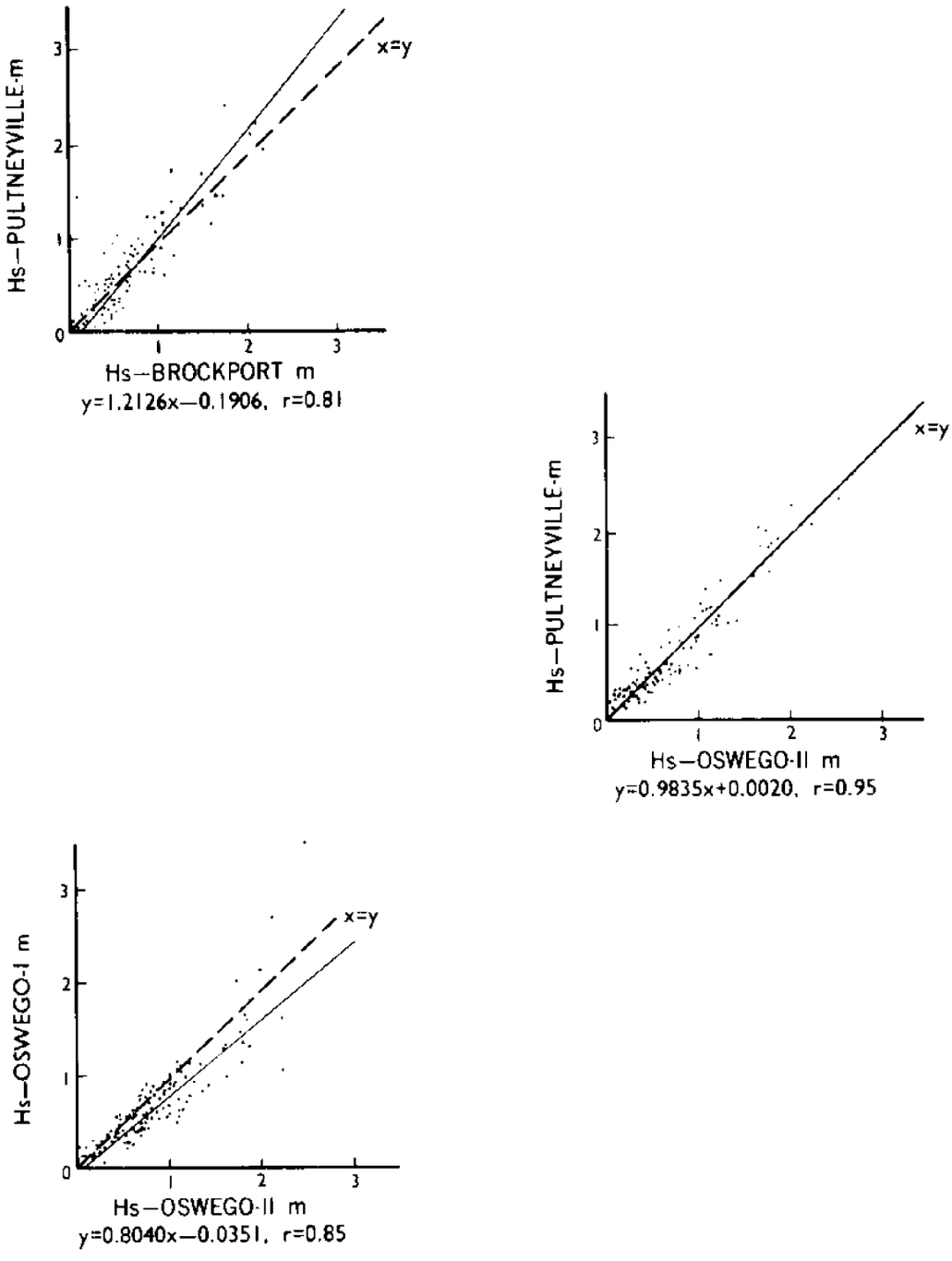

Figure 39 Significant wave heights recorded at one wave rider buoy versus significant wave heights recorded at a second wave rider buoy. The dashed line indicates the line x = y that the data would be expected to follow if significant wave heights were the same at both stations. The solid lines is the best fit obtained by least squares linear regression. The equation below each graph refers to this line. r is the correlation coefficient.

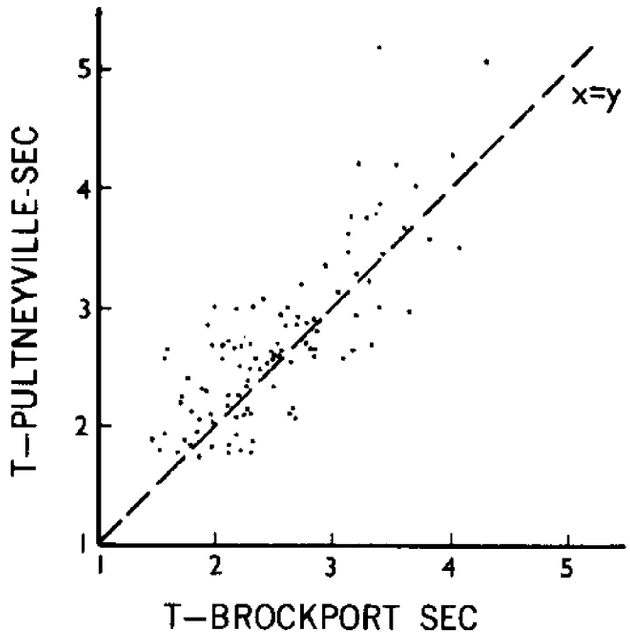

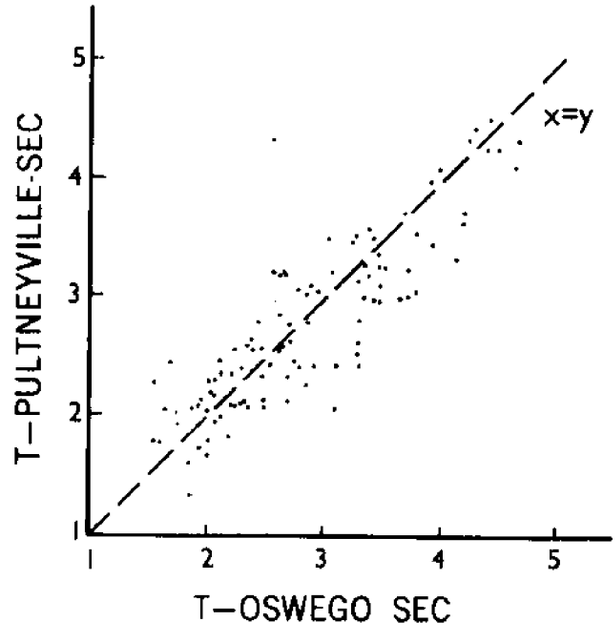

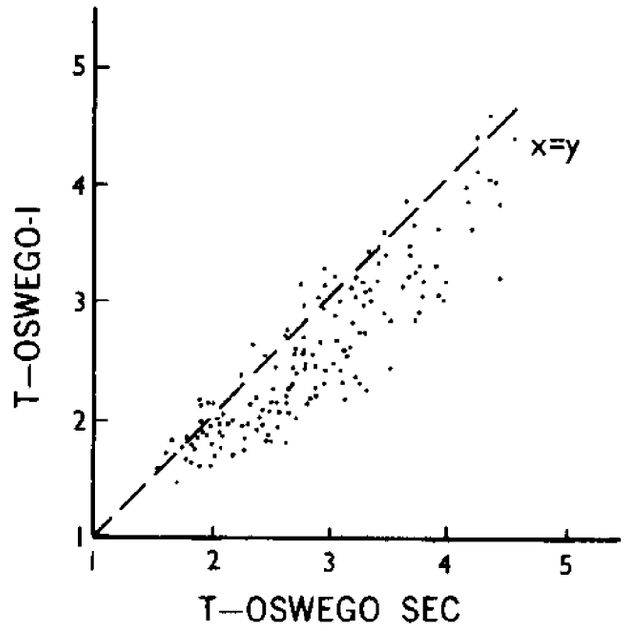

Figure 40 Average wave period recorded at one wave rider buoy versus average wave period recorded at a second wave rider buoy. The dashed line indicates the line x = y that the data would be expected to follow if the average periods were the same at both stations.

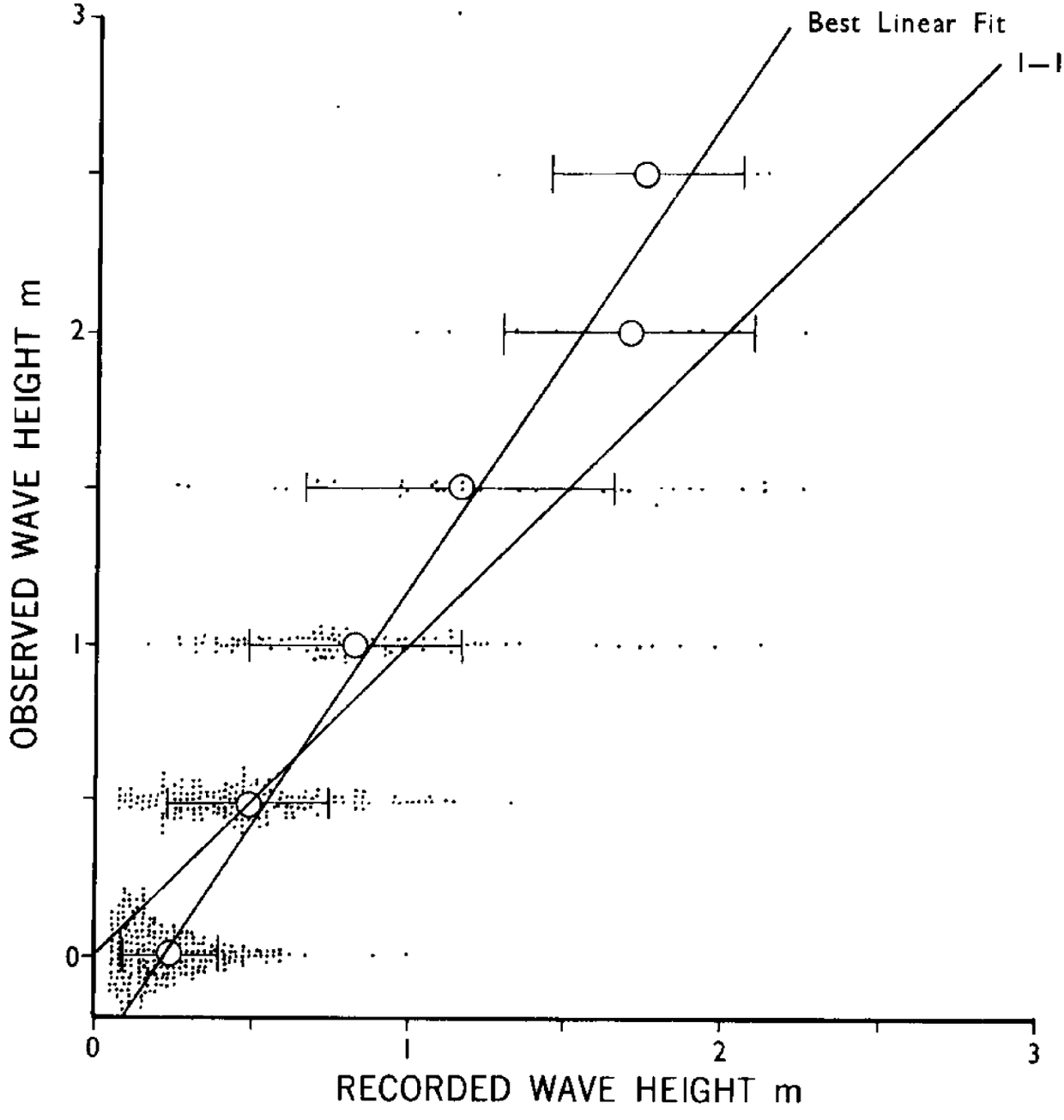

Figure 41 Recorded versus observed significant wave height on Lake Ontario.

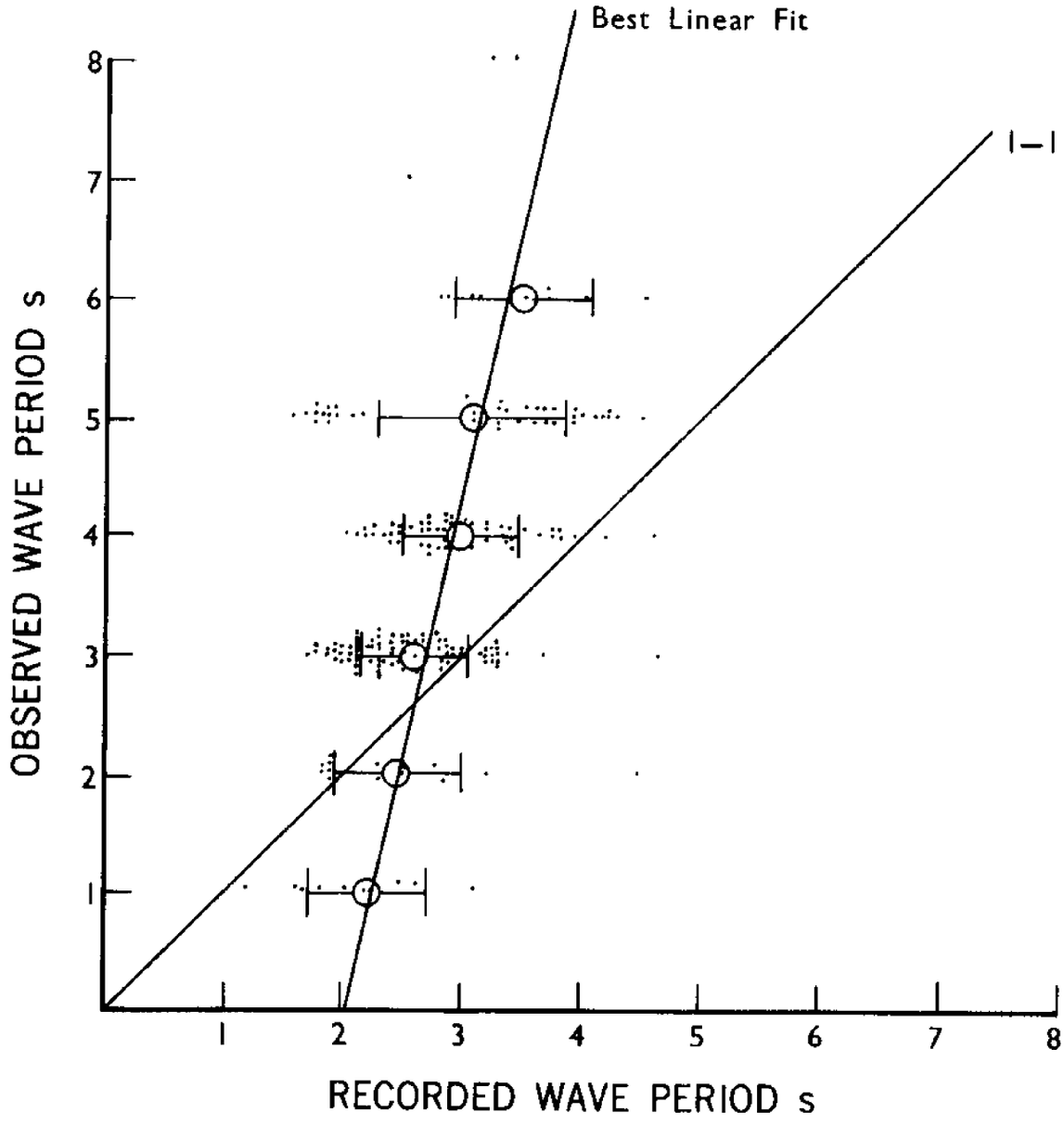

Figure 42 Recorded versus observed average wave period on Lake Ontario.

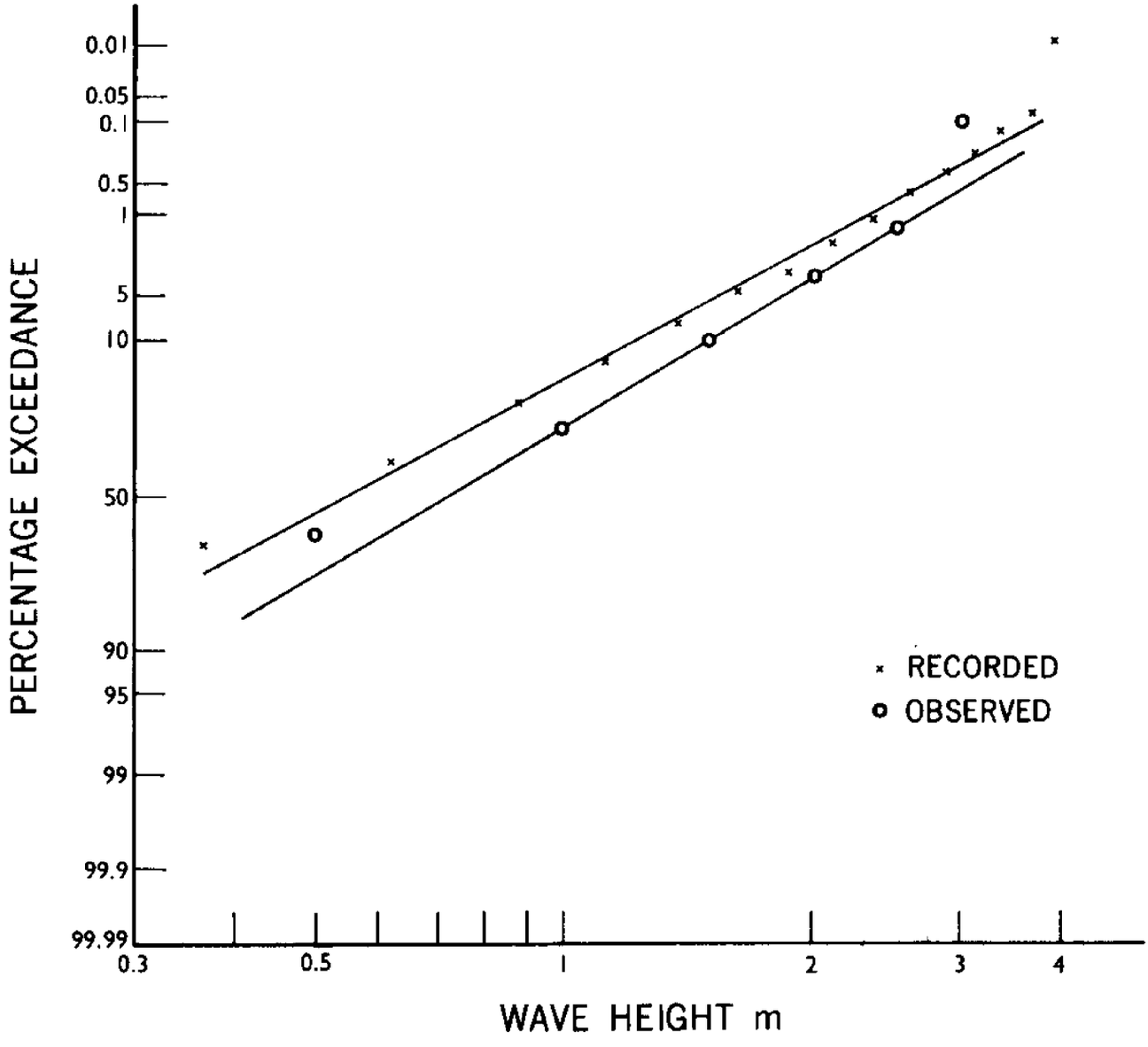

Figure 43 Percent of time a given significant wave height was exceeded from wave rider buoy measurements of Liu and Kessenich (1975) and by shipboard visual observation.

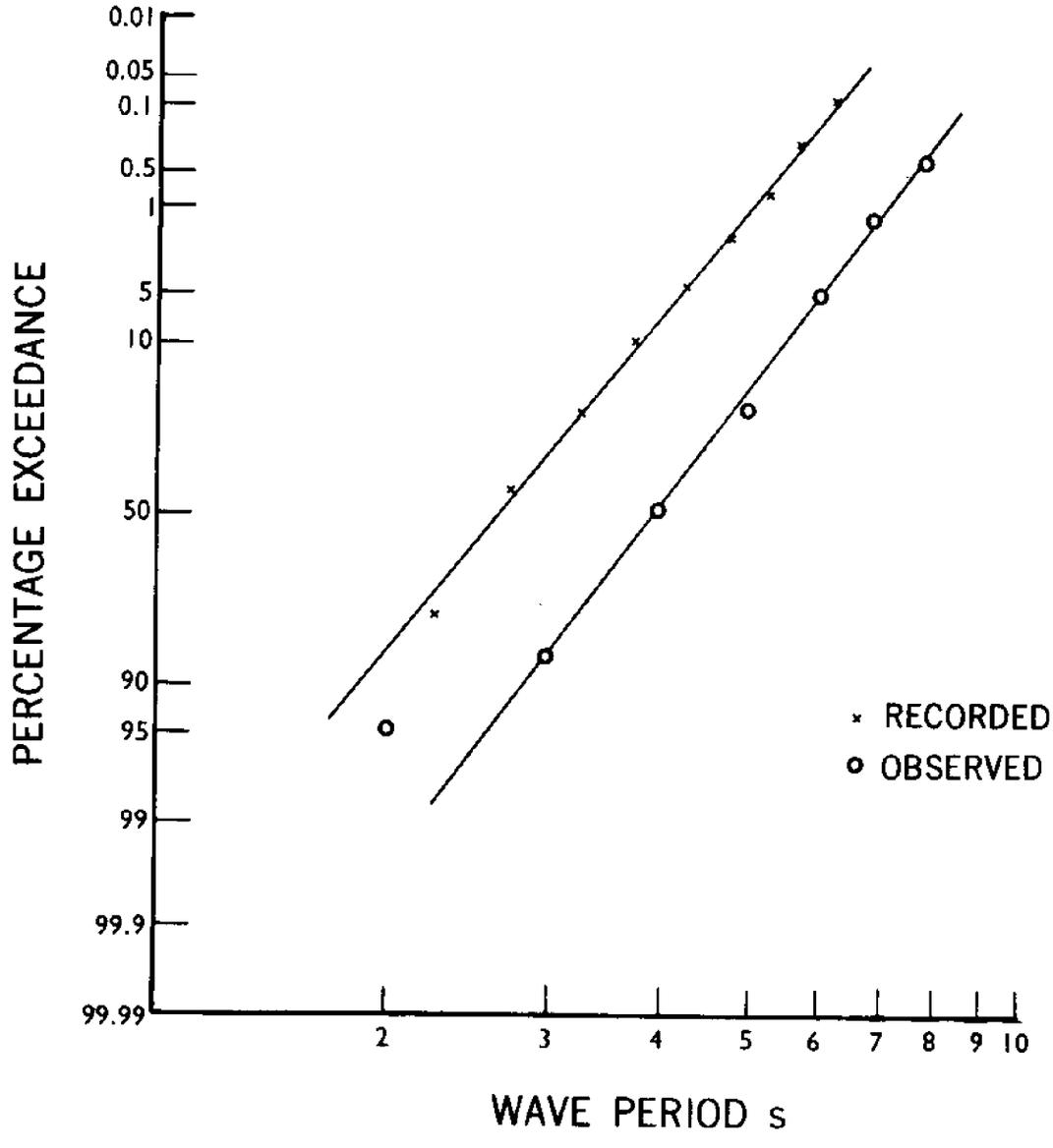

Figure 44 Percent of time a given average wave period was exceeded from wave rider buoy measurements of Liu and Kessenich (1975) and by shipboard visual observation.

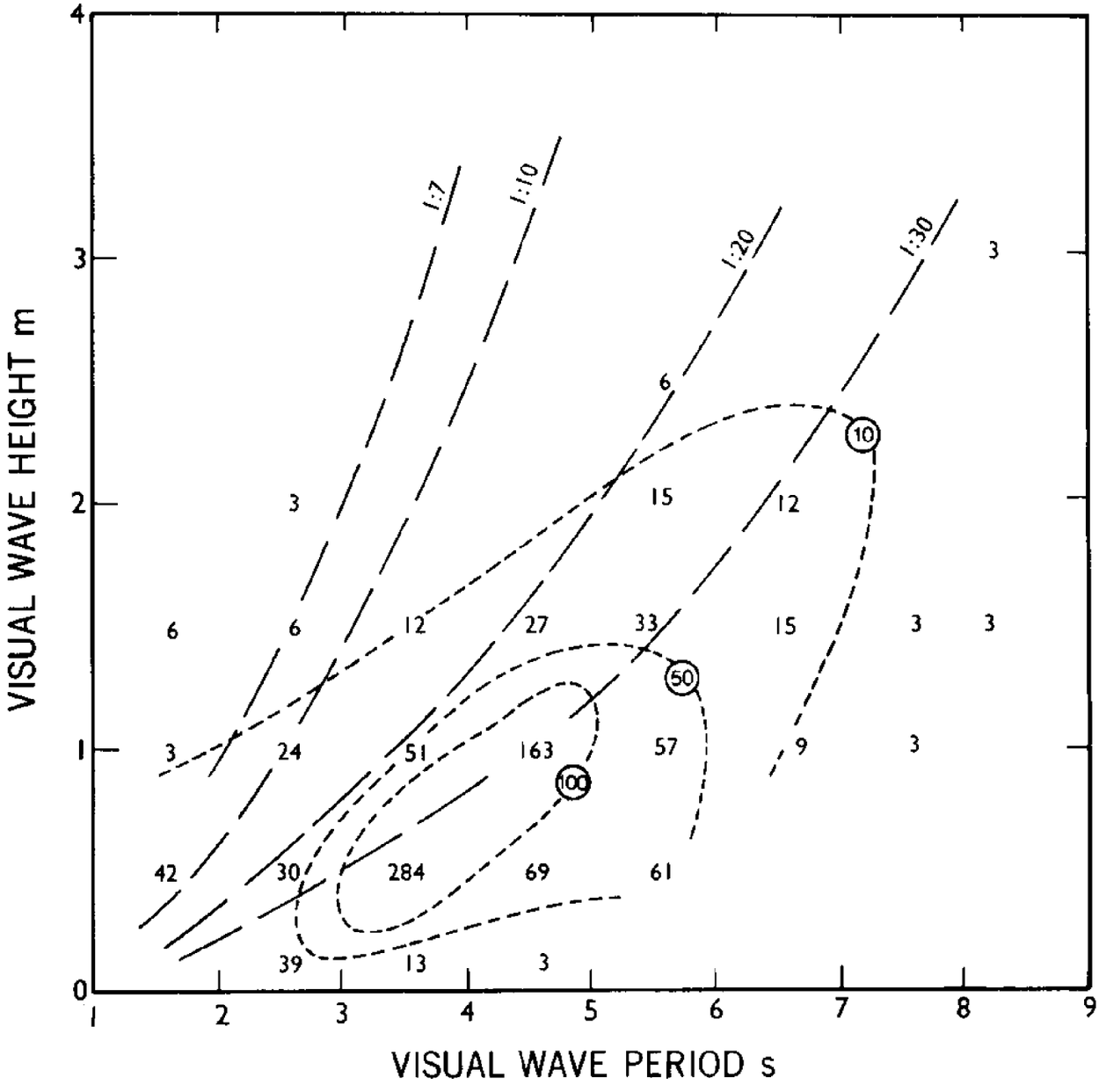

Figure 45 Scatter plot of shipboard observations of wave heights versus periods. The numbers represent number of points. Dotted lines represent contours of frequency of occurrence. Dashed lines represent steepness of waves.

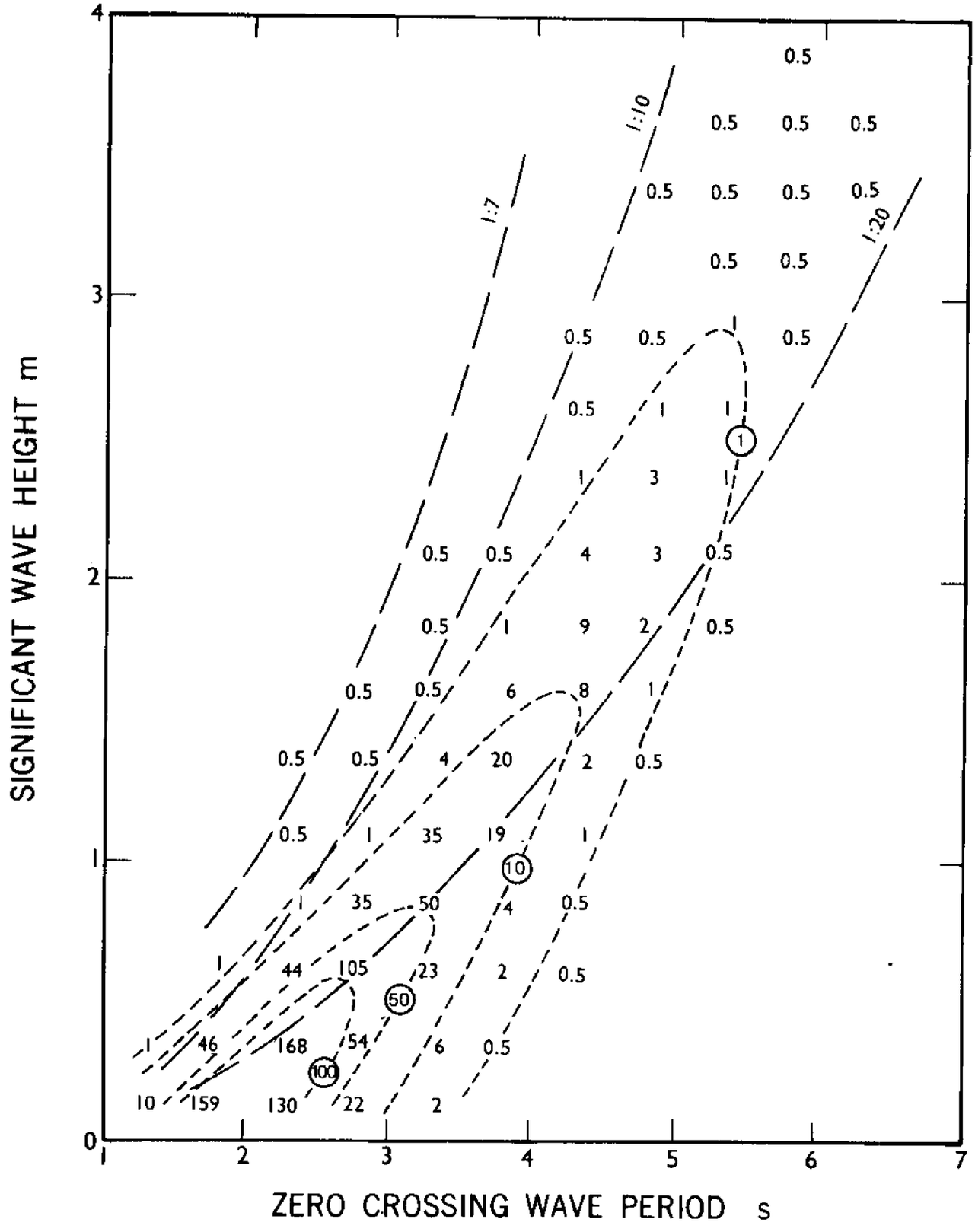

Figure 46 Scatter plot of recorded significant wave height versus average zero crossing wave periods. The numbers represent the number of points. Dotted lines represent contours of frequency of occurrence. Dashed lines represent steepness of waves.

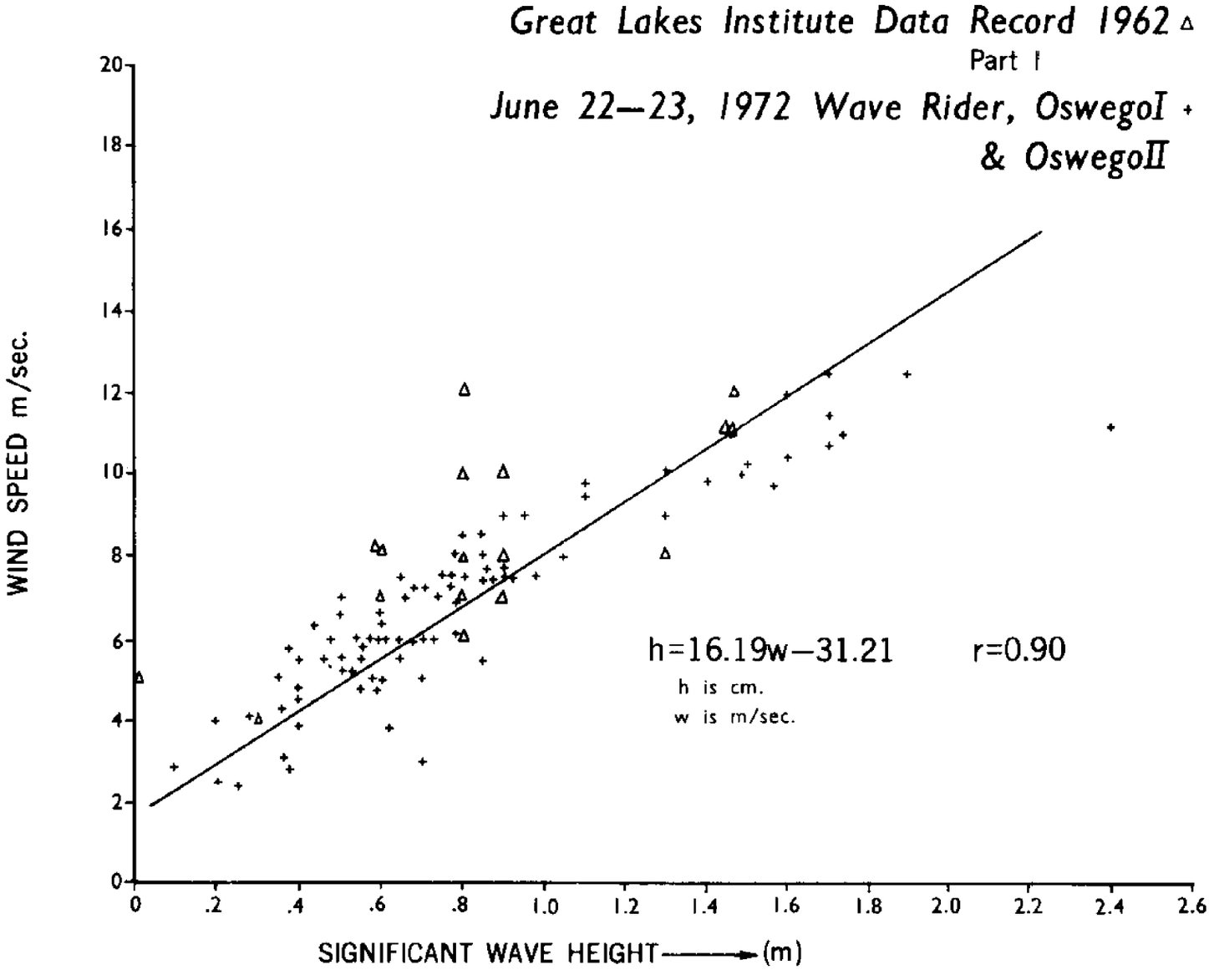

Figure 47 Significant wave heights from Oswego I and II wave rider buoys and Great Lakes Institute shipboard data versus wind speed. Line represents best fit by least squares linear regression. r is the correlation coefficient.

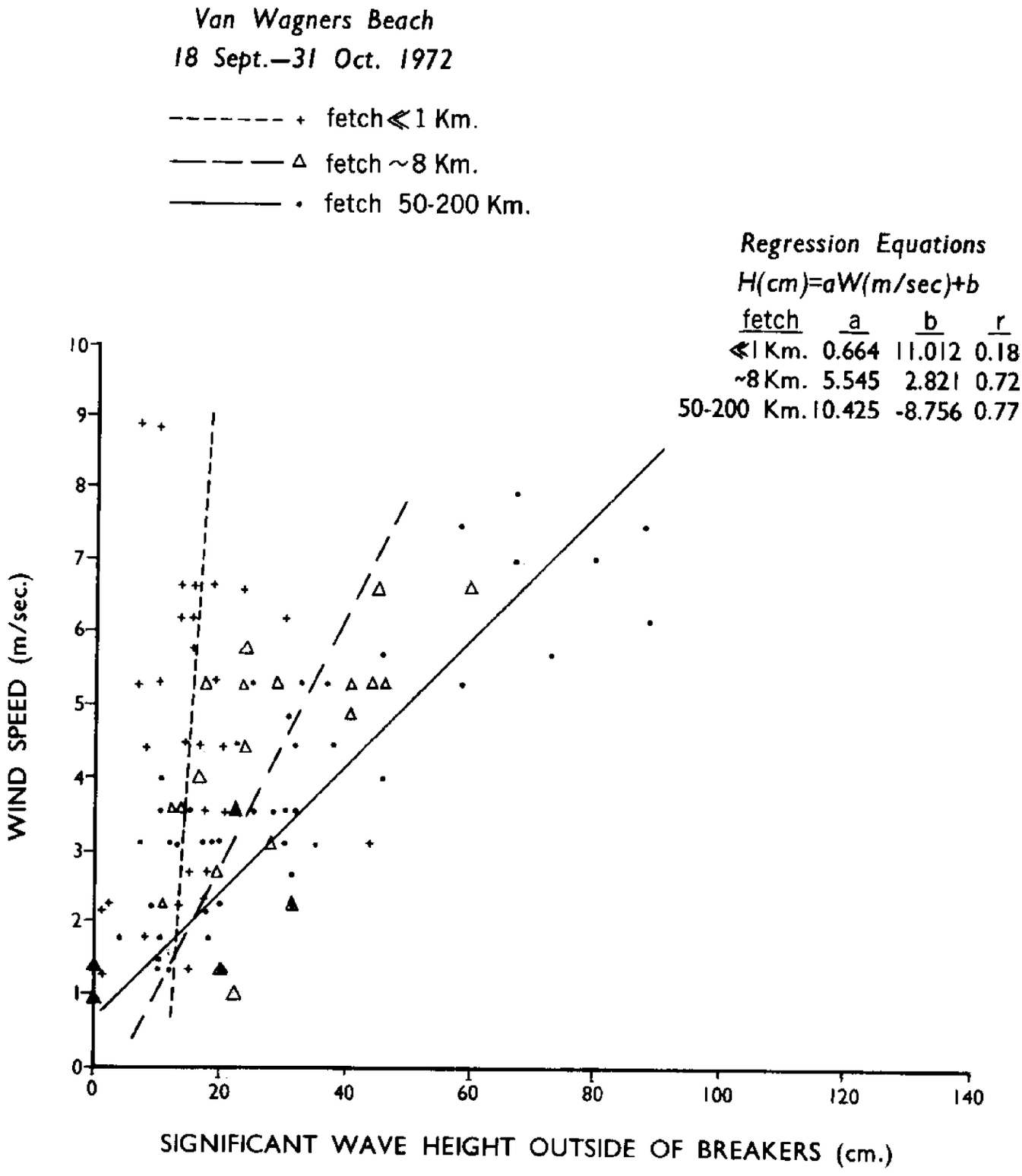

Figure 48 Significant wave heights from station just lakeward breaking waves off Van Wagners beach versus wind speed. The three lines represent best fit by least squares linear regression to data points with three different ranges of fetch. r is the correlation coefficient.

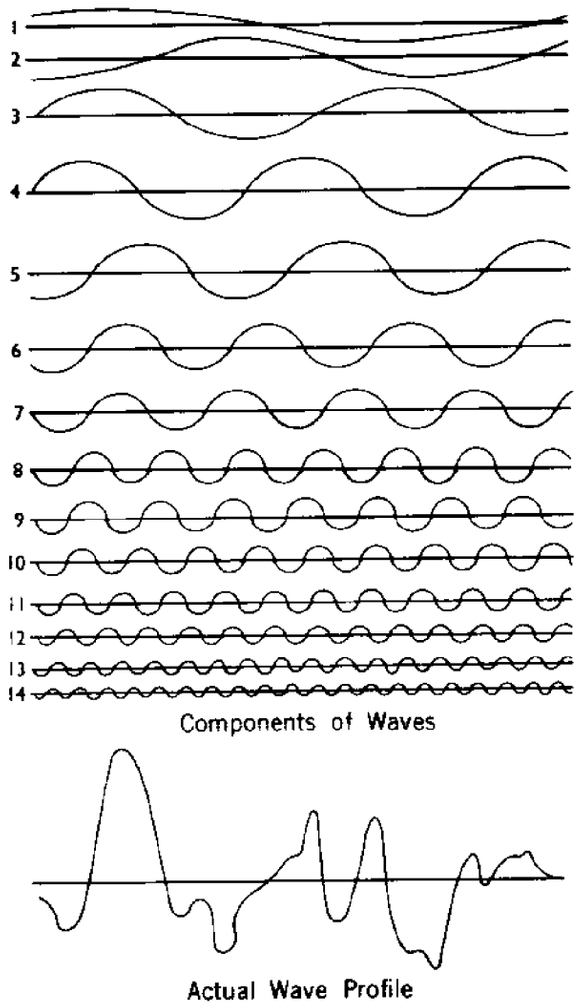

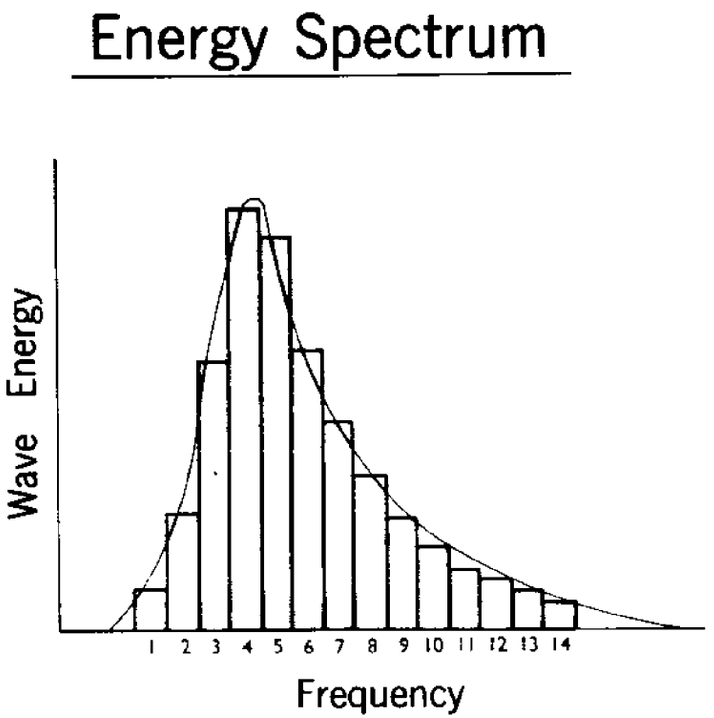

Figure 49 Representation of actual wave profile as the sum of 14 sinusoidal component waves. The relative energy density spectrum for a wave profile formed from the 14 sinusoidal waves shown on the left side of the figure is represented on the right side of the figure.

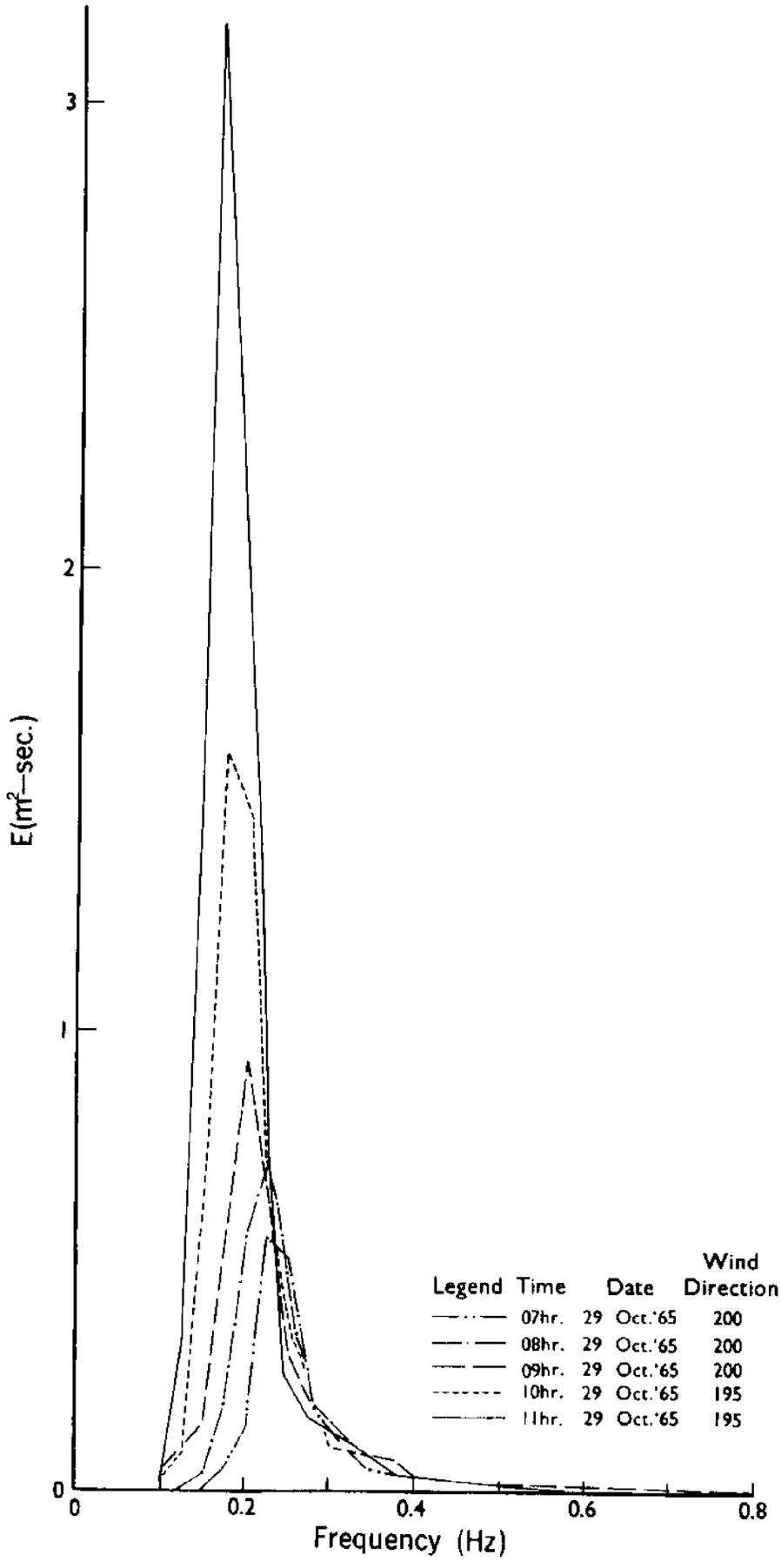

Figure 50 Relative energy density spectrum versus frequency plotted for an episode of wave growth.

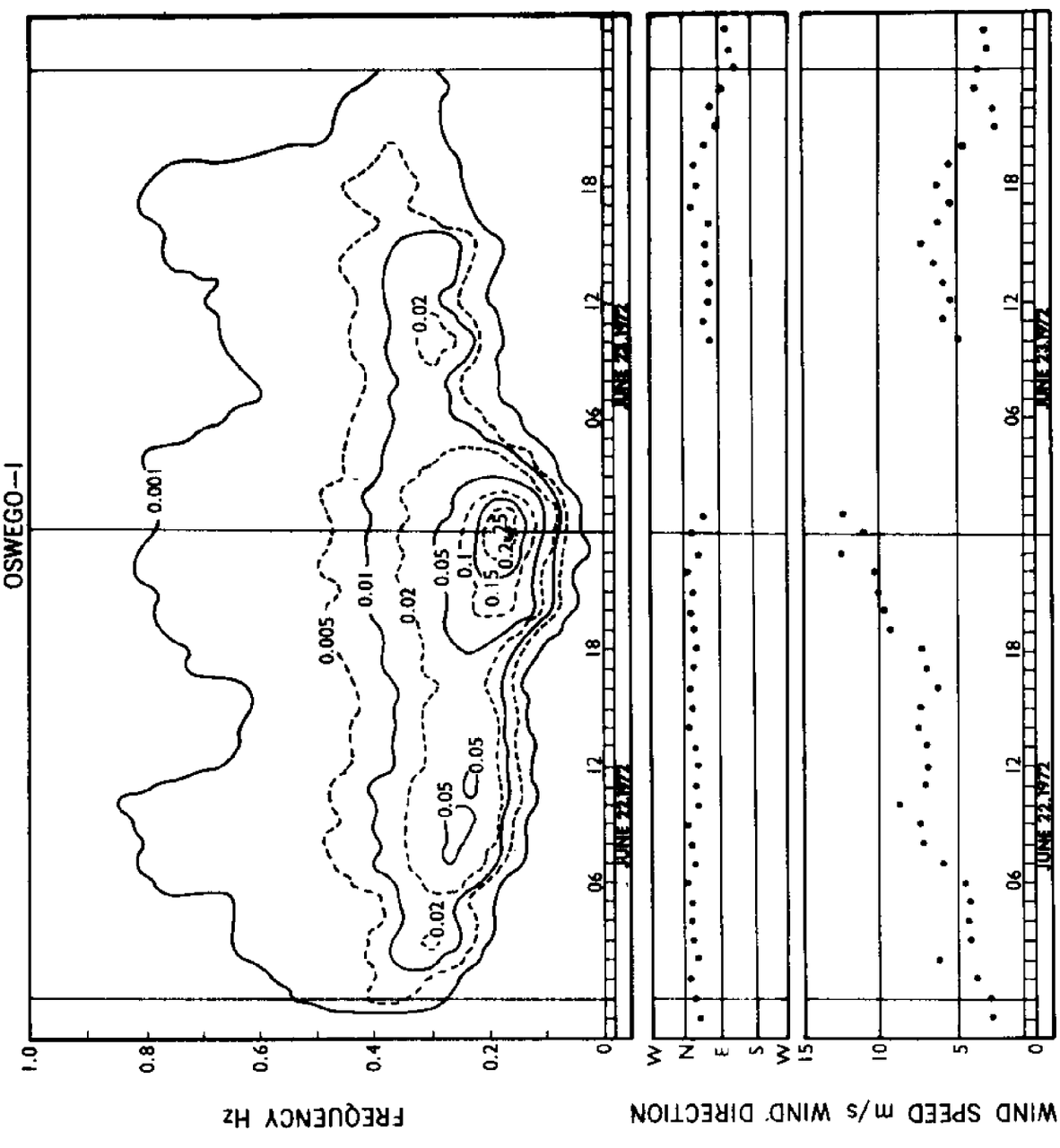

Figure 51 Wind speed and direction and frequency of waves versus time for the storm of June 22-23, 1972 at wave rider buoy Oswego I. The upper diagram of time versus frequency is contoured in terms of relative spectral energy density.

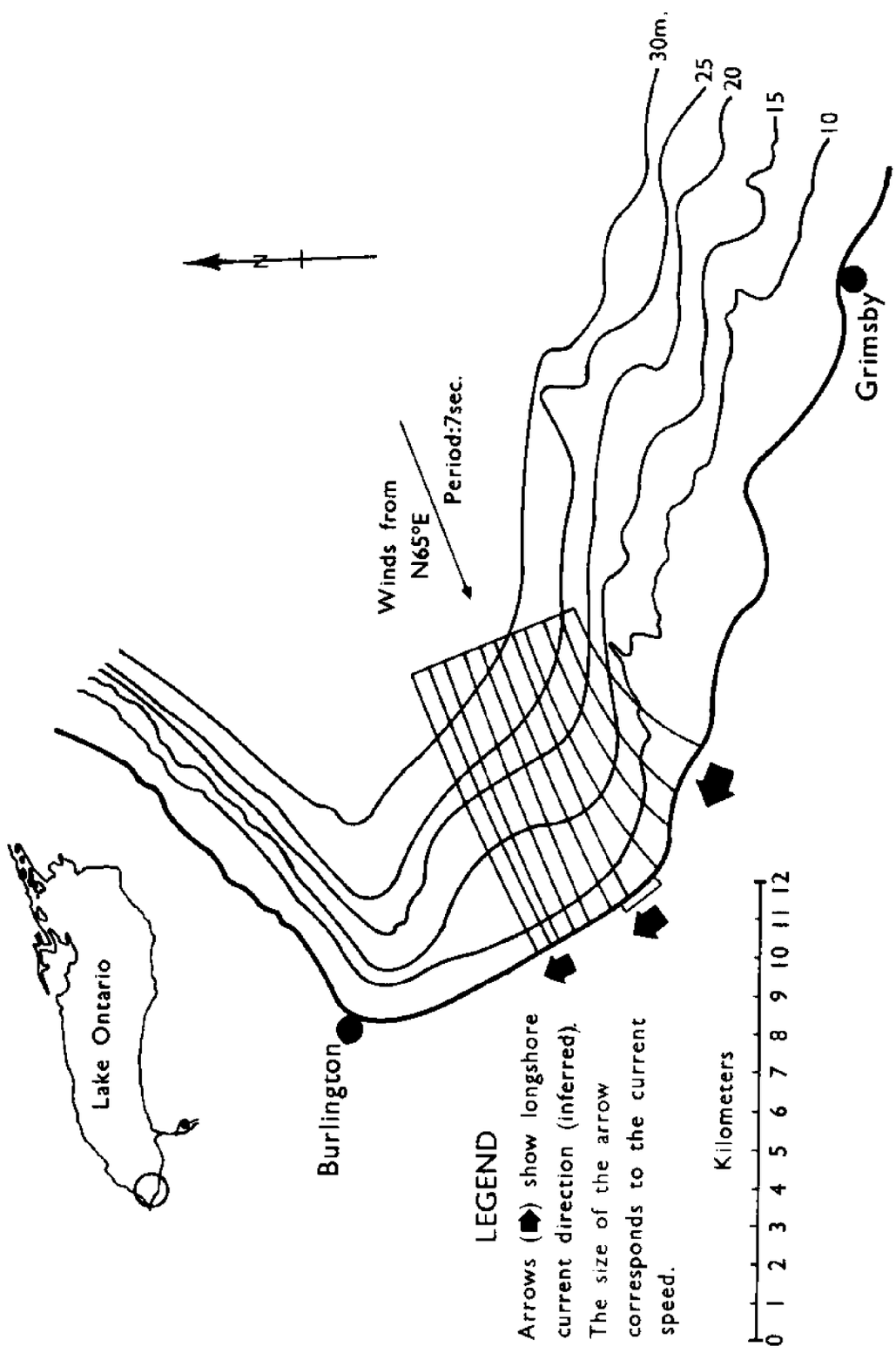

Figure 52 Computed refraction of wave paths initially from N65E near Van Wagners beach, Lake Ontario.

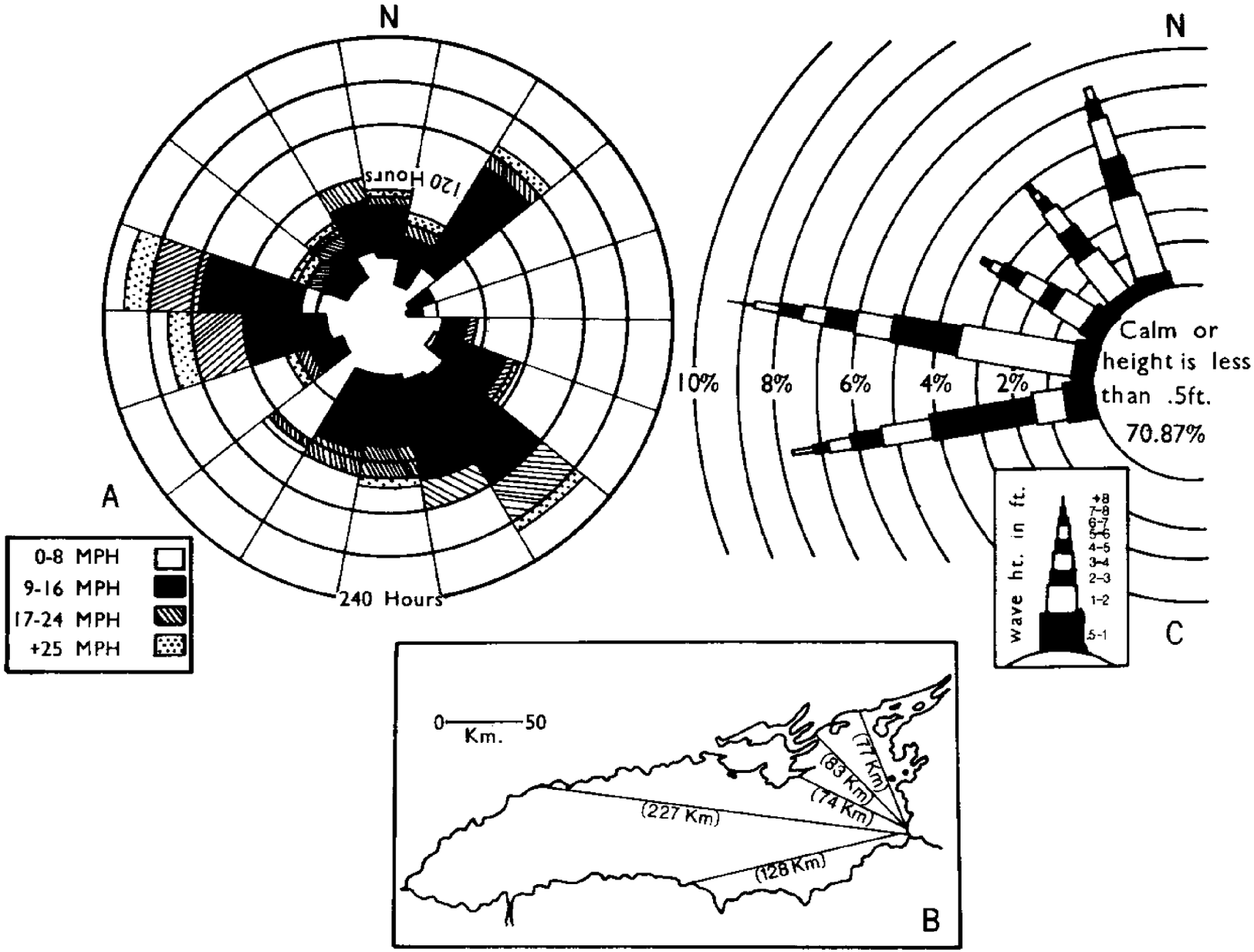

Figure 53 Wind rose and hindcasted wave rose obtained by Cohn (1973) for October 1972-October 1972 at Selkirk Shores region of Lake Ontario near Pulaski, N.Y. Insert map shows fetch for several directions of wind.

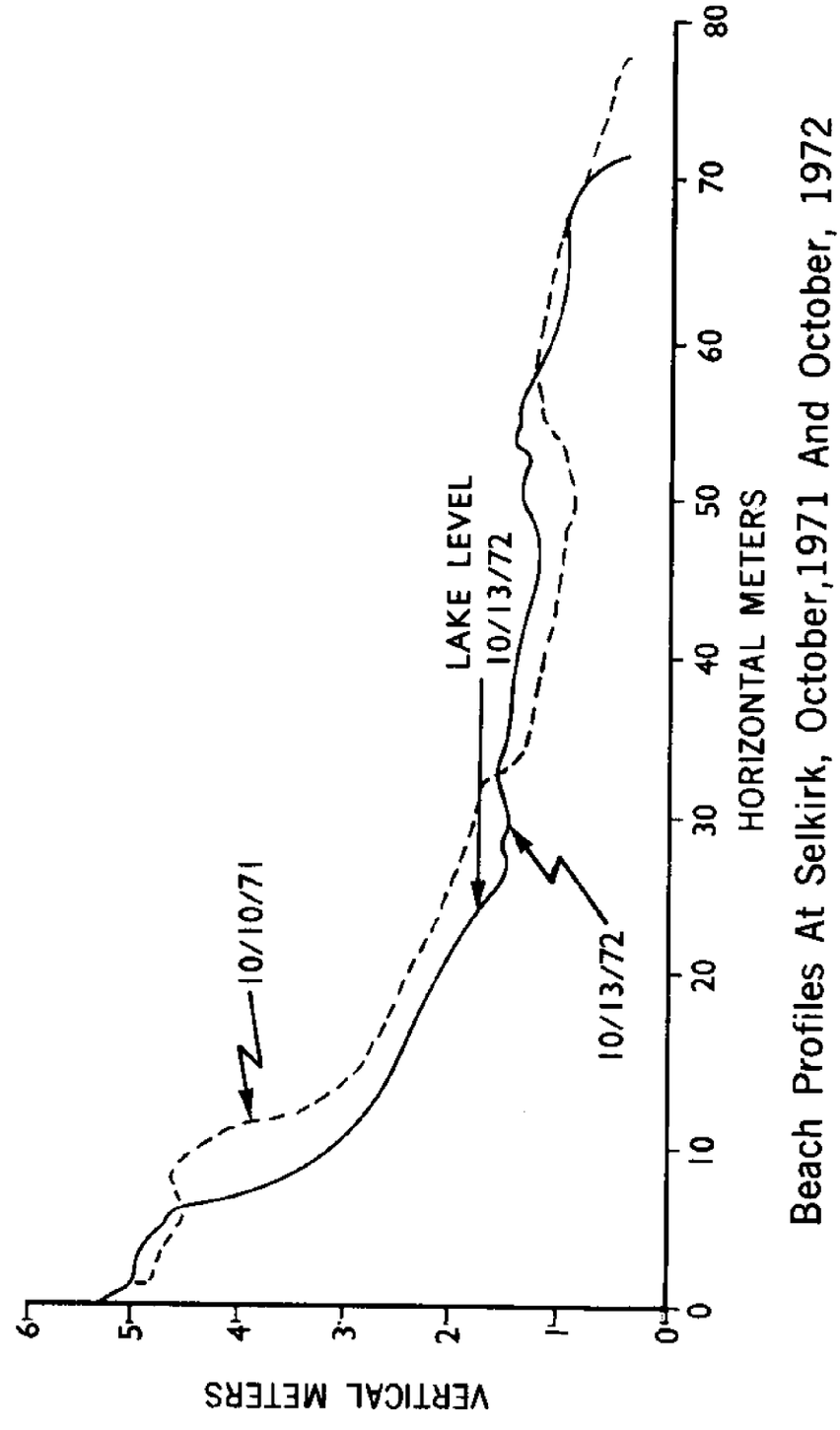

Figure 54 Beach profiles at Selkirk Shores region of Lake Ontario for October 1971 and October 1972.

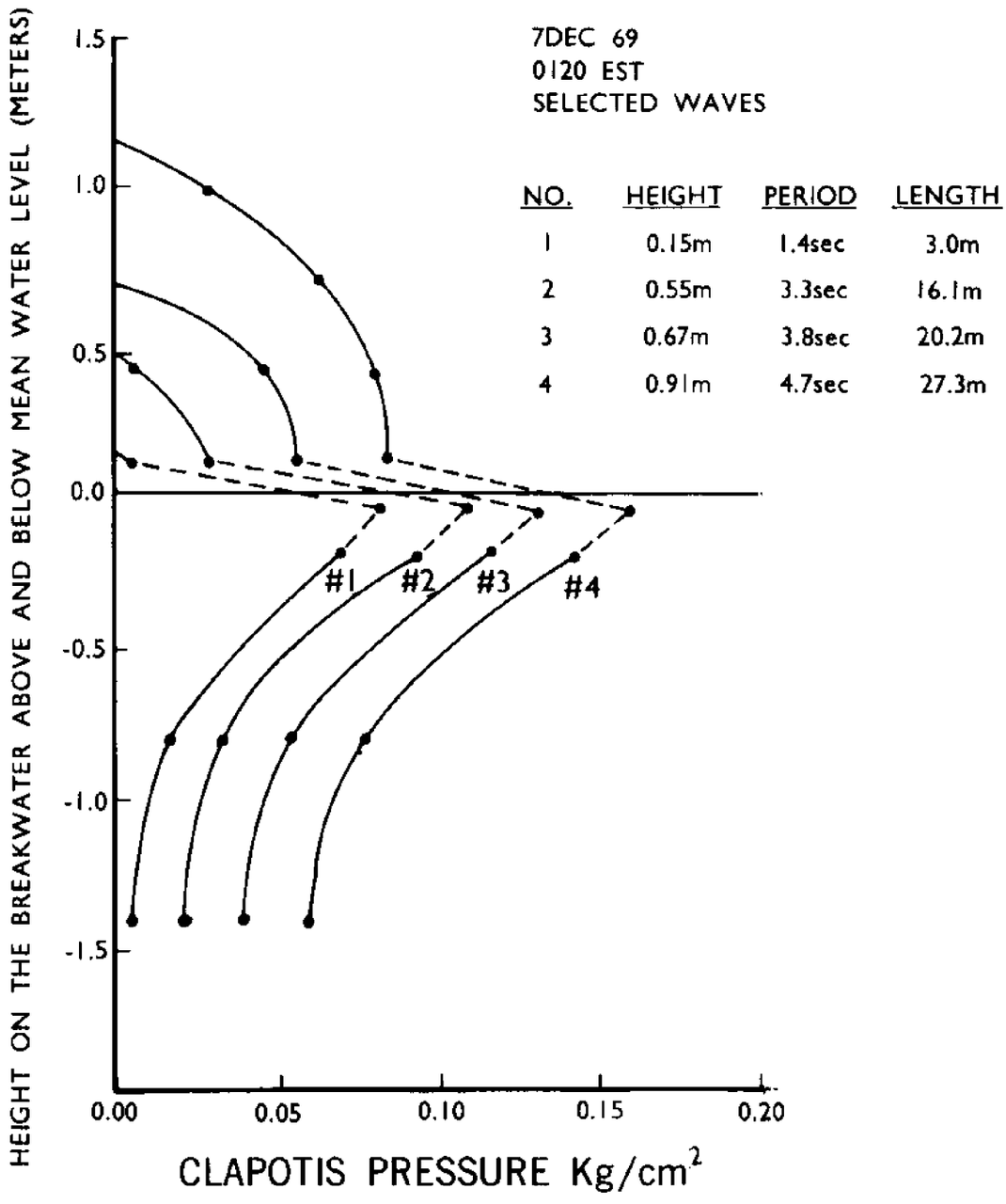

Figure 55 Clapotis wave pressure vs. height on a vertical breakwater for four different wave heights measured by Cole (1973).

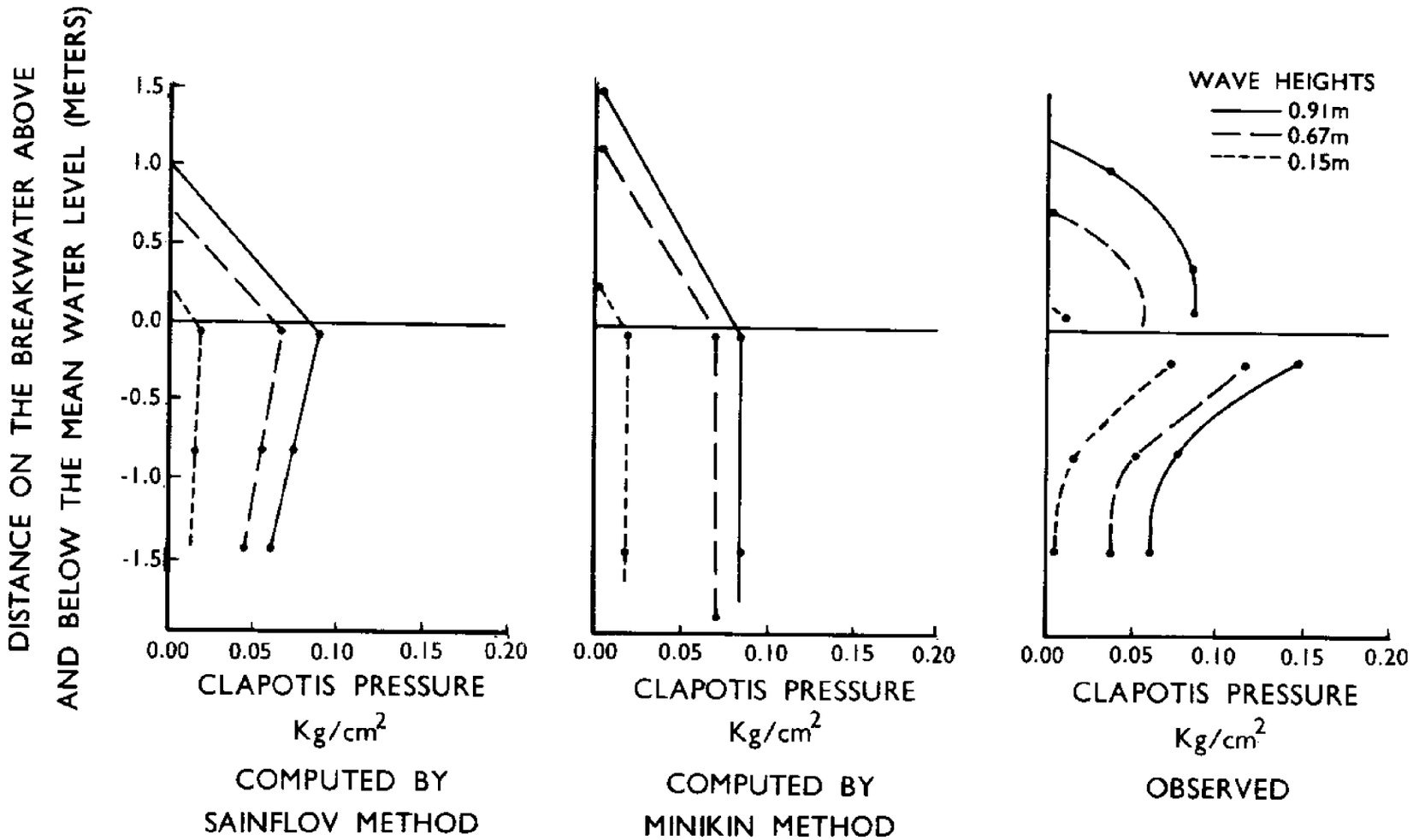

Figure 56 Clapotis wave pressure vs. height on a vertical breakwater for three wave heights. Left graph is for computed values using Sainflou's method. Center graph is for computed values using minikin's method. The right graph is for values measured by Cole (1973).

OTHER SEA GRANT TITLES OF INTEREST

New York Bight Atlas monograph series. 33 titles. Ask for free flyer.

US IFYGL Coastal Chain Program Report 2: Transport, Currents and Temperature from the United States and Canadian Coastal Chain Studies. Dennis R. Landsberg and Jon T. Scott. 215 pp. August 1976. $3.00

Order publications from NEW YORK SEA GRANT INSTITUTE
State University of New York
99 Washington Avenue
Albany, NY 12246
ATTN: Distribution Officer